ABSTRACT

Title of Document: **EVALUATION OF THE AASHTO EMPIRICAL AND MECHANISTIC-EMPIRICAL PAVEMENT DESIGN PROCEDURES USING THE AASHO ROAD TEST**

Sarah Beth Fick
Master of Science, 2010

Directed By: Professor, Charles W. Schwartz, PhD.
Department of Civil & Environmental Engineering

The American Association of State Highway and Transportation Officials (AASHTO) adopted the Mechanistic-Empirical Pavement Design Guide (MEPDG) in 2008 and state agencies are now transitioning from the classical empirical procedures derived from the American Association of State Highway Officials (AASHO) Road Test. This thesis focuses on the practical implications of this transition: specifically, the changes to required pavement thickness. The AASHO Road Test pavement distress histories are compared against the MEPDG and AASHTO 1993 performance predictions using several performance measures (PSI, IRI, rutting, and cracking). No existing relationships from the literature were found to fit the AASHO Road Test recorded data so new relationships were developed to relate measured PSI to MEPDG predicted distresses. The findings, although somewhat inconclusive due to inherent difficulties in modeling the conditions at the Road Test for the MEPDG, suggest that the MEPDG predicts thinner pavement sections at higher traffic levels.

EVALUATION OF THE AASHTO EMPIRICAL AND MECHANISTIC-EMPIRICAL PAVEMENT DESIGN PROCEDURES USING THE AASHO ROAD TEST

By

Sarah Beth Fick

Thesis submitted to the Faculty of the Graduate School of the
University of Maryland, College Park, in partial fulfillment
of the requirements for the degree of
Master of Science
2010

Advisory Committee:
Dr. Charles W. Schwartz (Chair)
Dr. M. Sherif Aggour
Dr. Dimitrios G. Goulias

This page has been intentionally left blank.

Preface

This thesis covers the topic of pavement design from 1958 through 2009, including the American Association of State Highway Officials (AASHO) Road Test, American Association of State Highway and Transportation Officials (AASHTO) Pavement Design Standards, and the Mechanistic-Empirical Pavement Design Guide (MEPDG). It is prepared by Sarah B. Fick in partial fulfillment of the University of Maryland, College Park, Master of Science degree requirements.

The research discussed herein was sponsored by the Federal Highway Administration (FHWA) Universities and Grants Programs under the supervision of the Design Guide Implementation Team (DGIT). It was carried out from September 2009 to November 2010 as part of the Dwight David Eisenhower Transportation Fellowship 2009 Grant for Research (GRF) project #6 "Assessing Sustainability: Pavement Construction and Network Sustainability Management."

The purpose of this Eisenhower GRF project was to aid state department of transportation agencies in the ongoing transition to mechanistic-empirical pavement design. It is a comparative study between the AASHTO 1993 design procedure and the MEPDG with respect to the practical differences in predicted performance, predicted service life, and the required structural thickness of the pavement. The two design methods were not only to be compared to each other, but also assessed for accuracy by comparing them with historical performance data from the AASHO Road Test.

Dedication

To my parents, thank you for supporting my education.

To my professors, thank you for guiding me through the last 6 years.

To my ‘Sheeples’, thank you for making sure I always got back in the saddle.

Acknowledgements

I would like to acknowledge Dr. Charles Schwartz for his generosity in providing me with a research assistantship and bringing me to the University of Maryland. Moreover, I thank him for his further assistance in obtaining and completing a Dwight David Eisenhower Transportation Fellowship. Without his support, I would not be where I am now.

I would also like to acknowledge Mr. Christopher Wagner, P.E., Mr. Henry Murdaugh, and the FHWA Universities and Grants team for seeing my potential and giving me this opportunity to explore the past and future of pavement design.

I also acknowledge Dr. Aggour and Dr. Goulias for participating in my thesis committee and supporting me in this last step towards my degree.

Table of Contents

List of Tables

List of Figures

Chapter 1: Introduction

The strength of a nations' transportation network is directly related to its economic health and growth. The need to rehabilitate our nation's crumbling infrastructure in the coming years is inescapable. The Department of the Treasury recently reported that public works projects repairing existing roadways, planning for new transit options, and increasing transportation capacity are of critical importance as America struggles through this recession. While the merits of investing in infrastructure are well documented, it is "not clear that policy makers should expect the same rate of return for [future] infrastructure investments…poorly planned, non-strategic investment is not only a waste of resources, but it can also lead to lower economic growth and production," (Department of the Treasury, 2010). With more trucks carrying heavier loads over longer distances, classical pavement design procedures are no longer cost effective and sustainable—making an evolution in how transportation engineers evaluate pavement performance more important than ever.

The paradigm-shifting "Interim AASHTO Mechanistic-Empirical Pavement Design Guide" (MEPDG) was officially adopted by the American Association of State Highway and Transportation Officials in 2008 (AASHTO, 2008). In 2003 and again in 2007, the Federal Highway Administration (FHWA) conducted a national survey to determine the state of practice for pavement design amongst state highway administrations. Both surveys indicate that current practice is use of an empirical design procedure derived from the 1950's AASHO Road Test. The most recent survey showed that 75% of state agencies use a version of the AASHTO empirical design procedure, 13% use a state procedure, and 12% use a combination of both. However, 76.9% of state

highway administrations intend to implement the new MEPDG, with 56% planning to make the transition in the next seven years. Moreover, the percentage of state agencies planning to implement the MEPDG nearly doubled between the 2003 and 2007 surveys. (Crawford, 2009)

The increasing interest and number of independent evaluations of the MEPDG are evidence enough of the transition underway. A significant and practical implication from adopting any new pavement design methodology is the resulting change in pavement structural thickness. The purpose of this thesis is to compare the AASHTO empirical and MEPDG procedures in terms of the required structural thickness for flexible pavements needed to perform satisfactorily under the designed traffic loadings. Specifically, the objectives are as follows:

1. Verify the accuracy of the 1993 AASHTO Pavement Design Procedure and the Mechanistic-Empirical Pavement Design Guide predictions in the context of the AASHO Road Test;
2. Evaluate existing pavement performance measures and identify thresholds of serviceability that permit the user to convert between the framework of either procedure;
3. Identify the key practical differences with regard to structural capacity between the MEPDG and AASHTO 1993 design procedures.

The research supporting these objectives as well as a discussion of the complications encountered during this study and the key results are presented in the following chapters:

Chapter 1: Introduction

The introduction covers the background necessary for understanding the research discussed herein and justifies the need for continued research in this field.

Chapter 2: Literature Review

Several papers and journal articles are reviewed and discussed in relation to this thesis. Literature is divided into two categories; those involving recent comparative studies between the MEPDG and AASHTO design procedures and those developing relationships between the parameters used by either procedure.

Chapter 3: Development of Pavement Design

This chapter is divided into three sections: the AASHO Road Test, AASHTO 1993 Pavement Design, and the Mechanistic-Empirical Pavement Design Guide. Each of these sections includes two discussion points. In the case of the Road Test, the design of the experiment along with pavement research is covered, and for the two design procedures, the specific inputs used for this study are defined. The second point covered in each section details problems that arose specific to this study.

Chapter 4: Pilot Study

The pilot study encompasses preliminary work aimed at evaluating the conditions of the Road Test and troubleshooting initial modeling problems.

Chapter 5: AASHO Road Test Modeling

This chapter covers the first study objective and addresses the accuracy of both design procedures in the context of the AASHO Road Test. Model predictions are presented and discussed. The second objective is also addressed in the context of shortcomings of existing performance measure relationships.

Chapter 6: Performance Model Development

This chapter discusses the data compilation and regression analysis attempts for developing a new statistically relevant relationship between PSI and pavement distresses.

Chapter 7: Key Insights and Lessons Learned

Final comments and key insights are discussed in this chapter as well as lessons learned. Additionally, recommendations for future research are made.

Chapter 2: Literature Review

Several studies relating to the AASHO Road Test, AASHTO empirical design procedure, and the MEPDG were consulted for this research. Included here is a summary of the technical reports most relevant to this study. Literature is divided into two categories: first, a representative synopsis of existing and ongoing comparative studies between the AASHTO Design Guide and the MEPDG; second, studies consulted to explore existing relationships between classical and contemporary pavement performance measures.

2.1 AASHTO vs. MEPDG Studies

Recently, many states have performed calibration studies to customize the MEPDG to specific regional conditions and standards in pavement design. Three representative studies are presented here that explore the accuracy of the MEPDG in comparison to the traditional AASHTO empirical design procedure and historical pavement performance data. The first paper by Kim *et al*. (2010) describes the results of Iowa DOT's most recent attempt to calibrate the MEPDG v1.0. Their findings are of particular importance to this thesis because they highlight potential problems that arise from using the nationally calibrated MEPDG models to simulate pavements in conditions similar to that of the AASHO Road Test. The second paper, Li *et al*. (2009) addresses the development of Washington State DOT's newest pavement design catalog. Their use of the MEPDG to check the AASHTO design method is applicable to the ultimate goal of this thesis in determining the practical implications to structural pavement thickness. The final paper by Schwartz (2009) is a sensitivity study examining the assigned contribution

of unbound layers to structural capacity for the MEPDG and AASHTO design procedures. This paper is included because the influence of material inputs and seasonal effects on unbound layers played a large role in pavement performance at the AASHO Road Test.

2.1.1 Kim *et al*. (2010)

Kim *et al*. (2010) explains the results of Iowa Department of Transportation's (DOT) most recent attempt to calibrate the MEPDG v1.0. Their findings are of particular importance to this thesis because they highlight potential problems that arise from using the nationally calibrated MEPDG models to simulate pavements in conditions similar to that of the AASHO Road Test. The objectives of this study were three-fold:

- To evaluate the information collected in the Iowa DOT's pavement management information system (PMIS) with respect to the MEPDG input and output parameters;
- To verify if the nationally calibrated MEPDG models provide reasonable predictions in relation to actual pavement performance;
- To examine if a correspondence exists between predicted and measured performance for Iowa highway conditions.

To accomplish these objectives, Iowa DOT's pavement management information system (PMIS) was queried for data on interstate and primary roads, which was then compared to the MEPDG information requirements. Sixteen pavement sections across Iowa were identified as having sufficient data and were not part of the national calibration in the National Cooperative Highway Research Program (NCHRP) Project 1-

37A, meaning the data could be used for independent verification of the MEPDG models. Of the sixteen sections, five were hot-mix asphalt (HMA) flexible pavements, five were jointed plain concrete pavement (JPCP) rigid pavements, and six were composite pavements with average annual daily truck traffic ranging from 208 to 7,525 trucks. Figure 2.1 shows a table of the details for each pavement section included in the study.

However, the Iowa PMIS did not have the detailed material properties or traffic characterization and distribution inputs required for MEPDG analysis. Only four of nine and three of seven MEPDG input parameters for HMA and PCC rehabilitation respectively were available in the PMIS database. Consequently, Kim *et al.* used MEPDG level 3 default inputs that corresponded with state standards for pavement design, but recommended that the Iowa DOT revise PMIS operations to include identification of the missing parameters for more successful implementation of the MEPDG in the future.

Type		Route	Direction	County	Beginning mile post	End mile post	Construction year	Resurface year	AADTT[a]
Flexible (HMA)		US218	1	Bremer	198.95	202.57	1998	N/R[b]	349
		US30	1	Carroll	69.94	80.46	1998	N/R	562
		US61[c]	1	Lee	25.40	30.32	1993	N/R	697
		US18	1	Kossuth	119.61	130.08	1994	N/R	208
		IA141	2	Dallas	137.60	139.27	1997	N/R	647
Rigid (JPCP)		US65[c]	1	Polk	82.40	83.10	1994	N/R	472
		US75	2	Woodbury	96.53	99.93	2001	N/R	330
		I80	1	Cedar	275.34	278.10	1991	N/R	7,525
		US151	2	Linn	40.04	45.14	1992	N/R	496
		US30	2	Story	151.92	158.80	1992	N/R	886
Overlaid (Composite)	HMA over JPCP	IA9	1	Howard	240.44	241.48	1973	1992	510
		US18[d]	1	Clayton	285.82	295.74	1967	1992	555
		US65	1	Warren	59.74	69.16	1972	1991	736
	HMA over HMA	US18	1	Fayette	273.05	274.96	1977	1991	2,150
		US59	1	Shelby	69.73	70.63	1970	1993	3,430
		IA76	1	Allamakee	19.78	24.82	1964	1994	1,340

a. Average Annual Daily Truck Traffic (AADTT) at construction year, b. N/R = Not Required, c. LTPP sites in Iowa, d. Resurfaced again with HMA in 2006.

Figure 2.1: Summary of information for selected Iowa Pavement Sections. (Kim *et al*., 2010)

Iowa DOT's PMIS did have most of the MEPDG performance data available for each section. The information was folded into a new database of historical pavement performance for each section that was then used for comparison against MEPDG distress predictions. However, the investigation revealed that the PMIS units for HMA alligator and thermal cracking as well as JPCP transverse cracking were different that those used in the MEPDG. As such, these distress measures were not included in the model verification and it was recommended that proper conversion methods for pavement distress measurement units from PMIS to MEPDG be developed for future local calibration efforts.

MEPDG v1.0 was used to simulate the chosen Iowa pavement sections and predictions were compared against actual distress measurements collected in the database. One example was provided for each pavement type due to space limitation in the report and only new construction HMA results are discussed here as relevant to this thesis. The results for HMA pavement US218 in Bremer County showed reasonable agreement for longitudinal cracking (m/km), IRI (m/km), and rut depth (mm), with IRI and cracking showing the best agreement (Figure 2.2).

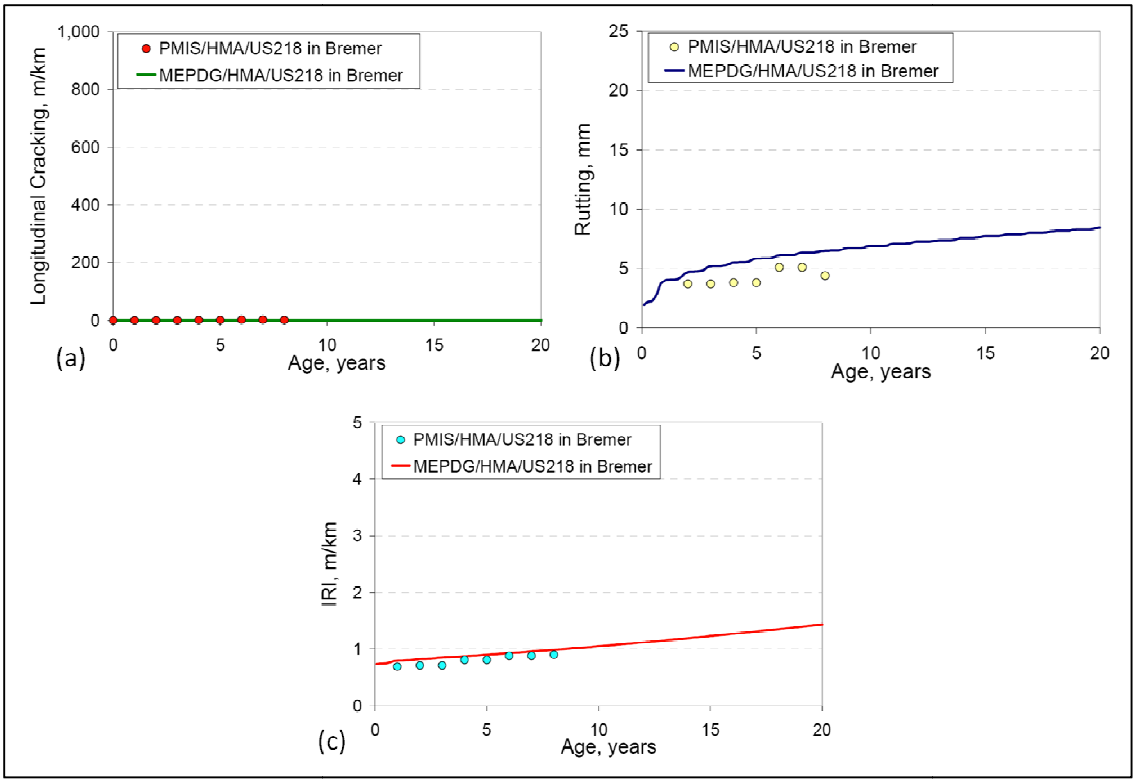

Figure 2.2: Nationally calibrated MEPDG (a)cracking, (b)rutting, and (c)IRI predictions for Iowa DOT structural section US218 in Bremer County. (Kim *et al.*, 2010)

A goodness-of-fit and null hypothesis statistical approach was taken in analyzing the bulk data. For this analysis, longitudinal cracking in HMA pavements was excluded because the NCHRP 1-40B study recommended exclusion for local calibration efforts due to questionable accuracy in predictions. The statistical results for the nationally calibrated model are presented below in Figure 2.3, along with the corresponding results for the locally calibrated model in parentheses. The rutting model for HMA pavements was analyzed using 27 data points and the nationally calibrated model coefficients. The results showed poor fit between the Iowa data and the MEPDG predictions using the national calibration. The HMA IRI model was analyzed using 52 data points, and was found to have a statistically reasonable fit between the Iowa data and the national MEPDG models (R^2=0.54). However, the null hypothesis—that no significant differences exist between the measured and predicted values of distress—is rejected (α<

0.05) for both HMA rutting (α< 0.001) and IRI (α< 0.046) models, indicating that there are "systematic differences [that need] to be eliminated by recalibrating the MEPDG performance models to local conditions and materials."

(a)

Type	Performance measures	N[a]	Goodness of fit statistics $e_{r(Mean)}$	S_e	S_e/S_y	R^2
HMA	Rutting, mm	27 (387)[b]	-1.86	2.16 (3.07)	1.51 (0.82)	Poor [c] (0.40)
	IRI, m/km	52 (353)	-0.06	0.25 (0.39)	0.68 (0.75)	0.54 (0.62)

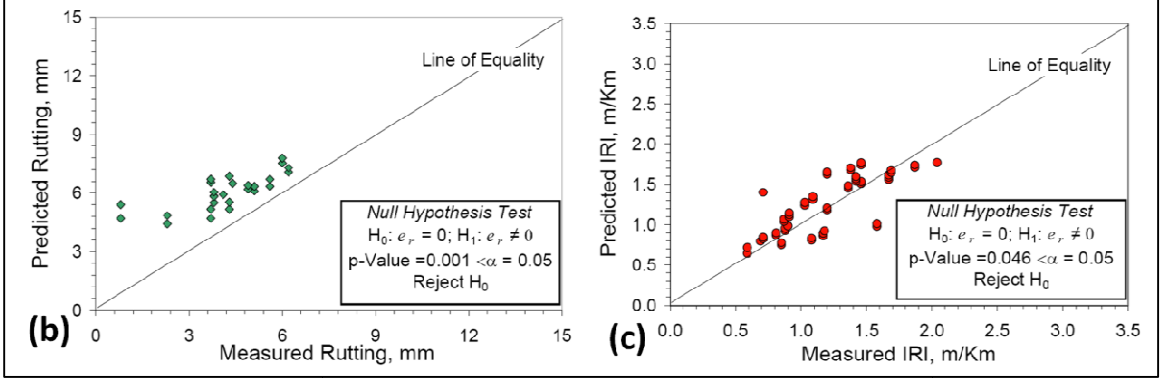

Figure 2.3: MEPDG nationally calibrated rutting and IRI model predictions verses Iowa historical pavement performance. (a) The table details the data and statistical results for both models. (b) Rutting shows a slight bias towards over predicting rutting and (c) IRI shows both good agreement and minimal bias. (Kim *et al.*, 2010)

Concerning HMA pavements, Kim *et al*. concluded that Iowa DOT's PMIS requires modification to collect the necessary input and output data relevant to the MEPDG and in the same units. Additionally, it was determined that more frequency and reliability was needed when collecting pavement performance data. They recommend that the MEPDG performance models be recalibrated to Iowa conditions to improve accuracy.

2.1.2 Li *et al.* (2009)

Li *et al*. (2009) developed a revised pavement thickness design catalog for Washington State DOT (WSDOT), with emphasis on documenting observations and issues between the AASHTO 1993 Guide and the MEPDG. Their use of the MEPDG to check the AASHTO design method is applicable to the ultimate goal of this thesis in determining the practical implications to structural pavement thickness. Both flexible and rigid pavements were examined in this study, but low-volume roads were excluded where the WSDOT standard of practice is to use bituminous surface treatments. The underlying design procedure in the new catalog remains, as the AASHTO 1993 design guide. Design thicknesses were used as inputs for the MEPDG to check and adjust the final pavement design. The focus was on high volume roads where the AASHTO 1993 design is thought to produce excessively thick pavement sections.

The methodology used in this study was as follows: pavements were designed according to the AASHTO 1993 guide; design thicknesses were used as input parameters to the MEPDG v1.0, locally calibrated for WSDOT; and MEPDG predictions were compared against historical performance data as a check on the original design. WSDOT policies for pavement design determined design inputs for both procedures and the study was conducted based on ESALs (design life). The study found that MEPDG still had some modeling issues and could not simulate all the distresses common in Washington State. For example, studded tires are permitted on vehicles from November to April, which results in increased surface wear and higher IRIs; MEPDG does not capture this effect in the models. More importantly, the results show that the AASHTO 1993 Guide was overdesigning pavement thicknesses for WSDOT at all ESAL levels. Table 2.1

shows the design thickness for AASHTO and the redesigned thicknesses based upon MEPDG results.

Table 2.1: AASHTO 1993 design thicknesses; MEPDG 'corrected' thickness in parentheses (Li *et al*., 2009).

50-YR ESALs (millions)	Reliability Level	Flexible Pavement Design Thicknesses (in.)	
		HMA	BASE
≤5	85%	7.5 (6.0)	6 (6)
5-10	95%	9.8 (7.8)	6 (6)
10-25	95%	11.3 (9.0)	6 (6)
25-50	95%	12.3 (11.2)	7 (7)
50-100	95%	13.4 (12.2)	8 (8)
100-200	95%	14.5 (13.3)	9 (9)

Historical performance also supports the observation that AASHTO 1993 overdesigns pavement thicknesses. Interstate HMA pavements constructed in the 1960's ranged in thickness from 9.5-18.6 inches and, other than regular maintenance of the wearing course, have required no rehabilitation. Furthermore, the base layer thicknesses were predetermined according to WSDOT standards and experience, and the MEPDG predictions confirmed the unbound layers to be adequate for the given design life, demonstrating the credibility of WSDOT's historical pavement performance.

It was concluded that the MEPDG still has modeling issues and was not ready to be implemented as an independent pavement design tool. However, it was capable of estimating reasonable values for major types of pavement distress when calibrated for local climate and material characteristics. The resulting pavement design catalog (Figure 2.4) has been officially adopted by WSDOT and is incorporated into the latest update of its pavement policy.

50-year ESALs	Reliability Level	Flexible Pavement		Rigid Pavement		
		HMA	Base	PCC	Base	
≤ 5,000,000	85%	6	6	8	GB only	4.2
5,000,000 to 10,000,000	95%	8	6	9	HMA over GB	4.2 + 4.2
10,000,000 to 25,000,000	95%	9	6	10	HMA over GB	4.2 + 4.2
25,000,000 to 50,000,000	95%	11	7	11	HMA over GB	4.2 + 4.2
50,000,000 to 100,000,000	95%	12	8	12	HMA over GB	4.2 + 4.2
100,000,000 to 200,000,000	95%	13	9	13	HMA over GB	4.2 + 4.2

Figure 2.4: WSDOT pavement design catalog. Pavement thicknesses designed using AASHTO 1993 and then corrected using the MEPDG. (Li *et al.*, 2009)

2.1.3 Schwartz (2009)

The final paper by Schwartz (2009) is a sensitivity study examining the assigned contribution of unbound layers to structural capacity for the MEPDG and AASHTO design procedures. This paper is included because the influence of material inputs and seasonal effects on unbound layers played a large role in pavement performance at the AASHO Road Test. The purpose of this paper was to quantify the contribution of unbound material characteristics, specifically layer thickness and stiffness, to pavement service life as predicted by the AASHTO and MEPDGE procedures. The objective was twofold:

- First, to determine the sensitivity of service life to subgrade modulus, base modulus, and base thickness for both the MEPDG and AASHTO 1993 pavement design procedures;

- Second, to verify the accuracy of both design procedures by comparing predictions to historical pavement performance data.

The sensitivity study was based loosely on the conditions of the AASHO Road Test, asphalt concrete (AC) over a crushed stone base over A-6 compacted subgrade. The variables analyzed are detailed in Table 2.2 and considered cases of 3, 6, and 9 inches of HMA. Design inputs for AASHTO and MEPDG were taken as defaults where AASHO properties were unavailable. Only one variable (in addition to HMA thickness) was allowed to change at a time. For example, when granular base thickness was allowed to change the base modulus and subgrade resilient were held constant at the values indicated in the fourth column of Table 2.2.

Table 2.2: Model variable input ranges and constants.

Case	Layer	Property	Range	Constant
1	Granular Base	Thickness	3 – 24 in.	12 in.
2	Granular Base	Modulus	20,000-45,000 psi	30,600 psi
3	Subgrade	Resilient Modulus	2,000 – 12,500 psi	5,000 psi

Results for case 1 where granular base thickness was varied showed good agreement between the design procedures for 3 and 6 inch AC thicknesses over moderate base thicknesses. However, AASHTO predicts substantially longer service life (larger structural contribution from unbound layers) when the base thickness is more than 12 inches (Figure 2.5a). Similar results were observed for case 2 where the base modulus was varied; good agreement existed between the design procedures for 3 and 6 inch AC layers, but for the 9 inch AC layer AASHTO showed a higher sensitivity to changing base modulus (Figure 2.5b). Finally, for case 3 where variations were made in subgrade modulus, good agreement was observed for both service life and sensitivity between the AASHTO and MEPDG models across all three AC layer thicknesses (Figure 2.5c).

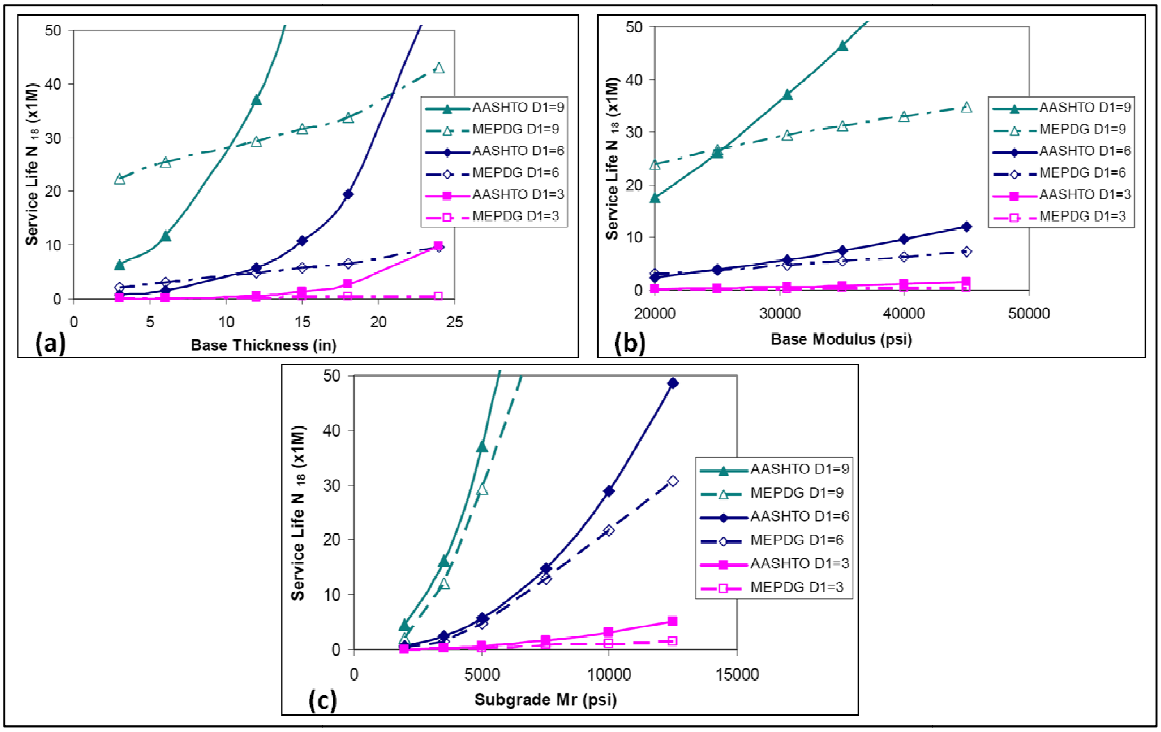

Figure 2.5: Predicted service life versus (a) base thickness, (b) base modulus, and (c) subgrade modulus. (Schwartz, 2009)

The overall conclusions drawn from this analysis were as follows:

- Service life predictions for AASHTO and MEPDG agree well for traffic loads less than 5 million ESALs;
- At traffic levels greater the 5 million ESALs, AASHTO and MEPDG assign significantly different weight to the structural contribution of the unbound materials;
- For higher quality materials, AASHTO assigns greater structural benefit to unbound materials, resulting in a higher service life prediction in comparison to the MEPDG.

To address the second objective of this study and verify the accuracy of both design procedures, Schwartz modeled the conditions of Loop 4, Lane 1 at the AASHO Road Test. The only variable component for this part of the study was the layer

thicknesses. An effective layer modulus value was used to combine the different stiffnesses between the base and subbase layers. Additionally, the fixed traffic configuration for that particular loop eliminated the need to convert between trucks and ESALs making service life a direct comparison between MEPDG and AASHTO.

As indicated in the sensitivity study, initial results for the second phase showed that the MEPDG predicted service life, defined as RD=0.5 inches at 50% reliability, was insensitive to varying effective granular layer stiffness while the AASHTO predicted service life, defined as ESALs to a PSI=2.5, was quite sensitive. Moreover, the AASHTO sensitivity to changing effective granular layer stiffness agreed well with the values for the AASHO Road Test (Figure 2.6).

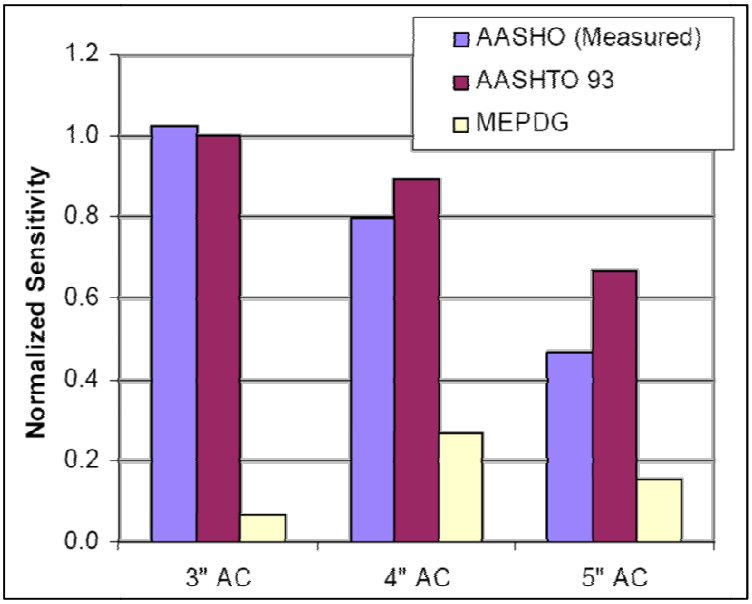

Figure 2.6: Sensitivity of service life to equivalent layer stiffness for the AASHO Road Test. (Schwartz, 2009)

Because the AASHTO Design Procedure was derived from the Road Test there is an implied bias in this comparative study. Therefore, the study was repeated using control sections from a full-scale APT experiment conducted by the University of Illinois. Three sections were used and once again predicted service life from the MEPDG and AASHTO design procedures was evaluated. However, it was found that both

procedures predicted service lives several magnitudes higher than the recorded number of axles to a 1 inch rut depth. Consequently, service life was normalized by the number of axle loads to failure for the structural section with an intermediate base thickness (Figure 2.7). The agreement in sensitivity for AASHTO predictions and the measured results is not as good as it was for the Road Test study. However, both show sensitivity to changing base thickness while the MEPDG shows minimal increase in service life with increasing base thickness.

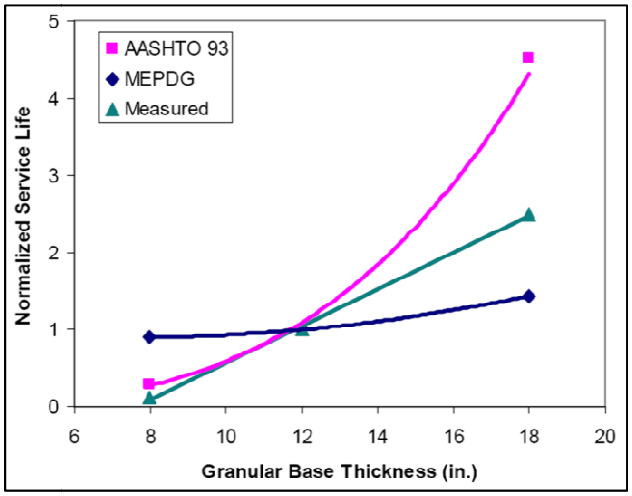

Figure 2.7: Service life versus base thickness for the Illinois APT control sections. (Schwartz, 2009)

This study is very limited and the results must be viewed within the context of material inputs and traffic configurations. Additionally, rutting was the controlling distress at the Road Test and conditions where fatigue distresses are the controlling failure mechanism may produce different results. However, the important conclusions from this study are that the predicted service life for the AASHTO and MEPDG procedures agree well at low traffic levels, as is expected based on the conditions for which the AASHTO procedure was derived form. At high traffic levels where the AASHTO design methodology is extrapolated, it over-predicts service life relative to the MEPDG. Reality likely falls between the two methods.

2.2 Present Serviceability and International Roughness Index Relationships

The AASHO Road Test resulted in the first correlation between pavement serviceability and observed distresses (Equation 2.1) in which observed slope variance (SV), rut depth (RD), cracking (C_F), and patching (P_F) were empirically correlated to present serviceability index (PSI).

$$PSI = 5.03 - 1.91\log(1 + SV) - 1.38(RD)^2 - 0.01\sqrt{C_F + P_F} \quad (2.1)$$

Additional relations that have been developed from experience relate terminal serviceability to an individual measure of distress. The conventional wisdom is that a terminal serviceability (p_t) equal to 2.5 corresponds to 20% fatigue cracking in the wheel path area or 0.5" of surface rutting.

The advantage of using PSI is that it is a single descriptive number for road roughness and ride quality. International Roughness Index (IRI), developed in the 1980's by World Bank as an alternative to PSI, describes pavement roughness in terms of a vehicle's vertical motion, in millimeters or inches, divided by the longitudinal distance covered. IRI was developed to provide a consistent way to measure pavement condition in any geographic location. PSI is subjective and can have dramatic discrepancies depending on the user's definition of an acceptable pavement roughness, whereas IRI is a measurable pavement property, which can be repeated with accuracy by any user.

This section reviews papers on the development of empirical correlations between measured IRI values and PSI. They are important to this thesis as a means to correlate the outputs from the AASHTO Design Procedure (PSI) and the MEPDG (IRI).

2.2.1 Paterson (1987)

An international study was undertaken by Paterson (1987) to evaluate technical options, maintenance strategies, and standards as well as the economic consequences therein of pavement performance. Part of Paterson's paper addresses a major concern that still exists today—how to relate PSI to the newly developed IRI. Paterson included four distinctly different geographic locations in his study: Brazil, Texas, South Africa, and Pennsylvania.

PSI ratings were found to vary widely across nations depending on the expectations of the user. Texan, Pennsylvania, and South African ratings represented users who had a high standard for paved roads, but the mean PSI still varied as much as one full point for a given roughness, implying that PSI was too subjective of a performance measure. The Brazilian raters, accustomed to rougher pavements, attached a much higher PSI rating for distressed pavements than did the other groups (Figure 2.8).

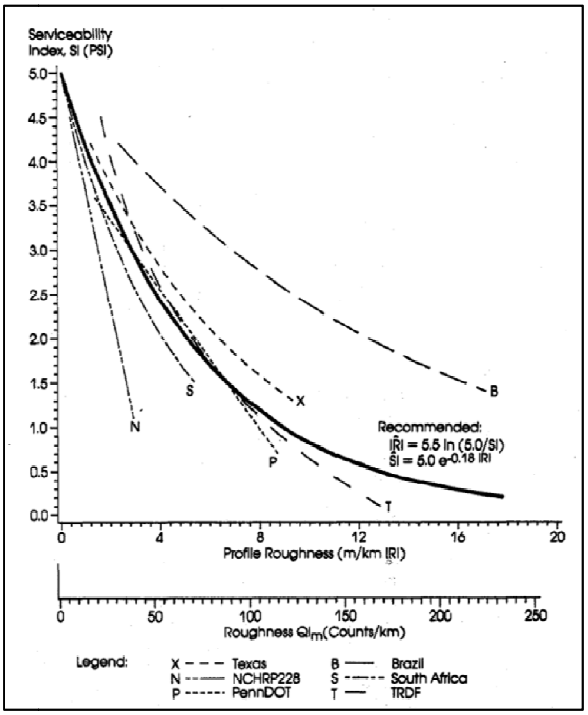

Figure 2.8: PSI vs. IRI relationships for each nation, The solid black line indicates the final recommended model. (Paterson, 1987)

Paterson used the individual data sources to develop a best-fit continuous model that was constrained such that when IRI (m/km) was zero, PSI would equal 5.0 (Equation 2.2). It was noted that use of the relationship presented below showed poor results for PSI values less than 1.5 and an alternative, linear equation was recommended for that range (Equation 2.3).

$$IRI = 5.5 \ln\left(\frac{5.0}{PSI}\right) \quad \text{or} \quad PSI = 5.0e^{-0.18IRI} \quad \textit{if } \text{PSI} \geq 1.5 \tag{2.2}$$

$$IRI = 12 - 3.6PSI \quad \textit{if } \text{PSI} < 1.5 \tag{2.3}$$

2.2.2 Gulen *et al.* (1994)

A study by Gulen *et al*. (1994), directed by the Indiana Department of Transportation (INDOT), involved ten randomly chosen raters evaluating twenty randomly selected pavement sections in Indiana. The purpose was to examine the relationship between PSI and IRI. The specific objectives were to develop a statistically significant model using a minimum number of raters and to define a serviceability threshold for unacceptable pavement distress.

Nine of the twenty pavement sections were AC and only the results pertaining to those sections will be discussed in this literature review. Similar to the AASHO Road Test procedures, evaluators were instructed on the road rating process and given forms to rate their ride quality. Participants were asked to rate the pavement quality as both the driver and the front seat passenger. Furthermore, tests were conducted on different days so that previous rides would not influence the raters. The resulting PSI ratings were found to have a normal distribution, and because the standard deviation was small, ratings were averaged. IRI data was also collected using a noncontact, laser-based

profilometer. Three readings were taken to verify the data collected and then the numbers were averaged for each pavement section.

Regressions were performed on the data to develop an empirical relationship between PSI and IRI. Twelve individual relationships were developed for bituminous, concrete, and composite pavements. Four of these characterized the relationship between PSI and IRI for AC pavements, the most successful of which had an R^2=0.92 (Equation 2.4).

$$PSI = 4.8 - 6.36\log(IRI) \quad \text{mm/m} \tag{2.4}$$

As discussed, the second part of this study was to determine the threshold at which pavements were no longer acceptable. Based on the results in Figure 2.9, passengers in the car were more tolerant of pavement roughness than drivers. Additionally, riders, regardless of position in the car, were more critical of roughness on concrete roads than on asphalt.

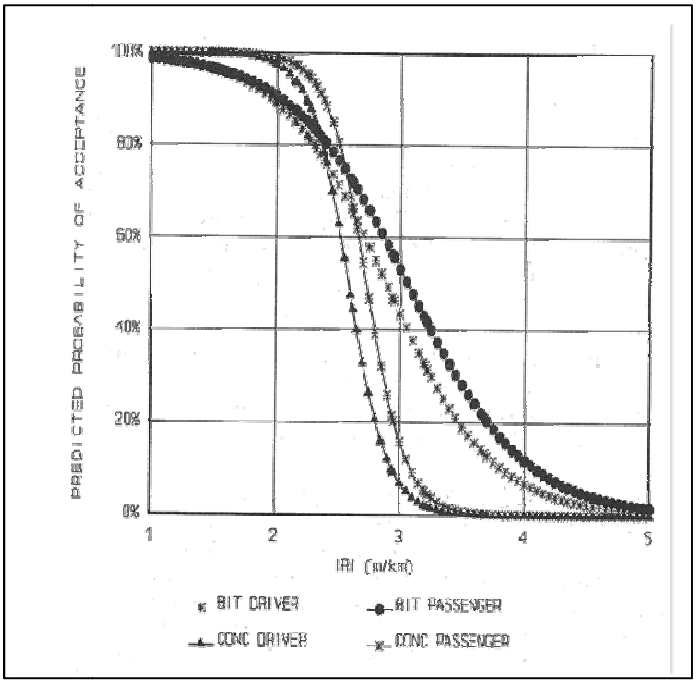

Figure 2.9: Probability of pavement performance acceptability versus IRI divided by position in the car and pavement surface. (Gulen, et al. 1994)

The conclusions of the study are as follows:

- Ten or fewer raters are sufficient to obtain PSI rating data.
- The location of the rater in the car is insignificant in practical application.
- All prediction equations are statistically sound for INDOT use.
- A terminal serviceability of 2.53 m/km is based on acceptance by 50% of road users, but a mean value of 2.3 m/km or 145in/mi is recommended for INDOT pavement management purposes.

2.2.3 Al-Omari and Darter (1994)

The primary objective of a study by Al-Omari and Darter (1994) was to develop a model for PSI in terms of IRI for flexible, rigid, and composite pavements. Additionally, they attempted to determine the relationships for key distresses to IRI and the thresholds for rehabilitation.

Al-Omari and Darter selected pavement data from five states in the National Cooperative Highway Research Program (NCHRP) Project 1-23 database as well as some sections from Indiana. The six states were Indiana, Louisiana, Michigan, New Jersey, New Mexico, and Ohio. Table 2.3 shows the number and type of pavement data contributed from each state.

Table 2.3: Number of pavement sections of each type contributed to the study from each state.

State	AC	COMP	PCC	*Total*
Indiana	42	-	24	*66*
Louisiana	13	13	22	*48*
Michigan	19	21	27	*67*
New Mexico	39	13	10	*62*
New Jersey	15	10	21	*46*
Ohio	34	32	23	*89*
Total	*120[sic]*	*89*	*127*	*378*

In this study there were a total of 162 HMA pavements, 71% of which were sections coming from Indiana, New Mexico, and Ohio. IRI was computed using the measured profile data. After compiling a database, several linear and non-linear regression models were evaluated. The most successful empirical correlation was of the form $PSR = 5*e^{(\alpha*IRI)}$. Analysis of the data revealed that there was very little difference between predictions for the states with the exception of New Jersey. Figure 2.10a shows the models for each state where all pavement types are combined and Figure 2.10b shows the models for each pavement type where all the state data is combined.

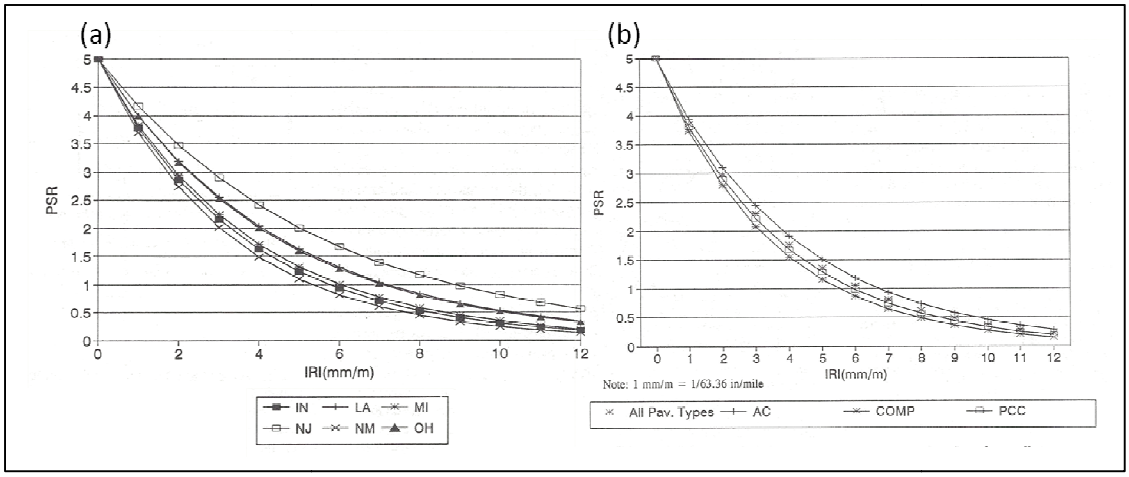

Figure 2.10: a) Model forms for all pavement types within each state. b) Model forms for all states within each pavement category. (Al-Omari and Darter, 1994)

There is very little difference between the best-fit curves for any of the cases presented above. This indicates that for practical purposes, the relationship between PSR and IRI can be described by one model for all pavement types (Equation 2.5).

$$PSR = 5e^{(-0.0041IRI)} \text{ (in/mi)} \qquad (2.5)$$

The final model form has an R^2=0.73, but it is important to note that the model is statistically biased to go through the point PSR=5, IRI=0. Figure 2.11 shows the

recommended model plotted against all the data points for pavement type across all states.

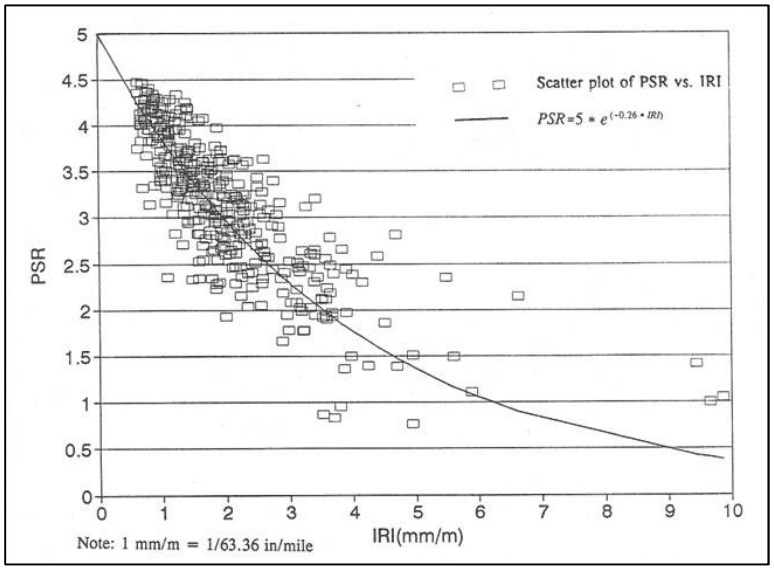

Figure 2.11: Final recommended model from Al-Omari and Darter plotted with the data points for all pavement types across six states. (Al-Omari and Darter, 1994)

2.3 Significant Research Points

The purpose of this thesis is ultimately to investigate the differences between the AASHTO 1993 procedure and the MEPDG. Research presented here is chosen for the direct implications to the results of this study. The existing and ongoing comparative studies between the AASHTO Design Guide and the MEPDG have different goals and methods, but collectively make several interesting points.

Kim *et al.* (2010) found that local calibration of the MEPDG significantly improved distress predictions. This result has been reported in several studies, but the proximity of Iowa to the AASHO Road Test (Ottawa, IL.) makes their findings particularly significant to this research. The nationally calibrated distress models for the MEPDG is used in this study, implying that some variability should be expected between the measured and predicted distresses.

The findings by Li *et al*. (2009) reiterated the point that local calibrated distress models predict pavement performance with increased accuracy. Additionally they found that MEPDG predicts thinner asphalt sections by 1-2 inches. These results are consistent with several other studies and address the practical implications of this research. They suggest that MEPDG distress predictions will be less than the corresponding AASHTO 1993 predictions.

Schwartz (2009) is applicable to this study in several ways. Both the sensitivity study and the distress verification were loosely based on the AASHO Road Test conditions, therefore the limitations of the study (specific material types, environmental conditions, controlling distresses, etc) are not a major concern in applying the findings to this thesis. The study found that AASHTO 1993 was sensitive to changes in unbound material properties which resulted in different service life prediction compared to the MEPDG. Consequently, this sensitivity is something to consider when interpreting the results of this thesis. Additionally, Schwartz found that service life predictions for AASHTO and MEPDG agree well for traffic levels below 5 million ESALs. This is contradictory to most other research unless considering that the other studies presented here were based on in-service roads and therefore subjected to traffic loadings well beyond the empirical range of the Road Test and AASHTO 1993 procedure. This is important to this study because it implies that there is the potential for the AASHTO and MEPDG distress prediction to not vary as much as suggested by studies based on high traffic loads.

The second group of studies consulted explored existing relationships between classical and contemporary pavement performance measures. The PSI-IRI relationships

suggested by Paterson (1987), Gulen *et al.* (1994), and Al-Omari and Darter (1994) are presented because they are both commonly used and fully encompassing measures of distress—that is, one can compare a measure of individual distresses (IRI) to ride quality (PSI). Al-Omari and Darter did not have the most statistically significant model, but it is the most applicable to this research because it is based on conditions throughout the United States; whereas the other models are either too limited or too broad in their geography.

Chapter 3: Development of Pavement Design Methods

The usual criticisms of the AASHTO 1993 design (performance based on one location, one environment, one set of materials, limited test duration, outdated construction practices and traffic loads) are instead benefits in this study. The high degree of control over the materials, climate, design details, and traffic removes several variables, ultimately aiding in the initial effort to understand the major practical differences in the AASHTO procedure and the MEPDG.

The purpose of this chapter is to familiarize the reader with the necessary components of the AASHO Road Test, AASHTO Design Procedure, and the MEPDG that are applicable to this thesis. For the AASHO Road Test, variables, conditions, results, and challenges specific to this study are summarized. For the AASHTO 1993 and the MEPDG methods, the design procedures are briefly discussed as well as the inputs specific to this thesis. Additionally, components of the input data that required in-depth analysis for this application are also explained.

3.1 AASHO Road Test

The AASHO Road Test was conceived and sponsored by the American Association of State Highway Officials and conducted under the guidance of the Highway Research Board (HRB) of the National Academy of Sciences-National Research Council from 1958 to 1961. Only two full scale attempts to characterize pavement performance had previously been undertaken. The first project, Road Test One-MD, was conducted on an in service portland cement concrete pavement in Maryland and the results were published in 1952 as HRB Special Report 4. The second

project, the Western Association of State Highway Officials (WASHO) Road Test, involved building two test loops of flexible pavement in Idaho; the results were published in HRB Special Report 18 (1954) and HRB Special Report 22 (1955). However, the AASHO Road Test was a considerably larger and more comprehensive attempt to resolve the progression and rate of pavement deterioration under moving loads of known magnitude and frequency. (AASHO, 1961)

The critical components of the Road Test were published in seven Special Reports (SR 61A-SR 61G) detailing the history and description of the project, materials and construction of the test facility, operation of the traffic, bridge research, pavement research, special studies, and a final summary report. Bridge research (SR 61D) and Special Studies (SR 61F) are not directly related to this thesis, but the remaining reports contain all the necessary information to model the Road Test using the AASHTO 1993 design procedure and the MEPDG software. (AASHO, 1961)

3.1.1 Design of the Experiment

The test site was in Ottawa Illinois, 80 miles south-west of Chicago and at the current site of Interstate 80 (Figure 3.1). This site was chosen because the borrow material available was thought to be 'uniform' and representative of that found throughout most of the country, because the climate was typical of that for most of the northern states in the nation, and because the earthwork could ultimately be used in the construction of a new interstate.

Figure 3.1: AASHO Road Test site location.

The test facility consisted of six two-lane test loops built upon a 36 inch embankment of A-6 borrow material locally sourced (Figure 3.2). Each loop had two test tangents, which were broken into structural sections roughly 100 feet long with 15 foot transitions between each section, creating a total of 468 flexible and 312 rigid pavement structural sections (Figure 3.3). Loop 1 was constructed solely for observing the influence of environmental factors on pavement distress initiation. Loops 2 through 6 constituted the main experiment (Design 1) as well as several special studies (Design 2 and Designs 4-6). Only the main factorial design (Design 1) was used in this study.

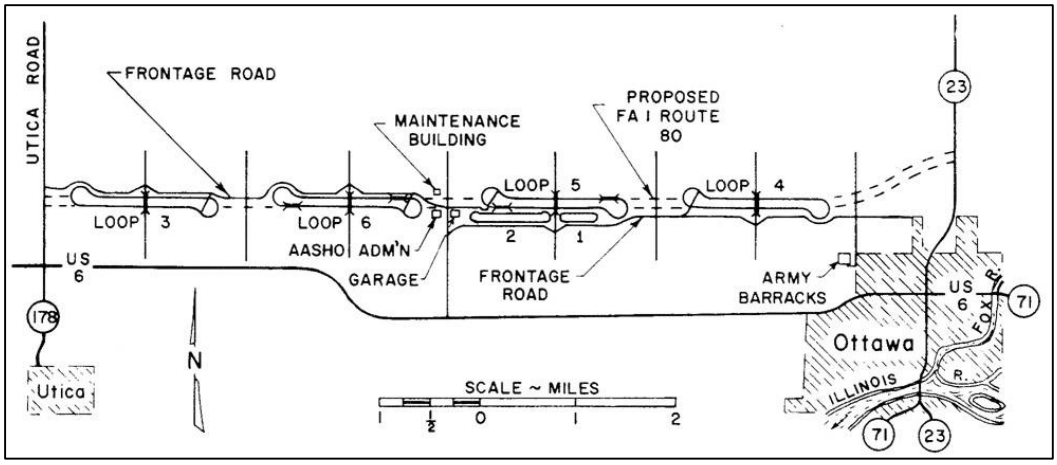

Figure 3.2: AASHO Road Test facility showing Loops 1-6, the proposed location of Interstate 80 (dashed line) and the proximity of Ottawa and existing roads. (AASHO, 1961)

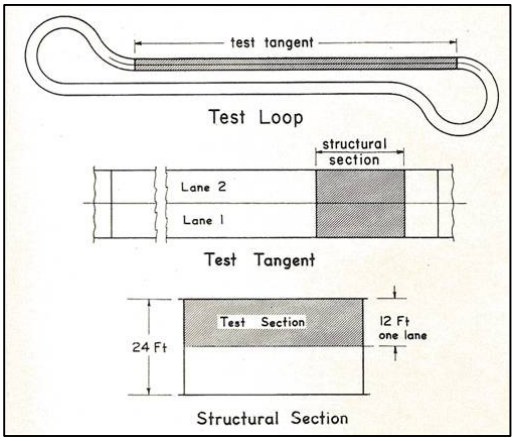

Figure 3.3: AASHO Road Test typical details (i.e. test tangent, lane 1 and 2, structural pavement section). (AASHO, 1961)

Factorial Design 1 in Loops 3 through 6 was 3x3x3; that is three levels of surface, base, and subbase thicknesses creating a total of 27 unique structural sections, 54 test sections per loop (inner plus outer lanes), with 3 duplicated structural sections (the factorial design for Loop 2 was 3x3x2). In the trafficked loops the surface, base, and subbase thicknesses were varied by 1 inch, 3 inches, and 4 inches respectively. Each test section was assigned a three-digit identification code; inner lanes assigned with odd numbers and outer lanes with even numbers, and then randomized within the loop. The typical cross section for each flexible pavement section is shown below in Figure 3.4.

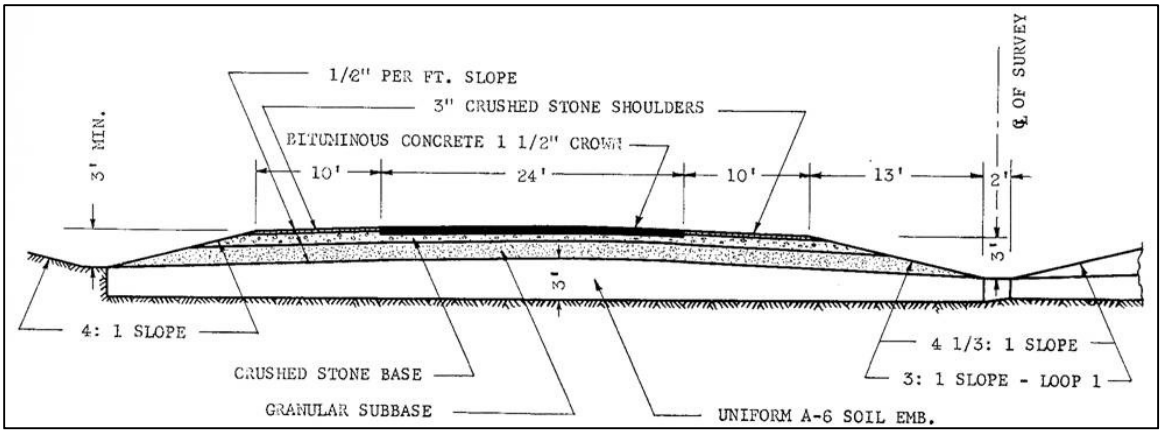

Figure 3.4: Typical flexible pavement cross-section showing the construction details of the embankment, subbase, base, and surface. (AASHO ,1961)

The embankment, referred to here as the subgrade, was constructed between September and November of 1956 using AASHTO designated A-6 borrow material (clayey soil) to ensure a uniform foundation and construction surface. During 1957 the remainder of the pavement structure was constructed; material properties are detailed in Figure 3.5. The subbase material used was a gravely-sand constructed with a uniform thickness across the pavement and shoulder cross-section. The base material was a crushed dolomitic limestone. The asphalt cement used as a surface for the flexible tangents was composed of crushed limestone and sand coarse aggregates and penetration grade 85-100 asphalt binder that met material standards as detailed in Figure 3.6. All construction and material testing was strictly overseen by the Illinois Division of Highways in accordance with AASHTO test standards (current as of 1956).

Item	Soil			Subbase			Base		
	No. Tests	Mean	Std. Dev.	No. Tests	Mean	Std. Dev.	No. Tests	Mean	Std. Dev.
Liquid limit	59	27.7	1.9						
Plastic limit	59	15.1	1.4						
Plasticity limit	59	12.6	1.8		N.P.			N.P.	
AASHO Classification (Group Index)	54	A–6(9)			A–1(0)				
Optimum moisture (%):									
AASHO T 99	44	13.5	1.0	35	7.7	1.0	27	7.6	1.2
AASHO T 180	8	10.4	1.0	10	7.1	0.6	8	6.6	0.4
Maximum density (pcf):									
AASHO T 99	44	119.2	2.2	35	133.1	3.3	27	137.9	4.2
AASHO T 180	8	128.8	2.4	10	137.4	2.2	8	142.1	2.5
Spec. gravity, apparent	53	2.72	0.04	34	2.70	0.05	37	2.74	0.05
Mech. anal.[3]:									
No. 4 sieve	58	96.6	2.2	48	73.5	4.5	43	48.9	7.0
No. 40 sieve	57	88.6	3.9	47	26.9	4.7	41	20.3	2.5
No. 200 sieve	58	75.5	3.2	29	8.1	2.0	24	9.9	1.7
0.02 mm	42	61.9	5.1	4	4	a	4	5	c
0.005 mm	47	40.3	5.4	4	2	b	4	3	d
Sand equivalent	1	6		5	51	e	5	46	f
Sodium sulfate soundness loss, 5 cycles							5	3.0	g
Los Angeles abrasion loss[4] (%)				6	31	h	18	27.3	2.2

[1] Latest standard AASHO test methods used (as of 1958).

[2] Ranges: a = 3-6; b = 2-4; c = 4-6; d = 2-4; e = 40-73; f = 41-54; g = 0.7-6.0; h = 25-35

[3] Percent finer than.

[4] 500 revolutions.

Figure 3.5: Summary of material characteristics for the unbound layers. (AASHO, 1961)

Characteristic	Mean Value
Specific gravity, 77 F/77 F	1.021
Penetration, 77 F, 100 g, 5 sec	88
Flash point (°F):	
Cleveland open cup	559
Pensky-Martens	510
Softening point (°F)	118
Ductility, 77 F, 5 cm/min (cm)	149
Loss on heating, 325 F, 5 hr (%)	0
Penetration of residue, 77 F, 100 g, 5 sec	77
Soluble in CCl_4 (%)	99.88
Spot test, standard naphtha	Neg.
Furol viscosity, 275 F	158
Thin film oven test, ⅛-in., 5 hr, 325 F:	
Change in weight (%)	+0.04
Tests on residue:	
Penetration, 77 F, 100 g, 5 sec	55
Percent of original penetration	63
Ductility, 77 F, 5 cm/min (cm)	152
Softening point (°F)	129

[1] Latest standard AASHO test methods used (as of 1958).

Figure 3.6: Summary of asphalt concrete material characteristics. (AASHO, 1961)

The load for each loop is an accumulation of axle applications. Typical 1950's trucks with axle loads ranging from 12kip (single) to 48kip (tandem) stressed the

pavements over a period of two years, reaching a maximum traffic loading of 1,114,000 axle applications per lane or 2 million 18-kip equivalent single axle loads (ESALs) (Figure 3.7). With the exception of Loop 2, inner lanes were trafficked by single axle trucks and the outer lanes were trafficked by tandem axle trucks; Loop 2 only had single axle trucks. This traffic combination meant that each structural section was subjected to two different load magnitudes and axle configurations.

Figure 3.7: AASHO test vehicles, loading, and axle configurations. (AASHO, 1961)

The AASHO Road Test provides good variation in structural numbers and slab thicknesses and, although not representative of today's traffic, a good range of axle loads. The experimental details discussed in this section are summarized in Figure 3.8 (AASHO, 1961). This thesis is focused only on flexible pavements; the exclusion of PCC pavements is elaborated upon at the end of this chapter.

Table 9 Designs for Flexible Pavement Experiment

Note: Shaded sections are replicates

Figure 3.8: AASHO Road Test Table 9 - Flexible Pavement Experiment. Factorial "Design 1" is the focus of this thesis. (AASHO, 1961)

3.1.2 AASHO Road Test Pavement Research and Results

As previously mentioned, the primary objective of the AASHO Road Test was to determine the relationship between pavement performance and loading rates. To define performance the concept of Present Serviceability Index (PSI) was created based upon the notion that a road's primary purpose is to service the traveling public. Serviceability was known to be influenced by longitudinal and transverse roughness, but was highly subjective. To determine a good estimate of the general user's assessment of road conditions, a Pavement Serviceability Rating (PSR) panel was used for the Road Test. The panel was composed of highway designers, maintenance engineers, administrators, and persons representing the interests of contractors, truckers, and automobile manufacturers. Each panel member made independent ratings for each pavement test section using the form in Figure 3.9.

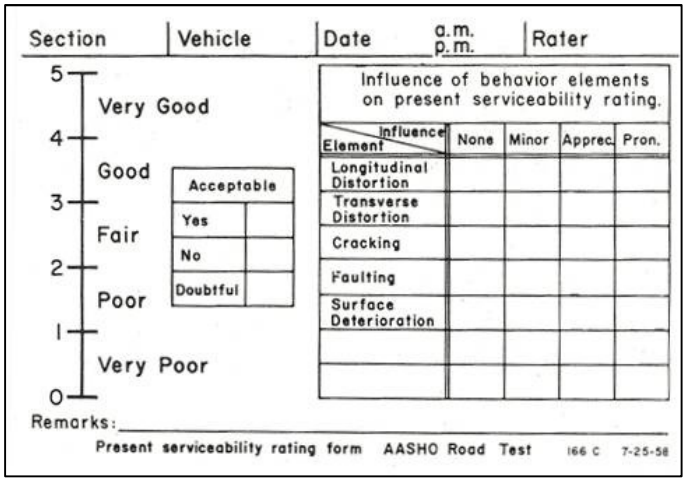

Figure 3.9: AASHO Road Test Present Serviceability Rating Form. (AASHO, 1961)

Ratings were taken every 2 weeks, averaged for each section, recorded with respect to the number of axle applications, and assigned to the final day in that 2-week period known as the Index Day. Index Days number 1 to 55 staring on November 5, 1958 and ending November 30, 1960. In conjunction with serviceability ratings, field

measurement crews measured variations in longitudinal and transverse profiles as well as the degree of cracking and patching in each test section using a longitudinal profilometer and a transverse profilometer. Figure 3.10 shows the typical distresses observed at the Road Test.

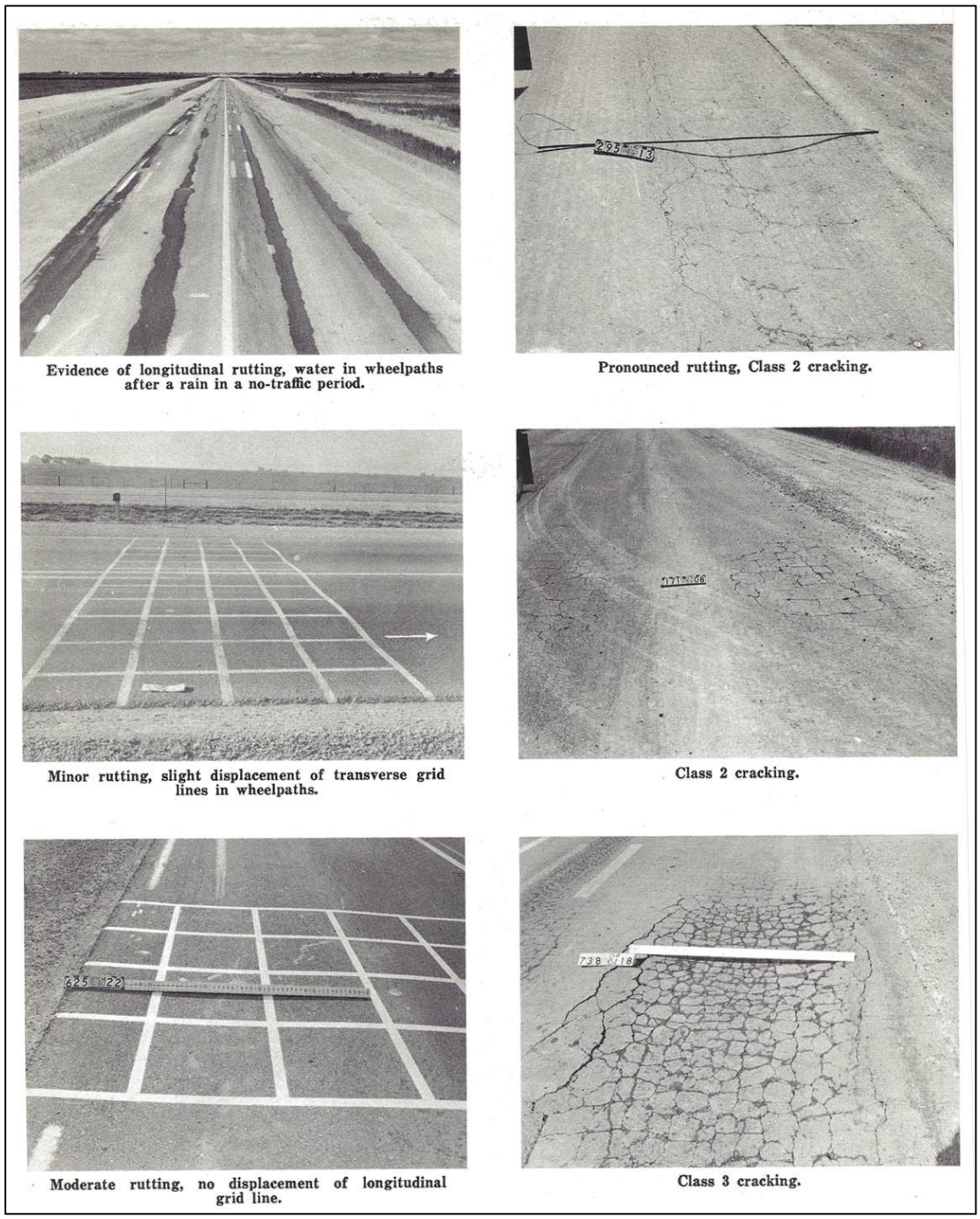

Figure 3.10: Typical flexible pavement fatigue and deformation distresses. Excessive rutting was the primary distress observed at the AASHO Road Test. (AASHO, 1961)

The Highway Research Board Special Report 61E details the pavement research program (AASHO, 1961). Published therein are the basic serviceability histories for each test section. Figure 3.11 is an example of the typical published data for each test section. The recorded PSR data from Index Days 11, 22, 33, 44, and 55 (22-week intervals) is available and shown in the right hand columns. The full distress histories were smoothed using a moving average technique. Presented on the left most columns are the logarithms of the number of axle applications at which the smoothed serviceability history curve crosses PSR levels 3.5, 3.0, 2.5, 2.0, and 1.5. These tables serve as the primary source for historical pavement performance data used in this thesis. These data are contained in full in the Flexible Pavement Database discussed in Appendix A.

Irregularities are occasionally observed in the test section distress histories, as is evident in the last two records for structural section 140 in Figure 3.11 where PSR increases from 3.1 to 3.3 with additionally axle applications. This phenomenon has been noted frequently in pavement performance projects. For example, irregularities in observed distresses have also reported in recent studies done by the Wisconsin, Washington, and Iowa Departments of Transportation (Kim *et al.*, 2010). Two possible explanations have been identified: first, minor maintenance may have been applied that was too insignificant to be considered restoration or reconstruction; second, the irregularities may be due to human factors. Given the high degree of control present at the Road Test the latter explanation is most likely in this case.

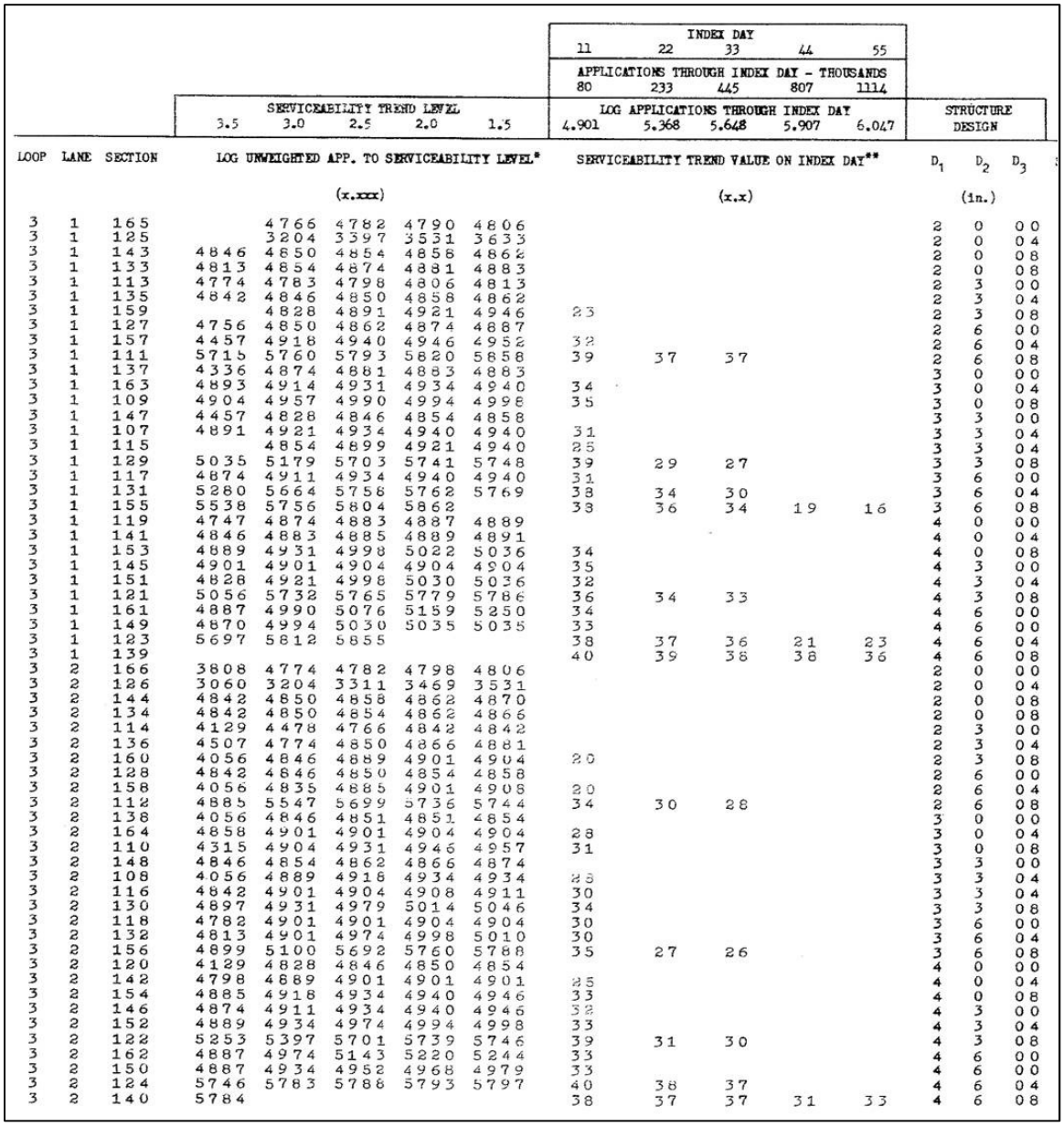

			INDEX DAY									
			11	22	33	44	55					
			APPLICATIONS THROUGH INDEX DAY - THOUSANDS									
			80	233	445	807	1114					
			SERVICEABILITY TREND LEVEL					LOG APPLICATIONS THROUGH INDEX DAY					STRUCTURE DESIGN			
			3.5	3.0	2.5	2.0	1.5	4.901	5.368	5.648	5.907	6.047				
LOOP	LANE	SECTION	LOG UNWEIGHTED APP. TO SERVICEABILITY LEVEL*					SERVICEABILITY TREND VALUE ON INDEX DAY**					D_1	D_2	D_3	
			(x.xxx)					(x.x)					(in.)			
3	1	165		4766	4782	4790	4806						2	0	00	
3	1	125		3204	3397	3531	3633						2	0	04	
3	1	143	4846	4850	4854	4858	4862						2	0	08	
3	1	133	4813	4854	4874	4881	4883						2	0	08	
3	1	113	4774	4783	4798	4806	4813						2	3	00	
3	1	135	4842	4846	4850	4858	4862						2	3	04	
3	1	159		4828	4891	4921	4946	23					2	3	08	
3	1	127	4756	4850	4862	4874	4887						2	6	00	
3	1	157	4457	4918	4940	4946	4952	32					2	6	04	
3	1	111	5715	5760	5793	5820	5858	39	37	37			2	6	08	
3	1	137	4336	4874	4881	4883	4883						3	0	00	
3	1	163	4893	4914	4931	4934	4940	34					3	0	04	
3	1	109	4904	4957	4990	4994	4998	35					3	0	08	
3	1	147	4457	4828	4846	4854	4858						3	3	00	
3	1	107	4891	4921	4934	4940	4940	31					3	3	04	
3	1	115		4854	4899	4921	4940	25					3	3	04	
3	1	129	5035	5179	5703	5741	5748	39	29	27			3	3	08	
3	1	117	4874	4911	4934	4940	4940	31					3	6	00	
3	1	131	5280	5664	5758	5762	5769	38	34	30			3	6	04	
3	1	155	5538	5756	5804	5862		38	36	34	19	16	3	6	08	
3	1	119	4747	4874	4883	4887	4889						4	0	00	
3	1	141	4846	4883	4885	4889	4891						4	0	04	
3	1	153	4889	4931	4998	5022	5036	34					4	0	08	
3	1	145	4901	4901	4904	4904	4904	35					4	3	00	
3	1	151	4828	4921	4998	5030	5036	32					4	3	04	
3	1	121	5056	5732	5765	5779	5786	36	34	33			4	3	08	
3	1	161	4887	4990	5076	5159	5250	34					4	6	00	
3	1	149	4870	4994	5030	5035	5035	33					4	6	00	
3	1	123	5697	5812	5855			38	37	36	21	23	4	6	04	
3	1	139						40	39	38	38	36	4	6	08	
3	2	166	3808	4774	4782	4798	4806						2	0	00	
3	2	126	3060	3204	3311	3469	3531						2	0	04	
3	2	144	4842	4850	4858	4862	4870						2	0	08	
3	2	134	4842	4850	4854	4862	4866						2	0	08	
3	2	114	4129	4478	4766	4842	4842						2	3	00	
3	2	136	4507	4774	4850	4866	4881						2	3	04	
3	2	160	4056	4846	4889	4901	4904	20					2	3	08	
3	2	128	4842	4846	4850	4854	4858						2	6	00	
3	2	158	4056	4835	4885	4901	4908	20					2	6	04	
3	2	112	4885	5547	5699	5736	5744	34	30	28			2	6	08	
3	2	138	4056	4846	4851	4851	4854						3	0	00	
3	2	164	4858	4901	4901	4904	4904	28					3	0	04	
3	2	110	4315	4904	4931	4946	4957	31					3	0	08	
3	2	148	4846	4854	4862	4866	4874						3	3	00	
3	2	108	4056	4889	4916	4934	4934	28					3	3	04	
3	2	116	4842	4901	4904	4908	4911	30					3	3	04	
3	2	130	4897	4931	4979	5014	5046	34					3	3	08	
3	2	118	4782	4901	4901	4904	4904	30					3	6	00	
3	2	132	4813	4901	4974	4998	5010	30					3	6	04	
3	2	156	4899	5100	5692	5760	5788	35	27	26			3	6	08	
3	2	120	4129	4828	4846	4850	4854						4	0	00	
3	2	142	4798	4889	4901	4901	4901	25					4	0	04	
3	2	154	4885	4918	4934	4940	4946	33					4	0	08	
3	2	146	4874	4911	4934	4940	4946	33					4	3	00	
3	2	152	4889	4934	4974	4994	4998	33					4	3	04	
3	2	122	5253	5397	5701	5739	5746	39	31	30			4	3	08	
3	2	162	4887	4974	5143	5220	5244	33					4	6	00	
3	2	150	4887	4934	4952	4968	4979	33					4	6	00	
3	2	124	5746	5783	5788	5793	5797	40	38	37			4	6	04	
3	2	140	5784					38	37	37	31	33	4	6	08	

Figure 3.11: Factorial Experiment – Design 1 Flexible Pavement, Unweighted Applications. (AASHO, 1961)

Excessive rutting was the primary form of distress observed at the Road Test for flexible pavements. A limited amount of measured rutting data was published in Special Report 61E (AASHO, 1961). Rutting for 21 structural sections (42 test sections) is provided in the context of transverse elevation changes at 0, 3, 6, 9, and 12 ft increments from the centerline (CL) starting from July 1959 until March 1960/Oct 1960. Measurements were converted into rut depths for the inner wheel path by taking the

average elevation between the CL and 6 foot readings and subtracting the 3 ft reading, and for the outer wheel path by using the same procedure for the 6, 12, and 9 foot readings respectively (Figure 3.12). Both raw data inputs and calculated rut depths for the 22 test sections over the course of two years are documented in Chapter 5.

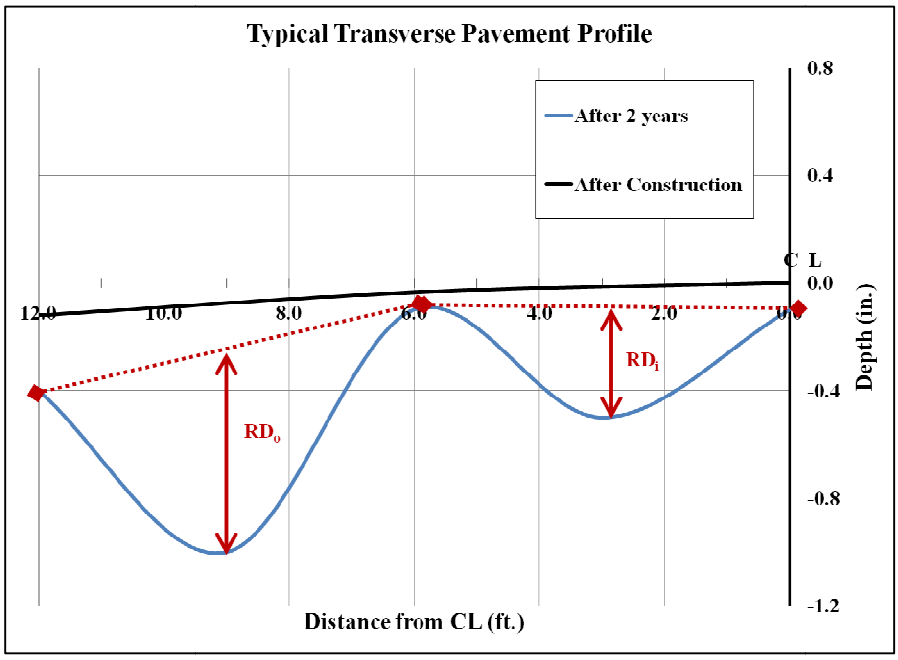

Figure 3.12: Conversion of AASHO Road Test transverse profile measurements to rut depth quantities.

3.1.3 Research Considerations When Using the AASHO Road Test

A preliminary step to this study required gaining an understanding of not only the conditions and available data from the AASHO Road Test, but also an awareness of the range of pavement structural capacity and performance over the 284 flexible pavement sections encompassed in the main factorial design. Furthermore, it is necessary to consider the most efficient way to consolidate and represent the data such that it was usable in evaluating the predictions from the MEPDG and AASHTO design procedures. This section covers aspects of the Road Test that are particularly applicable to this

specific study. Because the materials used at the Road Test were consistent across all the pavement sections, only layer thickness was variable; Structural number (SN) is used as a proxy for structural capacity. Traffic is also considered as equivalent single axle loads (ESALs) to accommodate the different types of truck axles and loads at the Road Test. The use of SN and ESALs normalizes the structural capacity and loads for each pavement section so that data can be compared across loops without bias.

Part of this preliminary study involved evaluating the statistical distribution of failure within the five trafficked loops both in the context of service life (ESALs) and pavement performance (PSI). Note that test sections included in this initial analysis were required to reach failure by the end of two years so that the exact number of ESALs to failure could be computed; failure was defined as a p_t=2.5.

Structural Numbers (SN) approximately follow a normal distribution over a range of 0.44 to 5.66 for the Road Test (Figure 3.13). However, performance is based upon both structural capacity and load. The frequency distribution of service life defined in terms of ESALs to failure reveals that a significant number of sections failed below 200,000 ESALs (Figure 3.14). However, there are no clear trends to explain this observation; early failures are most likely the result of inadequate structural support for the loading configuration in many sections.

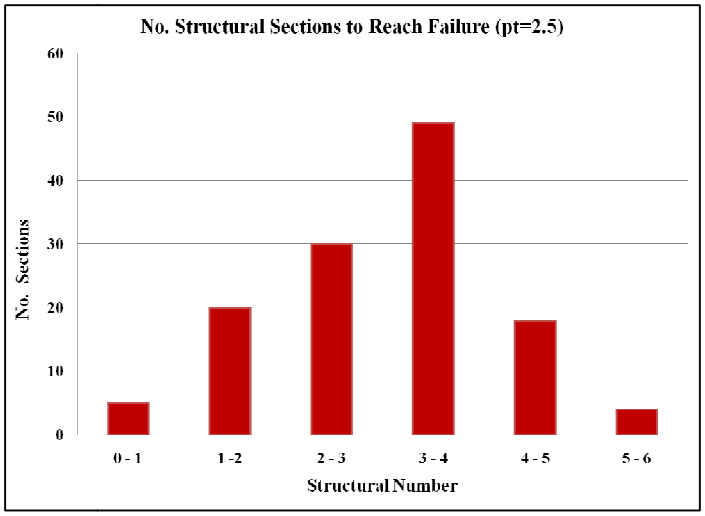

Figure 3.13: Distribution of structural numbers for AASHO test sections that failed (p_t=2.5) within 2 years.

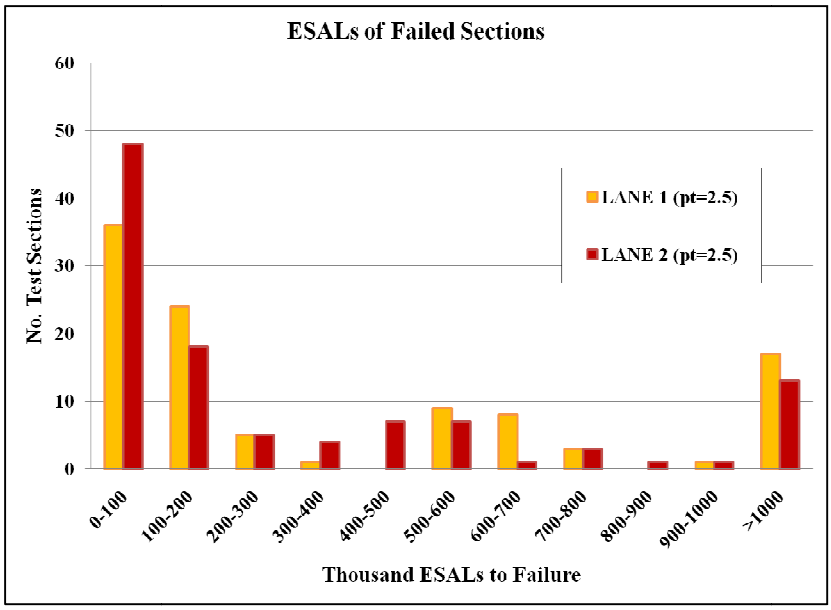

Figure 3.14: Service life distribution for AASHO test sections that failed (p_t=2.5) within 2 years divided by lane.

To explore the relationship between structural capacity and applied load at the AASHO Road Test a statistical distribution approach was employed. Figure 3.15 shows the distribution of SNs within each loop. It is observed that the range of SNs within each loop is approximately 1.7 and, more importantly, the range is consistent. It is known that the applied load increases for each loop and, because the range of SNs does not change significantly but the mean increases slightly for each loop, it can be inferred that there are

both under loaded and overloaded test sections in each loop. Furthermore, considered with the SN distribution in Figure 3.13, Loops 3-5 encompass the majority of pavement sections with a SN between 2.5 and 4.5 and represent the median for loading configurations. This implies that there no bias in structural load or capacity across the loops.

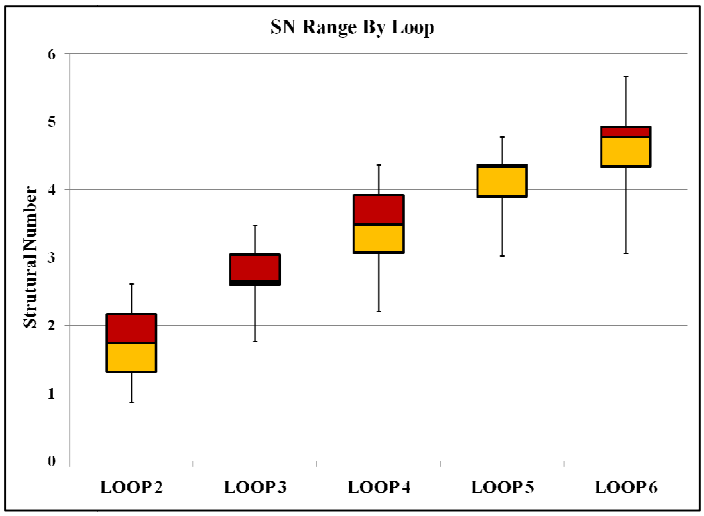

Figure 3.15: Statistical distribution of structural numbers by loop.

However, during the course of analysis, abnormalities between Loop 2 and the rest of the trafficked loops were noticed prompting further investigation. Loop 2 was initially observed to have minimal serviceability deterioration, but this could be considered to represent the lower extreme of the traffic to distress relationship. Figure 3.16 decisively shows that Loop 2 is inconsistent with the rest of the experiment; the load to structural capacity ratio is significantly less than that of the other loops.

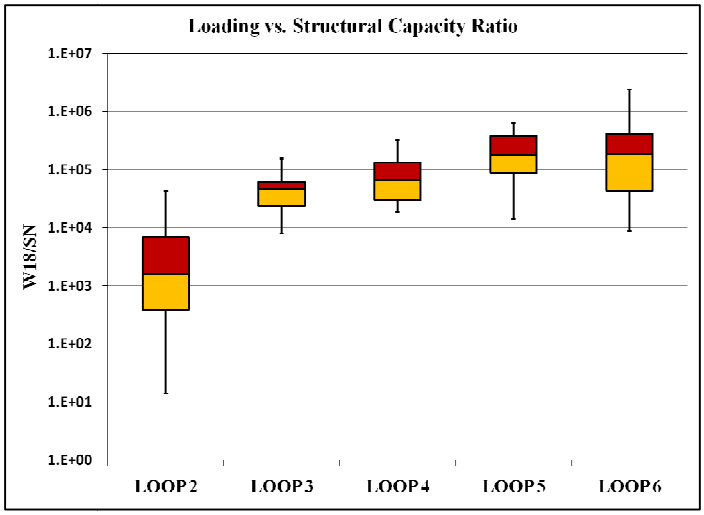

Figure 3.16: Statistical distribution of load to structural capacity ratio for Loops 2-6.

It was observed early in the AASHO Road Test that pavement sections inadequately designed for the applied load deteriorated at a rate that was directly related to seasonal changes. Figure 3.17 shows that the distress accumulation for Loop 2 was not seasonal, but rather the pavement deteriorated at a linear rate. If Loop 2 had a similar load to structural capacity ratio as the other loops, the seasonally influence would manifest as large drops in the mean 50% distribution between February to August 1959 and January to June 1960. Figure 3.18 demonstrates the season-distress rate observation was particularly pronounced in the remaining flexible pavements, where the load to capacity ratios were much higher.

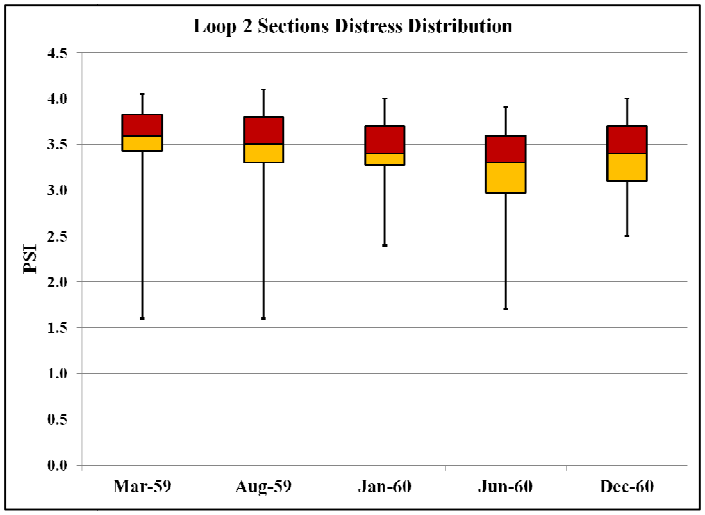

Figure 3.17: Statistical distribution of distress accumulation for Loop 2.

Further examination of the raw AASHO distress histories for selected typical Section IDs (SID) in Figure 3.19 shows three distinct trends typical of the Road Test:

- SID 333 shows a nearly linear decrease in PSI over time
- SID 256 shows a mild decrease in PSI with a large rate of change in the second year, which may be attributed to either an increase in traffic and/or a seasonal influence
- SID 155 shows a distress history with large drops in PSI just after February 1959/1960 and minimal change during the winter months suggesting a significant seasonal influence.

Figure 3.19 presents the data on the same x-axis scale as Figure 3.18. It is clear that while the range of distress accumulation does not vary much over the 2-year experiment, the inter-quartile range (IQR) shows a distinct seasonal influence on the data. PSI decreases significantly in the spring months and stabilizes in the winter months each year. While there are anomalies in the data, the majority of the AASHO Road Test sections follow this seasonal distress trend.

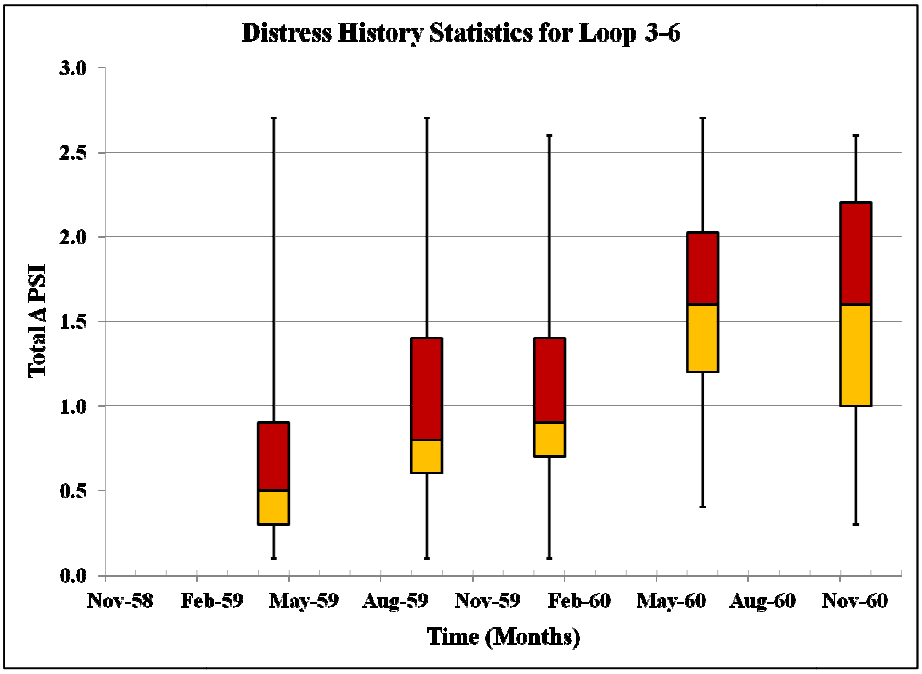

Figure 3.18: Statistical distribution of the change in PSI for Loops 3-6.

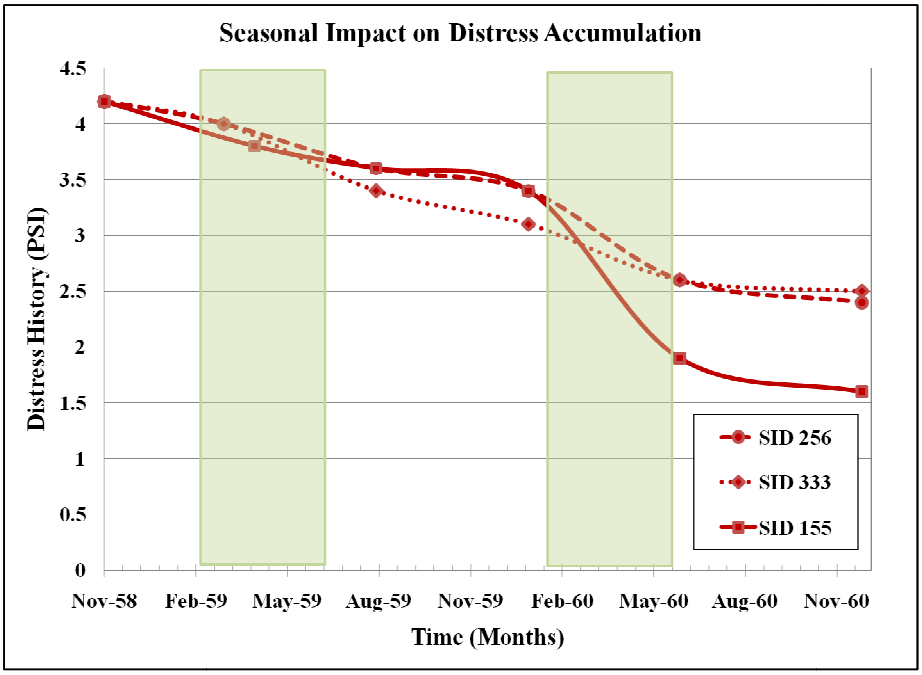

Figure 3.19: Typical AASHO distress histories showing the seasonal influence on distress accumulation.

3.2 AASHTO Guide for Pavement Design (1993)

The results of the AASHO Road Test were used to develop the AASHTO Design Procedure and, though it has gone through multiple editions since its original publication in 1961, modifications have improved but not significantly altered the original methods. Because the AASHTO procedure is an empirical regression between the structural capacity, traffic, and performance observed at the AASHO Road Test, it inherits all the limitations as well; the most glaring of which is that engineers use the AASHTO design procedure for ESALs that are far beyond of those from which it was created. Regardless, the AASHTO procedure has been used in excess of 50 years proving that it is a robust model capable of predicting reasonable pavement structures. However, it is thought to produce excessively thick pavements at the upper traffic range where there is no data to support the model and, in a time when resources are growing more scarce and come at higher prices, it is necessary to optimize the structural design of pavements.

3.2.1 Design Procedure

Two performance measures can be considered in relation to the AASHTO 1993 Design Guide—service life (defined in terms of accumulated traffic) and distress (defined in terms of PSI). The first case utilizes the standard design equation shown below that predicts ESALs to failure. The structural design number (SN) and terminal serviceability decrease (ΔPSI) as recorded from the Road Test are input and accumulated traffic (W_{18}) is output. This case allows comparisons of predicted vs. measured service life (Equation 3.1).

$$\log W_{18} = z_R S_o + 9.36 \log(SN + 1) - 0.20 + \left\{ \frac{\left(\frac{\log(\Delta PSI)}{(4.2-1.5)}\right)}{\left(0.4 + \frac{1094}{(SN+1)^{5.19}}\right)} \right\} + 2.32 \log M_R - 8.07 \qquad (3.1)$$

W_{18} = predicted number of 18kip ESALs
Z_R = standard normal deviate
S_o = standard error
SN = structural number
ΔPSI = difference between the initial (p_o) and terminal (p_t) serviceability
M_R = subgrade resilient modulus (psi)

Variable	Selected Design Values
W_{18}	AASHO measured or predicted
Z_R	0.00
S_o	0.40
$SN = D_1a_1 + D_2a_2m_2 + D_3a_3m_3$	a_1=0.44, a_2=0.14, a_3=0.11 m_2=m_3=1.0
$\Delta PSI = p_o - p_t$	p_o=4.2 p_t as measured or defined
M_R	3,000 psi

The second case considers the predicted terminal serviceability (p_t) under a specified traffic load. This can be achieved by inverting the standard AASHTO 1993 design equation. The recorded AASHO Road Test ESALs are input and the corresponding serviceability is output. This predicted serviceability is compared to the actual value measured at the Road Test. This corresponds to comparing predicted vs. measured distress.

$$p_t = 4.2 + 2.7 * 10^{(\log W_{18} + 0.203 - 9.36 \log(SN+1) - z_R S_o) * (0.4 + (\frac{1094}{(SN+1)^{5.19}})} \qquad (3.2)$$

3.2.2 Application of the AASHTO 1993 Design Procedure

Traffic, Structural Number, initial serviceability, and terminal serviceability are defined by the records of the AASHO Road Test and are cataloged by Section Identification (SID) number in the Flexible Pavement Database. For Case 1 discussed in the previous section, inputs are relatively straightforward—terminal PSI and structural

number come directly for the Road Test records. Subgrade resilient modulus is not directly measured for the Road Test, but can be established based upon material classification, physical properties, and CBR test results.

The A-6 borrow material used to construct the embankment and subbase layer did not drain freely and was highly susceptible to frost heave as was observed in the published rutting data. The California Bearing Ratio (CBR) values reported in Special Report 61B were very low for this clay (AASHO, 1961). Lacking any specific test data for the subgrade resilient modulus (M_R), an average CBR value of 5 corresponding to M_R=5000 psi was used initially. However, this was observed to produce discrepancies between the reported AASHO traffic and the predicted AASHTO 1993 design life as large as 15 million ESALs, especially at higher structural numbers. As previously noted, it was expected that the AASHTO 1993 predictions should agree well with the results of the AASHO Road Test. This was indeed the case after M_R was reduced to 3000 psi; this subgrade stiffness produced close agreement between the actual traffic from the road test and the predicted ESALs from the AASHTO 1993 design procedure (Figure 3.20).

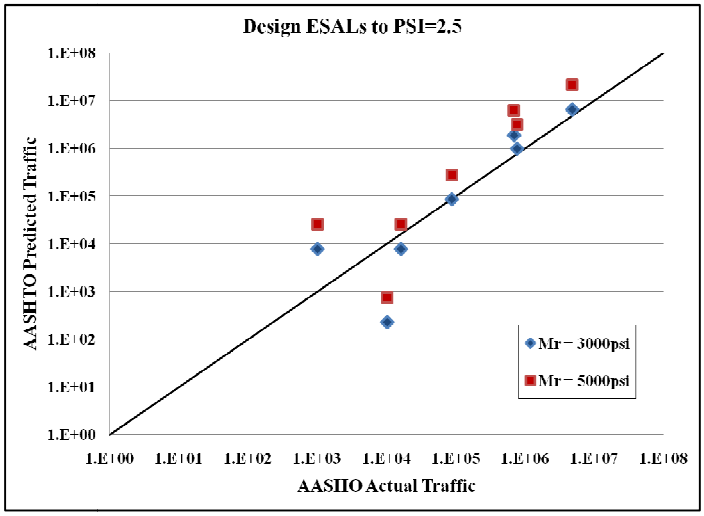

Figure 3.20: Influence of subgrade resilient modulus on predicted service life.

Moreover, if the subgrade resilient modulus is assigned a value of 3000 psi, the last two terms of the AASHTO design equation (Equation 3.1) resolve to zero and yield the original 1961 design equation.

For Case 2 both the inputs and outputs require some additional work to prepare. In this case, where pavement distress is the performance measure, inputs include the AASHO traffic and SN. Because traffic at the Road Test was recorded as axle applications it must be converted to ESALs for use in the AASHTO 1993 design equation either by use of Truck Factors or Equivalent Axle Load Factors (EALF). Based on application to the database, EALFs were the chosen method to avoid the need to looking up individual truck factors for every load combination (Equation 3.3

$$EALF = \log\left(\frac{W_{tx}}{W_{t18}}\right) = 4.79\log(18+1) - 4.79\log(L_x + L_2) + 4.33\log L_2 + \frac{G_t}{\beta_x} - \frac{G_t}{\beta_{18}} \quad (3.3)$$

). (Huang, 1993)

$$EALF = \log\left(\frac{W_{tx}}{W_{t18}}\right) = 4.79\log(18+1) - 4.79\log(L_x + L_2) + 4.33\log L_2 + \frac{G_t}{\beta_x} - \frac{G_t}{\beta_{18}} \quad (3.3)$$

Where:

W_{tx}	=	number of axles application at time t
W_{t18}	=	number of 18-kip single-axle applications at time t
L_x	=	load (kips) on one single, tandem, or tridem axle
L_2	=	axle code (1 for single, 2 for tandem, etc)
SN	=	structural number
p_t	=	terminal serviceability
G_t	=	$\log\left(\frac{4.2-p_t}{4.2-1.5}\right)$
β_x	=	$0.40 + \left\{\frac{(0.08(L_x+L_2)^{3.23})}{(SN+1)^{5.19}(L_2{}^{3.23})}\right\}$
β_{18}	=	β_x; L_x=18, L_2=1

All variables are known except for the W_{t18} (ESALs). The equation can be rearranged to yield the desired value. Once AASHO traffic has been converted into ESALs, it can be plugged into Equation 3.2 to yield a predicted PSI. However, it is

important to note that when the AASHTO 1993 design procedure is used in the inverted form (Case 2), it is not capable of handling pavement sections with low structural numbers. For any given traffic level, the left side of Equation 3.2 goes to infinity as the SN is decreased. Therefore, there is a theoretical limiting SN for each traffic configuration, as indicated in Figure 3.21.

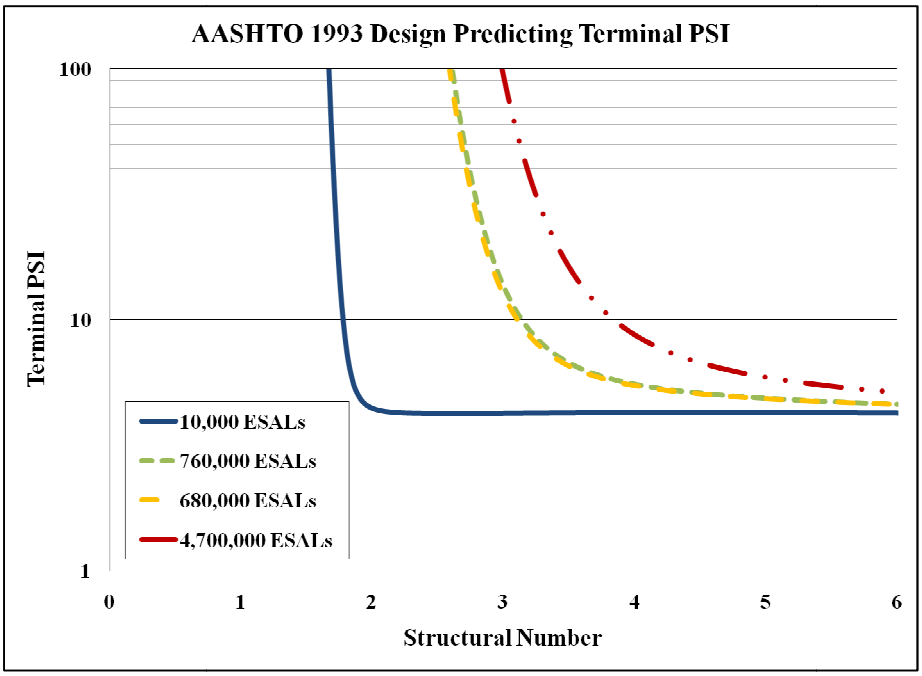

Figure 3.21: Limiting PSI for a given structural number and traffic configuration.

3.3 Mechanistic-Empirical Pavement Design Guide

First released in 2002 and currently on version 1.1 (released 2009), MEPDG was created in recognition of the limitations of AASHTO design procedure. The nationally calibrated pavement performance models are based on historical data from the Long-Term Pavement Performance (LTPP) program. The most notable changes from the AASHTO 1993 Design Procedure include:

- Incorporation of environmental parameters;

- Structural credit for superior construction materials and methods via their resilient modulus values as opposed to generic structural coefficients (a_1=0.44, a_2=0.14, a_3=0.11);
- Use of load spectra and volume distribution as opposed to ESALs;
- Use of mechanistic analyses to determine critical stress, strain, and deflections induced in a pavement by a given load magnitude and configuration;
- Prediction of individual distresses instead of a composite serviceability parameter.

The empirical part of the MEPDG relates calculated stress and strains to observed distresses accumulated over the design life. MEPDG is not a direct design method, rather it provides a prediction of pavement performance. The user must iterate to an economical structure that provides adequate performance.

3.3.1 Design Procedure

MEPDG v1.1 (national calibration) is used in this study. The AASHO Road Test sections are modeled as accurately as possible from information available in the research reports. Where data is unavailable the MEPDG Level 3 defaults are used instead.

Each *project name* uses the following format:

L5 . D5-6-8 . No469 . SN3.dpg

Where 'L' designates loop, 'D' is the layer thickness of AC-Base-Subbase respectively, 'No' is the Section Identification (SID) number, and 'SN' is the structural number rounded to the nearest integer. Accordingly, the example file name is AASHO Road Test section 469 from Loop 5 which is 5 inches of asphalt over 6 inches of base material

underlain by 8 inches of compacted subgrade that accounts for a total structural number of approximately 3.

All projects are analyzed for a *design life* of 2 years unless otherwise noted (UON) and construction phasing (i.e. *base/subbase construction, pavement construction, and traffic open*), though loop-dependant, is roughly August 1958, September 1958, and November 1958 respectively. The *type of design* is by definition flexible pavement.

The *default analysis parameters* are used, however an *initial IRI* of 45 in/mi is chosen (UON) instead of 63 in/mi because the existing PSI vs. IRI models suggest this to be a more equivalent representation of a 4.2 serviceability index. This change was important for comparative analyses that related PSI to IRI and, as will be discussed more fully in a subsequent chapter, it was observed the Al-Omari and Darter (1994) model fit the AASHO Road Test data better using a lower initial IRI. Moreover, initial IRI is not relevant in subsequent analyses, which were based solely on distresses, so there was no bias introduced to the other regression models in doing so.

Traffic is modeled with an *initial two-way AADTT* of 509 and a *linear traffic growth* of 99.9% at the end of each year. The traffic is constrained to 1 *lane* that services 100% of the trucks operating at a *design speed* of 30 mph. The *monthly traffic volume adjustment factors* are set to equal 1.0 (UON), however the *axle load distribution factors* are variable based on loop and lane. Site-specific Level 1 data is input to exactly model the traffic for each loop. The truck types used at the Road Test are detailed in Figure 3.22 below. MEPDG also accommodates seasonal truck traffic with monthly adjustment factors. These were all assigned 100% (i.e. axles carry 100% of the total assigned load every month). *Lateral traffic wander, axle configuration, and wheelbase* were set to the

Level 3 defaults. However, the *number of axles/truck* is specified as 3 single axles for Class 8 trucks and 1 single axle and 2 tandem axles for Class 9 trucks.

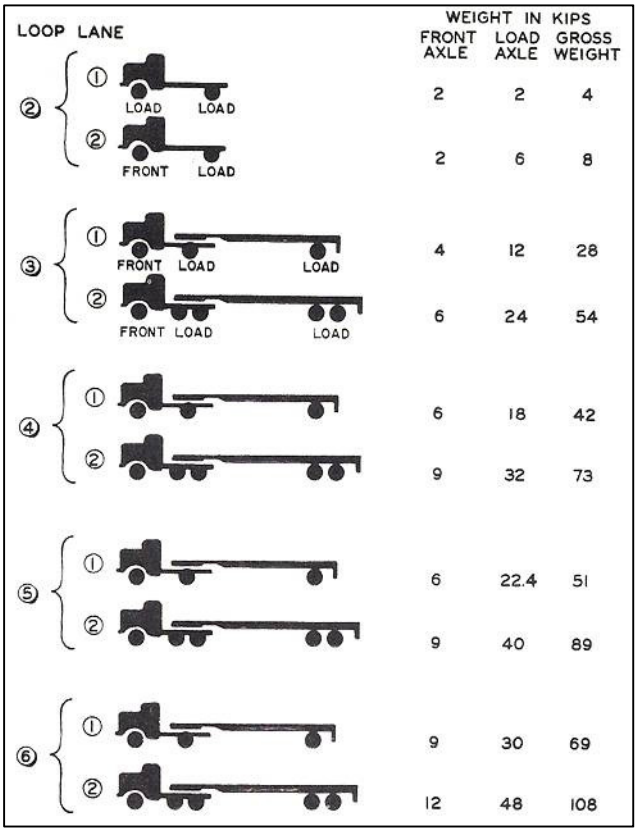

Figure 3.22: AASHO traffic configuration. (AASHO, 1961)

Climatic data is generated based on latitude of 41 degrees 20 minutes, longitude of -88 degrees 50 minutes, an elevation of 610 feet, and average annual water table depth of 20 feet. The MEPDG default weather stations are detailed in Table 3.1.

Table 3.1: Weather stations details.

Name	Distance (mi)	Lat.	Long.	El. (ft)
Aurora Municipal Airport	35.0	41.46	-88.9	709
Dupage Airport	50.3	41.55	-88.15	758
Greater Rockford Airport	61.2	42.12	-88.05	731
Greater Peoria Rgnl. Airport	63.9	40.4	-89.41	716
Chicago Midway Intl. Airport	64.0	41.47	-87.45	619
O'Hare Intl. Airport	65.2	41.59	-87.55	658

Project structures contain a maximum of 5 layers. *Asphalt material properties* are defined as level 3 using the actual mix gradation as noted in Figure 3.23 with a Pen

85-100 binder grade and MEPDG default gravimetric and volumetric properties, which were a close match to the conditions at the Road Test. *Base and Subbase material properties* are defined by level 2 inputs using an AASHTO classification of A-1-a and A-1-b, a modulus of 30,600 psi and 15,200 psi, and ICM specifications as noted in Figure 3.24 and Figure 3.25. Two *subgrade layers* are defined for all project structures: the first represents the compacted embankment each loop was built upon and the second is the uncompacted foundation soils. Excluding compaction, these two layers are identically defined as A-6 soils with a modulus of 3,000 psi (restricted to be a representative design value) and ICM specifications as noted in Figure 3.26.

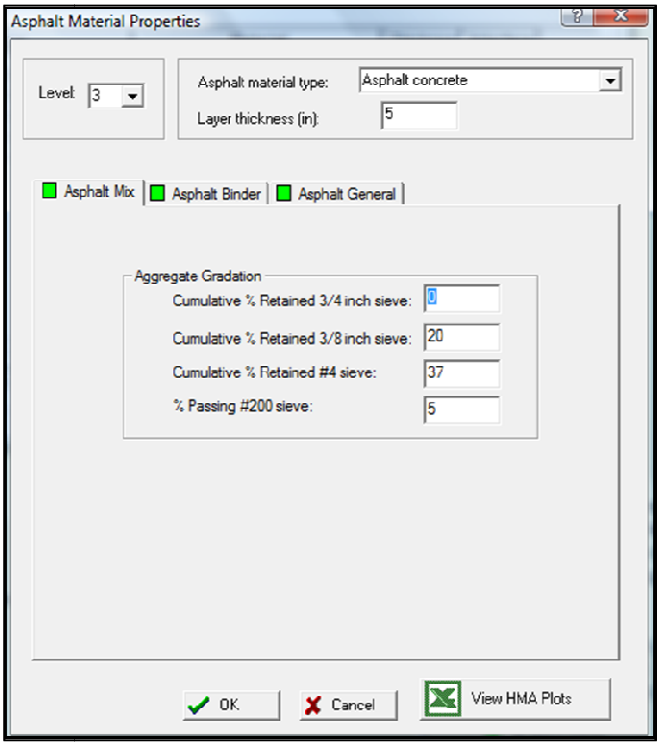

Figure 3.23: AC material inputs.

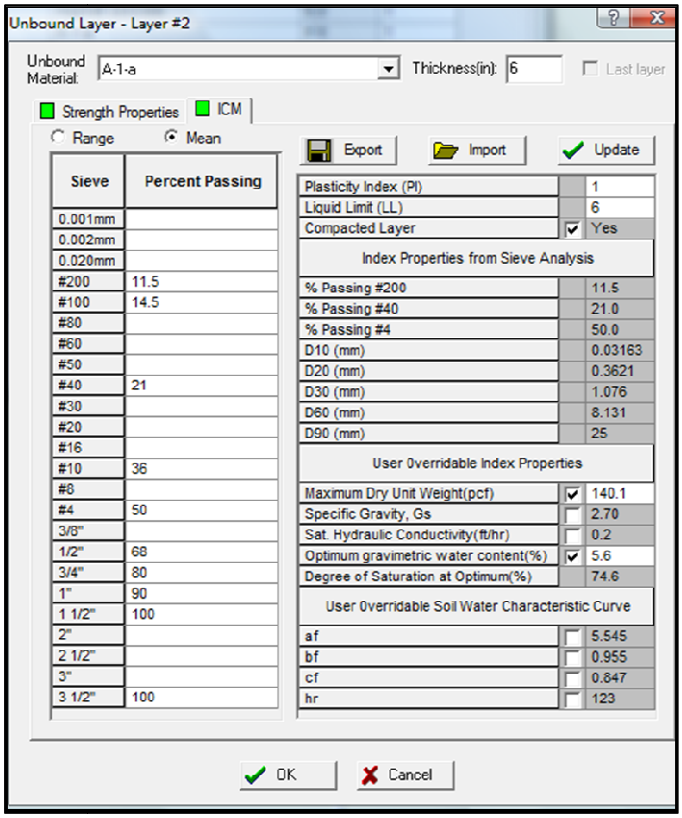

Figure 3.24: Base material inputs.

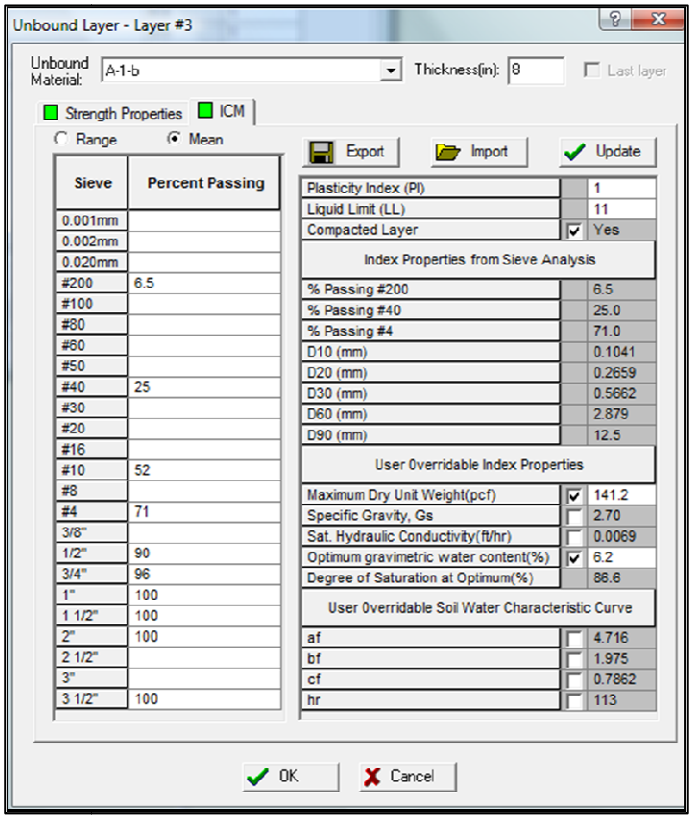

Figure 3.25: Subbase material inputs.

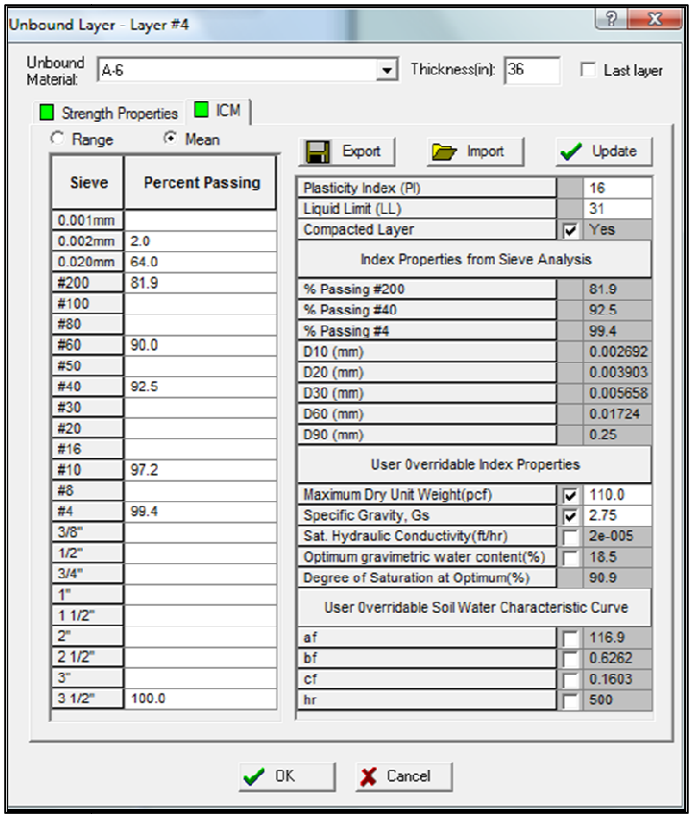

Figure 3.26: Subgrade material inputs.

3.3.2 Application of the MEPDG

The AASHO Road Test traffic did not progress in a linear fashion over the course of 2 years, but rather accumulated at an approximate rate of 513 trucks/day for the first year and then more than doubled to a rate of 1,190 trucks/day for the second year. Additionally, as previously discussed, there is a seasonal influence on distress accumulation; meaning that there are two variables that directly control pavement deterioration fluctuating at the same time. In order to compare the design procedures over the entirety of each distress history it was necessary to align the traffic and climate models for the MEPDG.

For the pilot study discussed in Chapter 4, a baseline traffic model (AADTT = 763, G=0) was used. This results in MEPDG having bias towards over-predicting distress at early times, when the actual AADDTT=512, and under-predicting at later

times (AADTT=1,190). Figure 3.27 shows the traffic models, particularly important is the rate or axle accumulations, i.e. the slope of the lines. This was acceptable for the pilot study because only distress rates at the end of two years were considered and the bias canceled out.

However, analysis of the complete AASHO Road Test distress histories makes it essential to model the actual applied traffic rates more accurately in the MEPDG. The monthly traffic adjustment factors in the MEDPG cannot be used for this purpose, as they can only be specified for a one year duration and are then repeated for all subsequent years. The traffic growth option can be employed, but unfortunately the MEPDG limits traffic growth to yearly increments and the annual growth rate to less than 100%. Given these constraints, the actual AASHO traffic can best be modeled with an annually adjusted traffic model having an initial AADTT = 509 and a linear growth rate = 99.9% as depicted in Figure 3.27 by the green line. This model approximates the rate of traffic very closely; it leads the actual traffic (i.e., predicts a given traffic volume earlier than actually occurs) by a variable shift that is most pronounced between June 1958 and November 1960 but is never more than a 3-month difference.

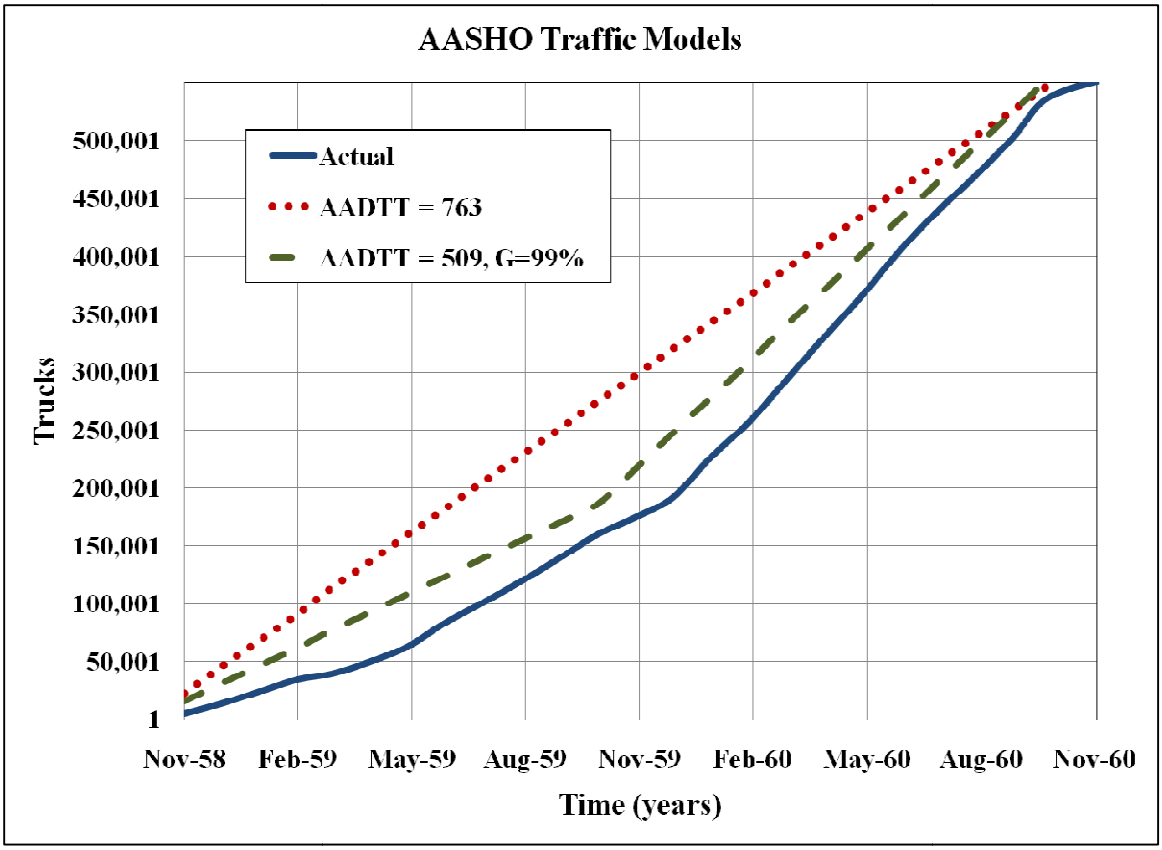

Figure 3.27: MEPDG traffic models vs. actual traffic at the AASHO Road Test.

To determine the significance of this time shift, as well as the practical differences between these two models and the actual AASHO traffic, six sections were chosen at random and analyzed for 1 year. Analyzing for only one year permits use of the monthly traffic adjustment factors in the MEPDG to simulate more closely the actual conditions of the Road Test. The first year predictions using the monthly-adjusted traffic rates can be compared to the predictions from the other two traffic models to determine if the time shift is significant. As shown in Figure 3.28, the time shift in the annually adjusted traffic model produces a slight bias toward over-predicting distresses. Figure 3.28 also shows that IRI and rut depth are least affected by the time shift. However, the *rate* of distress accumulation is nearly identical for all modes of failure, so the annually adjusted traffic model with AADTT=509, G=99.9% is considered acceptable.

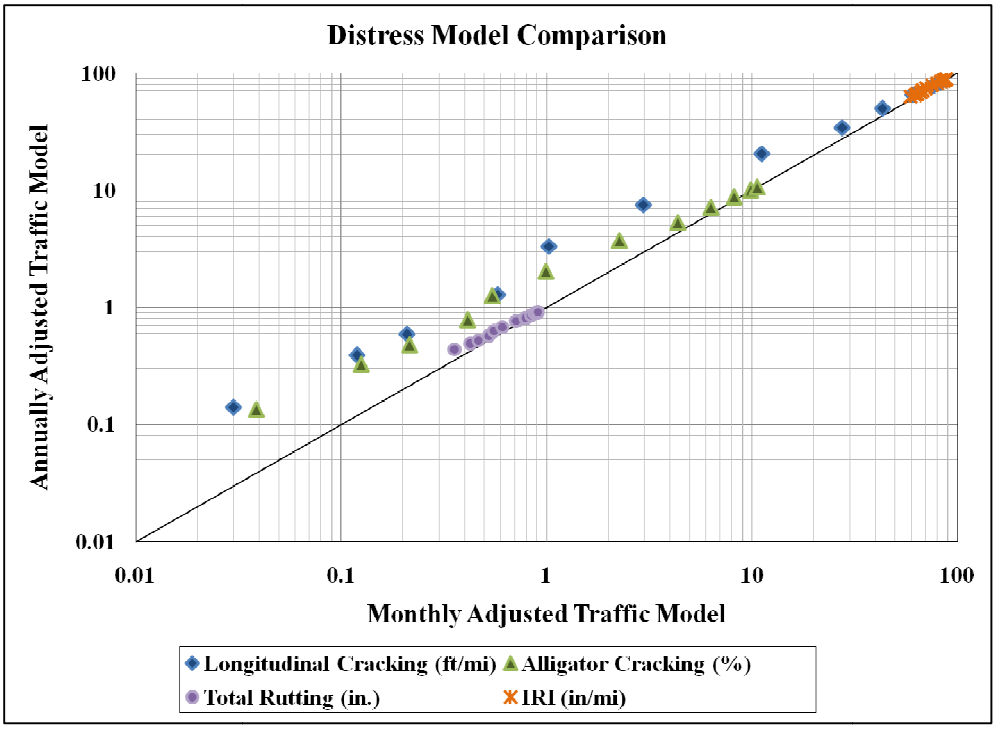

Figure 3.28: Effect of traffic model on MEPDG predicted distresses.

There are several factors to consider during the final year of the Road Test. Figure 3.27 shows that beginning around January 1960 there is a significant increase in the rate of axle applications. However, there is no additional pavement distress until the March when PSI decreases by an average of 0.5 (see Figure 3.18). Although the rate of traffic continues, distress accumulation is once again arrested in September 1960. This observation further suggests that distress accumulation in the AASHO Road Test was highly seasonal.

3.4 Rigid Pavements

As mentioned, the Road Test loops were composed of both flexible and rigid tangents. The experimental details for rigid pavements are summarized in Figure 3.30. However, rigid pavements are not included in this study because there was no significant deterioration observed in ride quality (PSI) over the two years (Figure 3.29). Because only a handful of pavements deteriorated to a PSI less than 4.0 there is no way to use serviceability as a performance measure.

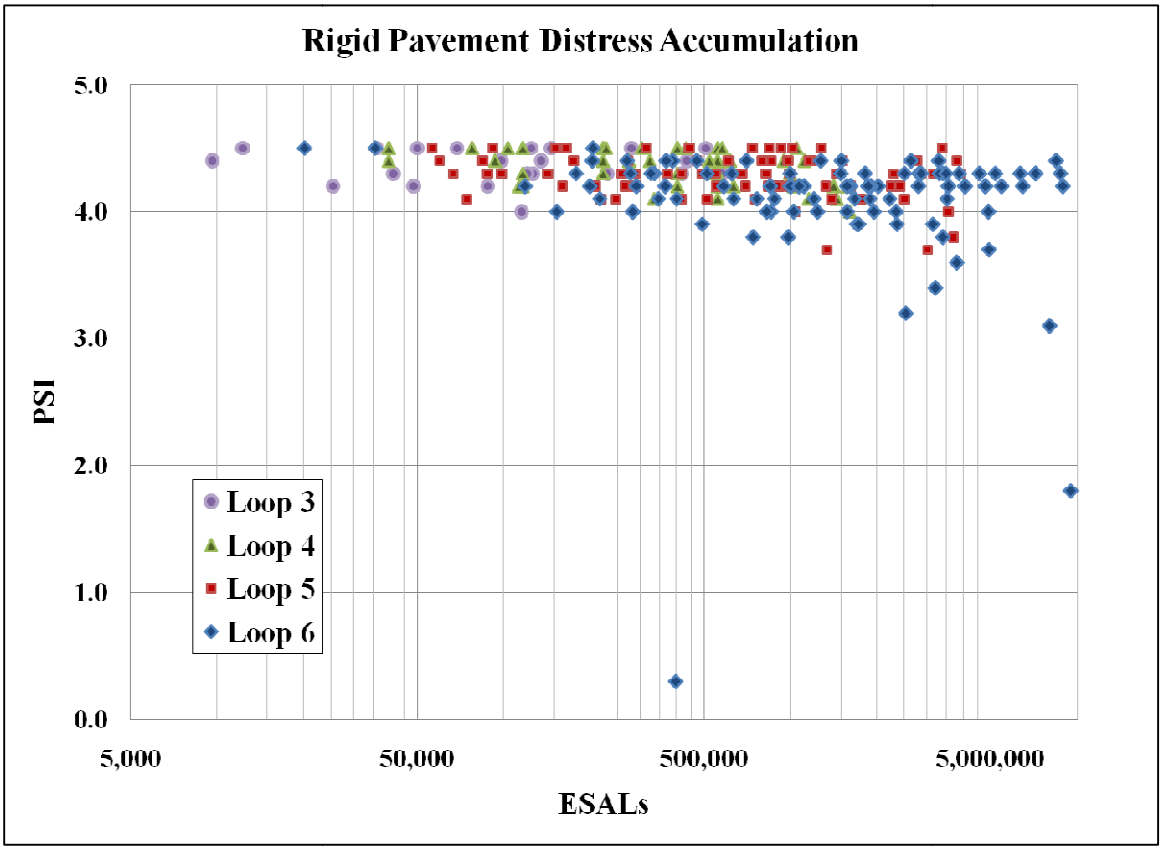

Figure 3.29: Rigid pavement distress accumulation.

However, while ride quality did not decrease there was still a significant amount of cracking and "pumping" observed at the Road Test as Figure 3.31 shows. The Highway Research Board Special Report 61E details the pavement research program

(AASHO, 1961). Published therein are distress records for Cracking Index and Pumping Index.

The Cracking Index (C*) was computed by totaling all the crack lengths in a given section and dividing by the area of the pavement; the recorded index was in units of projected cracks per 1,000 square feet. The Pumping Index (P*) was a measure of the volume of unbound material ejected per unit length of pavement; it was computed as cubic inches of material averaged over the length of the test section in inches.

The cracking and pumping indices are empirically correlated to PSI, thus theoretically it may be possible to use C* and P* to develop a relationship between MEPDG predicted and AASHO measured distresses. However, the average value of C* at a theoretical PSI=1.5 was 168 with a standard deviation of 71. For P* a mean value of 134 was correlated with a PSI=1.5, but there was "not a clear-cut definition of the value of the pumping index associated with serviceability…one section failed with a P*=5 while another survived with a P*=209," (AASHO, 1961). These measures of serviceability unfortunately have the opposite issue of the PSI records, they are too variable.

Furthermore, it is ill-advised to attempt to correlate poorly defined measured distresses to predicted ones. The cracking index is well defined using crack classifications, but the pumping index is misleading. Pumping is generally accepted as instability in the unbound layers due to saturation that causes a loss in structural support and may lead to fatigue cracking. However, the 'pumping' at the AASHO Road Test does not fit this description. It is noted in the reports that 'pumping' was observed particularly after rain events and in some cases as much as 3 cubic yards of material was

ejected from under one 40 foot panel overnight (AASHO, 1961). Trench studies showed that the unbound material left under rigid pavements was not overly saturated or disturbed in anyway. The loss of material from under the slabs at the Road Test is better described as erosion. It is noted in the report that the base material was not stabilized properly. Rain likely seeped under the slab and washed the top layers of unbound material out as axle loads were applied to the pavement. Moreover, it was noted that had there not been a loss of base support there would have been minimal failures in the rigid tangents. (AASHO, 1961)

Because the performance measures are poorly defined it was decided to exclude analysis of rigid pavements from this study.

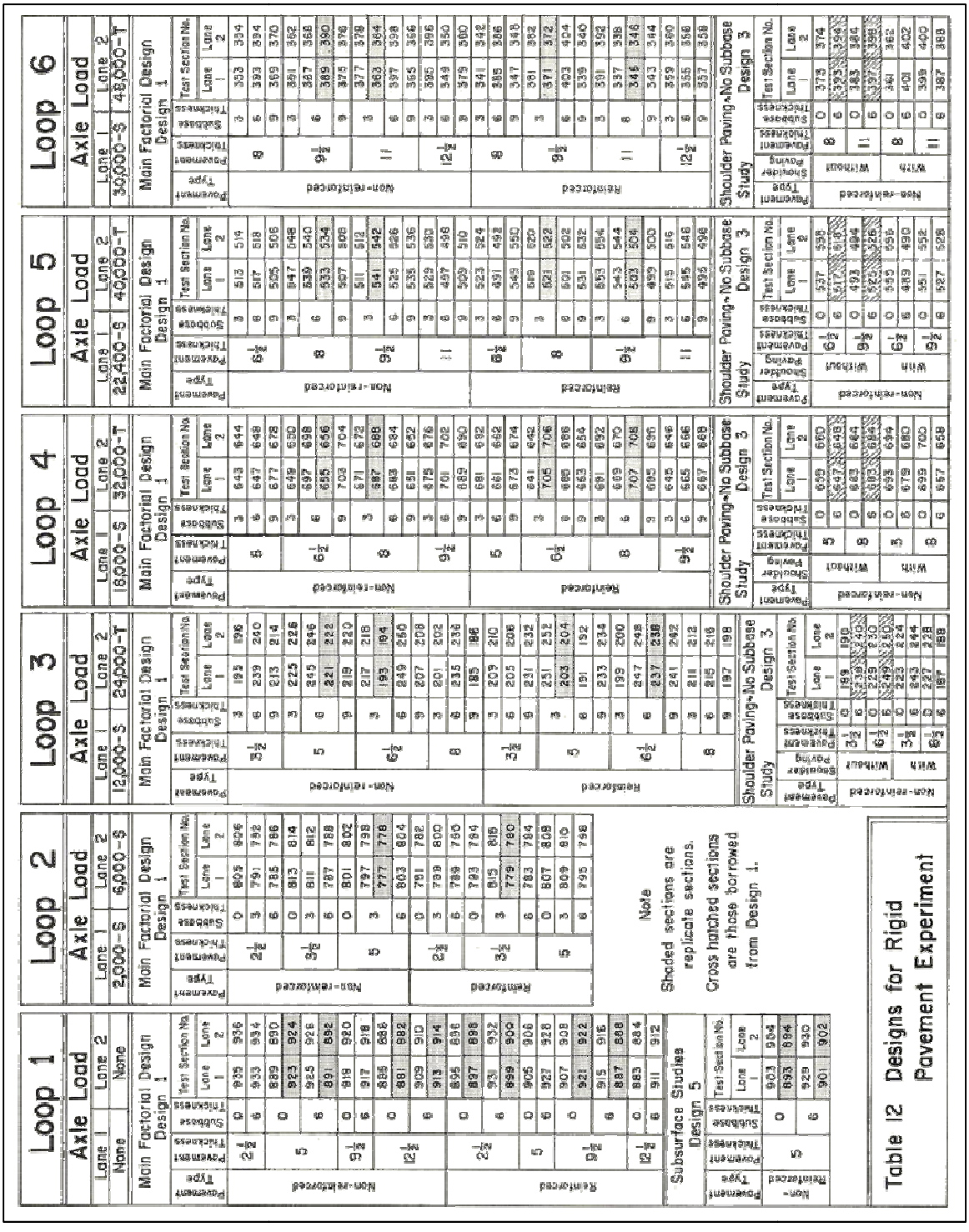

Figure 3.30: AASHO Road Test Table 12 - Rigid Pavement Experiment. (AASHO, 1961)

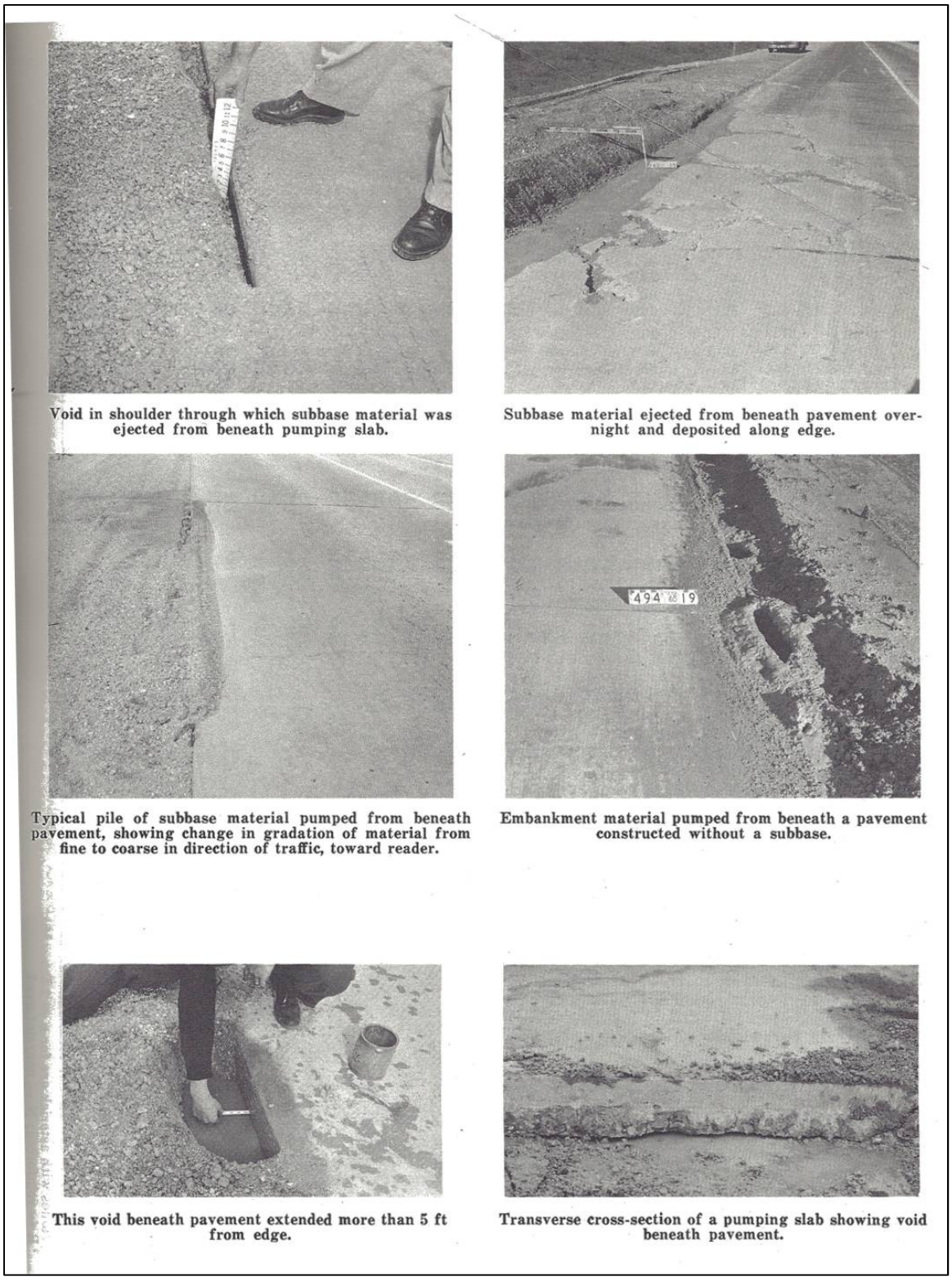

Void in shoulder through which subbase material was ejected from beneath pumping slab.

Subbase material ejected from beneath pavement overnight and deposited along edge.

Typical pile of subbase material pumped from beneath pavement, showing change in gradation of material from fine to coarse in direction of traffic, toward reader.

Embankment material pumped from beneath a pavement constructed without a subbase.

This void beneath pavement extended more than 5 ft from edge.

Transverse cross-section of a pumping slab showing void beneath pavement.

Figure 3.31: Rigid Pavement distress types. Loss of subgrade ("Pumping") caused significant problems. (AASHO, 1961)

Chapter 4: Pilot Study

4.1 Objective

The pilot study addressed whether the AASHO Road Test was a useful baseline in the comparison between the AASHTO 1993 and MEPDG procedures using PSI as a measure of performance. The AASHTO 1993 procedure was derived directly from, and characterizes pavement performance in the same terms as, the Road Test (PSI). Therefore, it was expected that these predictions would correspond well with the actual experiments.

The usual criticisms of the AASHTO 1993 design (performance based on one location, one environment, one set of materials, limited test duration, outdated construction practices and traffic loads) were instead benefits in this study. The high degree of control over the materials, climate, design details, and traffic allowed for more robust inputs to the MEPDG. This was expected to aid the initial effort in understanding the major practical differences between the current design procedures and the MEPDG.

The principal limitation of using the AASHO Road Test in this comparison is that performance was evaluated in terms of the semi-qualitative PSI index, while the MEDPG predicts performance in terms of individual distresses and a composite roughness measure IRI. Part of the pilot study was dedicated to evaluating the most commonly accepted relationships between PSI and IRI.

4.2 Methodology

Several sections were chosen at random to represent the full structural range of the Road Test. The study was conducted in two phases. Phase I was a small exploratory study that evaluated seven random AASHO Road Test sections spanning the full range of

structural numbers (0.88-5.22). Phase II expanded upon this by evaluating every section from Lane 1 in Loop 4 (18-kip single axle traffic). This traffic configuration eliminated the need to convert between trucks and ESALs. The same methodology was used in both phases. Table 4.1 below gives the details for all structural sections included in the study.

Table 4.1: Characteristics of AASHO Road Test sections studied in the pilot study.

LOOP	F-BLOCK	SECTION ID	THICKNESS			SN
			SURFACE	BASE	SUB-BASE	
3	1	165	2	0	0	0.88
3	1	163	3	0	4	1.76
4	1	633	3	0	4	1.76
4	2	607	3	0	8	2.20
4	3	571	3	0	12	2.64
4	2	599	3	3	4	2.18
4	3	573	3	3	8	2.62
4	1	617	3	3	12	3.06
4	3	585	3	6	4	2.60
4	1	623	3	6	8	3.04
4	2	601	3	6	12	3.48
4	3	583	4	0	4	2.20
4	1	619	4	0	8	2.64
4	2	603	4	0	12	3.08
4	1	627	4	3	4	2.62
4	2	589	4	3	8	3.06
4	3	575	4	3	12	3.50
4	2	595	4	6	4	3.04
4	3	577	4	6	8	3.48
4	1	625	4	6	12	3.92
4	2	605	5	0	4	2.64
4	3	587	5	0	8	3.08
4	1	621	5	0	12	3.52
4	3	579	5	3	4	3.06
4	1	631	5	3	8	3.50
4	2	593	5	3	12	3.94
4	1	629	5	6	4	3.48
4	2	591	5	6	8	3.92
4	3	581	5	6	12	4.36
6	2	297	6	3	8	3.94
6	1	325	6	6	8	4.36
6	2	311	6	9	12	5.22

The structural sections used represent the full range of structural numbers, layer thicknesses, and single axle loading conditions used in the AASHO Road Test as nearly as possible (Table 4.1). Structural Number (SN) and Equivalent Single Axle Loads (ESLAs) were used as a proxy for structural capacity and traffic respectively in this Pilot Study. Doing so normalized the structural capacity and loads for each pavement section, meaning data could be compared across lanes and loops without bias. Several problems were encountered during Phase I of the study that had to be addressed before progress could continue—material inputs being chief among these. Chapter 3 details the selected values for both AASHTO 1993 and the MEPDG procedures and provides supporting evidence.

The AAHSO Road Test, AASHTO 1993, and MEPDG design procedures were compared using PSI as a performance measure. Two cases were considered representing evaluation based on pavement performance and design life (Chapter 3):

- Input the reported AASHO traffic at failure (p_t=2.5) and compare the predicted terminal serviceability from AASHTO 1993 and MEPDG;
- Compare the predicted ESALs to failure from the AASHTO 1993 and MEPDG procedures against the corresponding reported traffic from the AASHO Road Test.

The principal limitation of this method was that AASHO and AASHTO evaluate performance in terms of the semi-qualitative PSI index, while the MEDPG predicts performance in terms of individual distresses and a composite roughness measure IRI. This was addressed using an empirical model proposed by Al-Omari and Darter (1994) which coverts IRI to PSI (Equation 4.1). Of the available options, the Al-Omari and

Darter model was chosen because it was derived from conditions that most nearly apply to the conditions of the Road Test.

$$PSI = 5 * e^{(-0.0041*IRI)} \quad (4.1)$$

For the first evaluation case, the actual AASHO Road Test traffic was used as an input to the MEPDG and the predicted IRI at the end of 2 years was converted to PSI for comparison against the AASHO p_t=2.5 and the AASHTO 1993 results. The second case required specifying the terminal PSI. As this is not a direct input to the MEPDG, an iterative process was used instead. Each section was run multiple times with an increasing Average Annual Daily Truck Traffic (AADTT) until an IRI=169 in/mile corresponding to p_t=2.5 based on the Al-Omari and Darter model was achieved at the end of 2 years. The AADTT to achieve that terminal serviceability was then converted to total ESALs.

4.3 Significant Findings

The relationships observed in the first stage of the pilot study ultimately were substantiated by the second, larger, stage and the two are therefore discussed together.

4.3.1 Case 1: Comparisons based on predicted distress

For Case 1 the dependant variable is terminal PSI and Figure 4.1 shows the results. The MEPDG was found to consistently over-predict the terminal serviceability (i.e., under predicts pavement deterioration) of the pavement sections. This is consistent with the findings of other studies that conclude the MEPDG often predicts thinner pavement sections for a given design life. However, the agreement between the

AASHTO 1993 predictions and AASHO Road Test measurements were more variable than expected.

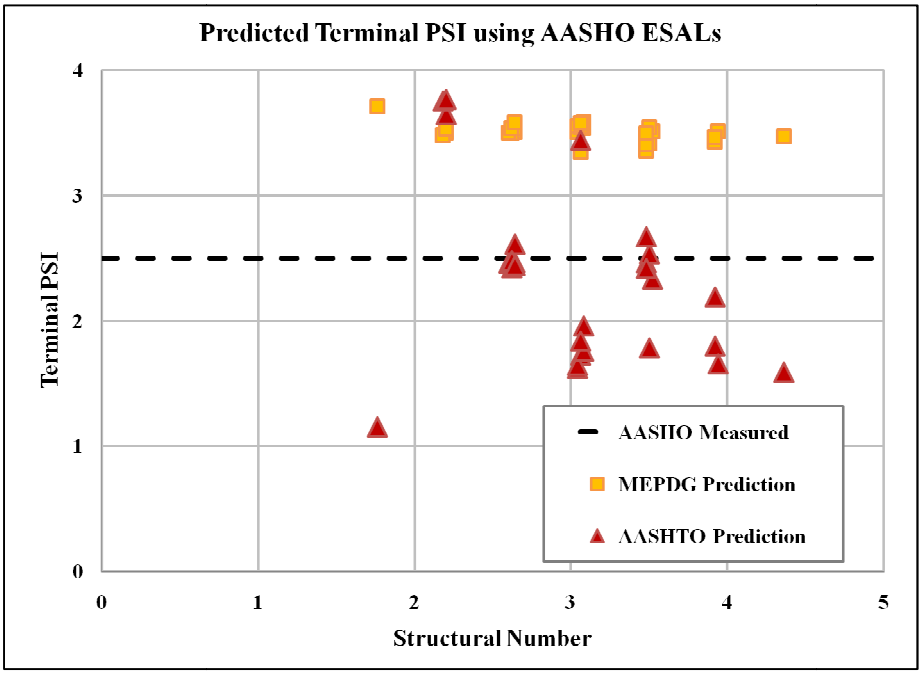

Figure 4.1: Prediction PSI using AASHO Road Test traffic that corresponds to p_t=2.5. (Case 1)

Figure 4.2 offers some insight towards understanding the discrepancies between AASHO measured and AASHTO predicted performance. This graph shows the AASHTO 1993 predicted PSI vs. traffic for various structural numbers and the AASHO Road Test measurements (PSI vs. actual 18-kip axle data) for six structural sections. The sections were chosen randomly but were required to have a minimum of six distress records and the same structural number as the AASHTO model they are compared against (Table 4.2). The AASHTO model for each SN approximates a best-fit-line for the corresponding AASHO measured data with reasonable accuracy given that the models were derived from much more data than what is plotted below. Note the initial PSI is taken to be 4.2 (IRI=42.5) as this corresponds with conventional methods and the AASHTO model is not equipped to handle PSI greater than 4.2.

Table 4.2: AASHO section data corresponding with Figure 4.2.

Structural Number		1.3	3.1	4.8
Section ID	'A'	755	121	309
	'B'	729	122	328

Immediately evident is the dramatic drop-off in the measured PSI vs. ESALs in the AASHO measured data. The drop-off in PSI is also pronounced in the AASHTO 1993 predictions, but less so than for the AASHO Road Test measurements. However, as mentioned above, the AASHTO models were derived from much more data then what is published and available for this study. For instance, the first index day, and thus plotted points in Figure 4.2, start from the 22nd week of the Road Test. It is reasonable to infer that the complete distress histories, with performance data every 2 weeks, would fit the AASHTO model forms well. The steepness in the PSI vs. ESAL model form is responsible for the variability between the AASHO measured terminal PSI values and AASHTO 1993 predictions (Figure 4.1); very small changes in traffic will cause very large changes in terminal PSI.

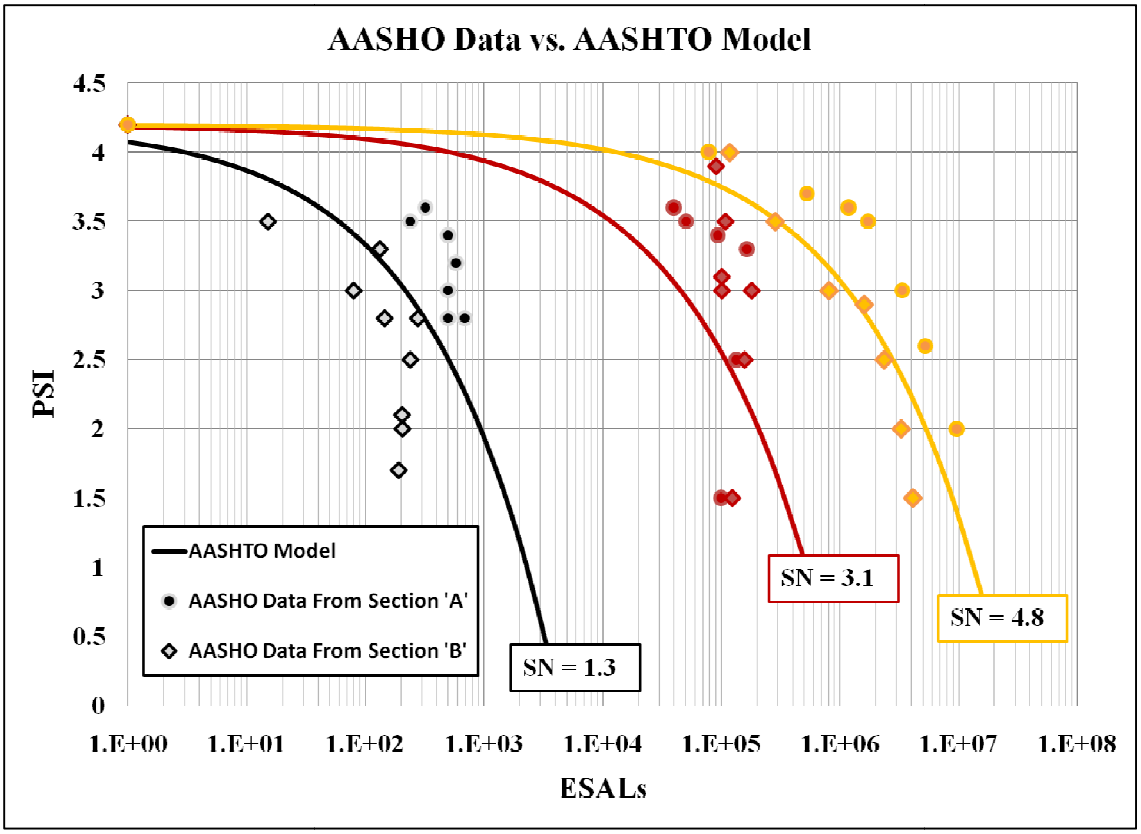

Figure 4.2: AASHTO 1993 design model and AASHO Road Test historical performance.

4.3.2 Case 2: Comparing based on predicted design life

For the second case, terminal serviceability is treated as an independent variable and maintained at 2.5 while the predicted ESALs from AASHTO 1993 and MEPDG required to reach failure are the dependant variable. The design predictions are compared against the measured traffic from the AASHO Road Test. Based on the previous case, the MEPDG is expected to overestimate the volume of traffic required to reach failure (p_t=2.5), and the results confirmed this to be the case (Figure 4.3).

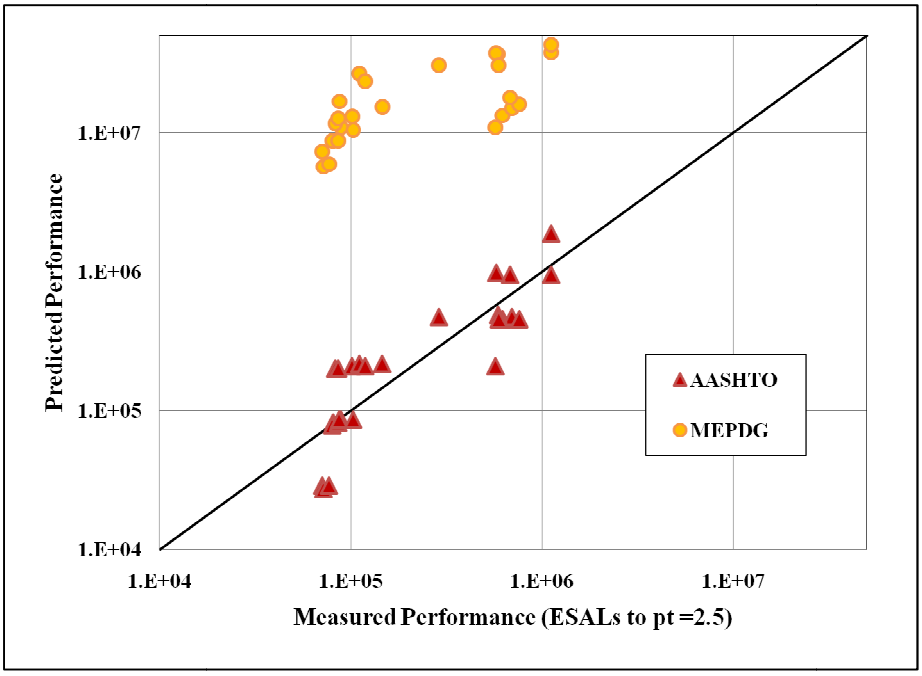

Figure 4.3: Predicted vs. measured design life using AASHO Road Test PSI is 2.5. (Case 2)

The above graph shows the when analyzing design life in terms of ESALs to failure, AASHTO predictions agree well with the actual AASHO measured data. This is of course expected given that the AASHTO design procedure was derived from the AASHO Road Test. Moreover, the opposite mechanism discussed in Figure 4.2 is true for this case; that is, changes in PSI produce minimal changes in ESALs. Additionally, it is observed that MEPDG has a significant bias towards over predicting design life. This would equate to thinner pavement sections as independent research suggests.

4.4 Discussion

The objectives of this pilot study were twofold: first, to explore whether the AASHO Road Test was a useful tool for evaluating the AASHTO 1993 and Mechanistic-Empirical design procedures, and second, to determine if PSI is a realistic measure of performance for this evaluation.

The purpose of this research is not just to evaluate how AASHTO and MEPDG predictions relate to each other, but also how close they match actual performance. The AASHO Road Test was chosen as a real-world comparison to put the design predictions in perspective. Furthermore, it was expected that the AASHTO predictions would correspond well with the AASHO measured data, making it possible to prove a hypothesis—even if only provisionally—before expanding the study to pavements in other locations and introducing more variables. As discussed, this hypothesis was indeed supported by the results, directly when evaluating service life and indirectly when evaluating distress predictions.

The second goal of the pilot study was to evaluate PSI as a composite performance measure. Problems were observed in the PSI vs. IRI empirical correlation developed by Al-Omari and Darter (1994). The model used in this Pilot study is their generalized equation. However there are no significant changes in the results when using their specific AC model ($PSI = 5 * e^{(-0.0038*IRI)}$). This is because their models are not very sensitive to changes in IRI; an increase of 10 in/mile in IRI decreases PSI by a tenth. Furthermore, the Al-Omari and Darter model was developed from data observed over relatively low IRI and high PSI ranges characteristic of real in-service pavements. This makes it less reliable in the lower PSI range ($0.75<p_t<3.0$) which is the focus of this study.

Additionally, the IRI model within the MEPDG is potentially adding variability to the results. IRI predicted by the MEPDG is not significantly influenced by many of the pavement distresses or environmental factors in the MEPDG method; rather, it is sensitive primarily to the initial IRI and predicted rut depth. The initial IRI used in this

study was the default value of 63 in/mile. Changing the initial IRI to 100 in/mile results in an overall decrease in terminal PSI of 0.5 to 3.0 and brings predictions closer in line with the AASHO Road Test measurements (Figure 4.4). This difference in IRI_o is well within the standard deviation of the MEPDG models. However, an IRI_o of 100in/mi is contradictory to the Al-Omari and Darter Model which relates a PSI of 4.2 to an IRI of approximately 45 in/mi, meaning one could just as easily argue the reverse that the data points should increase to a terminal PSI of approximately 4.0.

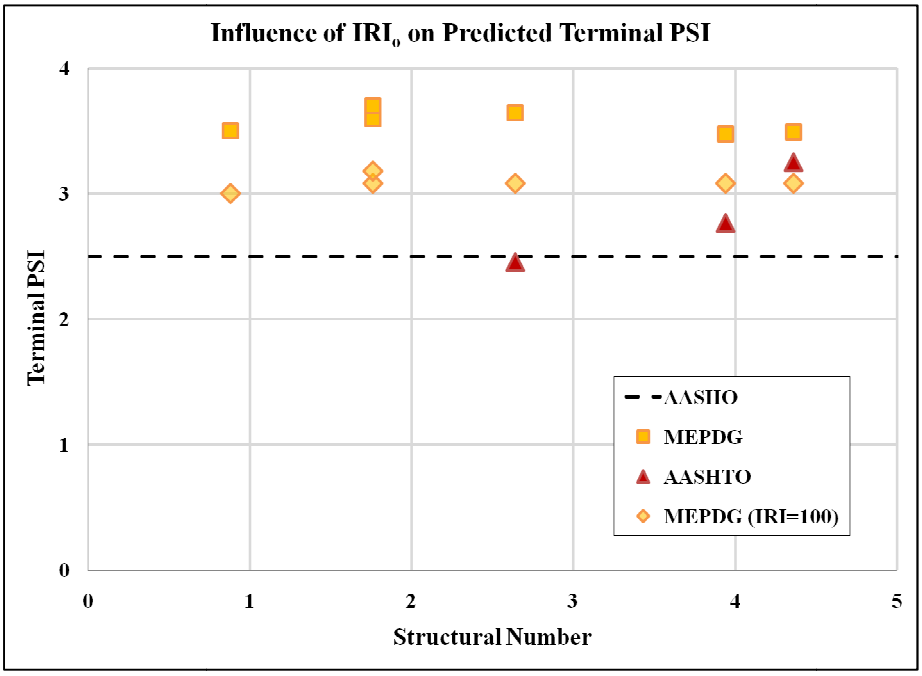

Figure 4.4: Influence of initial IRI on predicted performance.

The overriding observations from the pilot study are that it is reasonable to continue using the AASHO Road Test in a larger scale study. However, more research is needed to determine a statistically sound relation between the PSI output of AASHTO and the IRI and distresses predicted by the MEPDG.

Chapter 5: AASHO Road Test Modeling Results

The principal limitation of the AASHO Road Test is that performance is evaluated in terms of the semi-qualitative PSI index while the MEPDG predicts individual pavement distresses. Chapter 3 presented the methodology and troubleshooting steps for modeling the AASHO Road Test using both the MEPDG and AASHTO 1993 design procedures. Chapter 4 detailed the findings of the pilot study including the difficulty in using existing IRI to PSI relationships. The purpose of this chapter is to discuss the results of the full-scale models for the AASHO Road Test using both design procedures and evaluate the accuracy of each procedure in relation to historical data.

The Flexible Pavement Database has been mentioned in passing several times and is fully detailed in Appendix A. The database was developed to organize the AASHO distress histories, AASHTO design predictions, and MEPDG distress predictions for each unique structural section encompassed in Design 1 for the Road Test. Loop 1 sections were excluded because they were strictly for environmental research.

Both design procedures were evaluated using the same methodology employed in the pilot study. The AASHTO 1993 Design Procedure was evaluated in terms of design life and pavement distress. However, the MEPDG was evaluated only in terms of distresses; evaluating in terms of design life is an iterative process and impractical for a large-scale study.

This large-scale study supports the initial observations of the pilot study. The AASHTO 1993 model and the Road Test results agree well, specifically when design life is used as a performance measure. Furthermore, agreement is improved by removing

Loop 2 data and using seasonally weighted traffic inputs. MEPDG predictions were compared directly to AASHO serviceability data, but no overriding trends were observed. A limited amount of rutting data from the AASHO reports were compared to MEPDG predictions with positive results, showing the rut depth can be predicted with confidence. However, there is not enough transverse profile data to apply these results across the whole of the AASHO Road Test. Existing relationships between PSI and IRI were also considered and found to be insufficient for modeling the Road Test.

5.1 AASHTO 1993 Model

The AASHTO design equation was empirically derived from the results of the AASHO Road Test with some additions over time and it is therefore reasonable to expect the predicted and measured PSI values to match closely. As discussed in Chapter 3 this model can be evaluated using two cases: Case 1 uses the AASHO Road Test pavement properties to predict design life; Case 2 uses AASHO traffic to predict serviceability.

5.1.1 Unweighted Predictions

Figure 5.2 shows the large-scale results when using design life to evaluate the AASHTO Design Procedure against historical pavement performance. The results observed in the pilot study are confirmed; AASHTO predicted design life agrees reasonable well with AASHO measured data (R^2=0.54) with negligible bias. Figure 5.3 shows the large-scale results for Case 2, predicted serviceability. Once again, results confirm the initial observations from the pilot study. The pilot study results showed poor agreement between AASHTO predicted PSI and AASHO measured values due to the steep drop off in PSI values with small increases in traffic. The poor fit (R^2=0.10) is due to the same inherent issues in the model previously discussed; that is for a small change

in traffic PSI changes dramatically. The original AASHO model, in the form of SN vs. load as shown in Figure 5.1, had a fit of +/- 14% (AASHO, 1961). The R-squared value in Figure 5.3 is too unreliable for practical use, but the one in Figure 5.2 is unexpectedly low in the context of the 1961 model statistics—even considering a different model form.

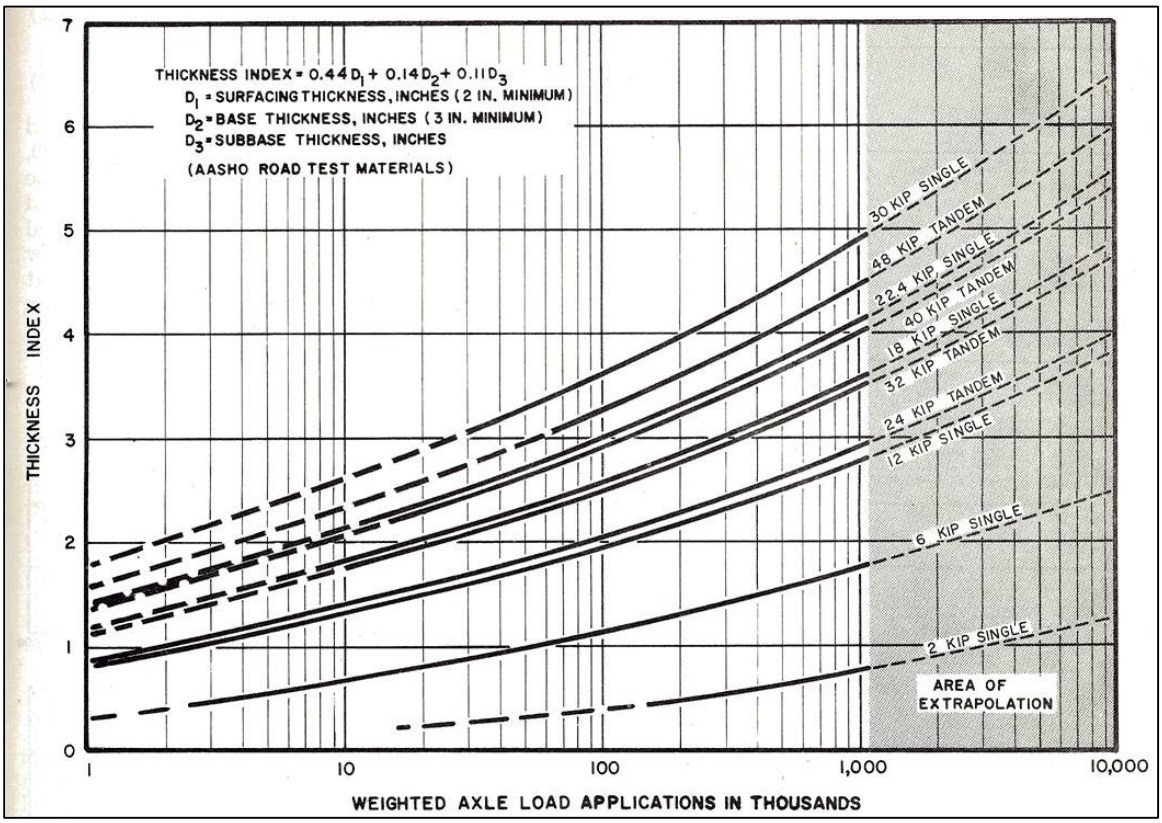

Figure 5.1: AASHO Road Test relationship between design and axle load application at p=1.5 from the Road Test Equations. (AASHO, 1961)

The Loop 2 results introduce extra scatter and artificially lower the measures of fit. It can be clearly observed in both figures that Loop 2 predictions do not follow the same trends as the other four loops. When using service life as a performance measure there is an unexplained banding in the Loop 2 data (Figure 5.2). Because service life is relatively insensitive to changes in PSI this banding does not introduce any bias, but it does decrease the coefficient of determination. Removing the Loop 2 data raises R^2 for the trend in Figure 5.2 to 0.75, a dramatic improvement. When serviceability is the

performance measure, the Loop 2 data shows a prominent bias towards over predicting PSI (Figure 5.3). In this case the Loop 2 trends do influence both bias and goodness-of-fit. Removing the data results in an R^2=0.4 for the trend in Figure 5.3. However, exclusion of Loop 2 imparts a global bias in the data to underpredict PSI. This is likely due to the issue discussed in Chapter 3 when using the AASHTO procedure in an inverted format (solving for PSI); for a given combination of traffic and structural capacity there is a limiting terminal PSI. All cases in which an unrealistic PSI was predicted were filtered from the results, but the borderline values (PSI<1.0) that cannot be systematically removed remain and this is likely influencing the bias.

The observations made in these figures (as well as those for the MEPDG) prompted the Loop 2 investigation discussed in Chapter 3. In summary, Loop 2 was substantially under-trafficked in relation to the available structural capacity and thus the results do not follow the same trends as in Loops 3 through 6.

Another source contributing to the spread in the data results may be the seasonal influence of distress accumulation. The AASHTO model was derived based upon seasonally weighted data, but unweighted axle applications are used in this present study. This could lower the coefficient of determination slightly and is discussed in the next section.

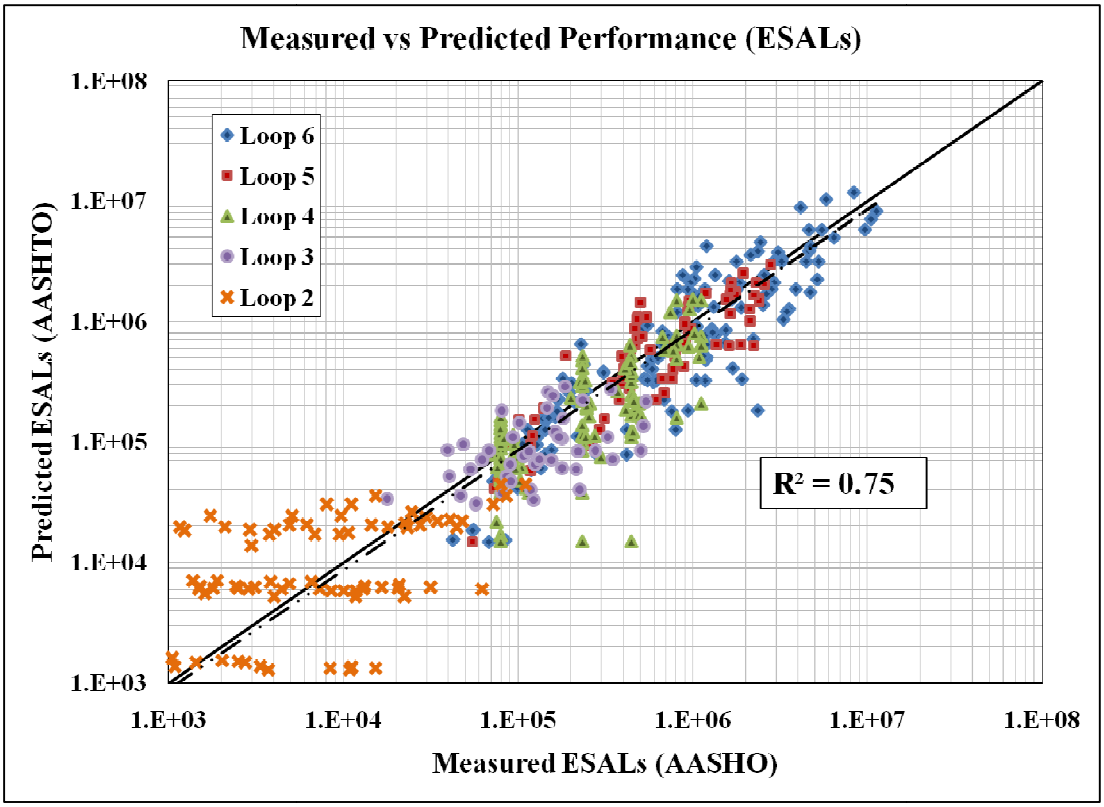

Figure 5.2: Evaluating predicted design life, AASHO measured traffic versus AASHTO predicted traffic. Best-fit line excludes Loop 2 data.

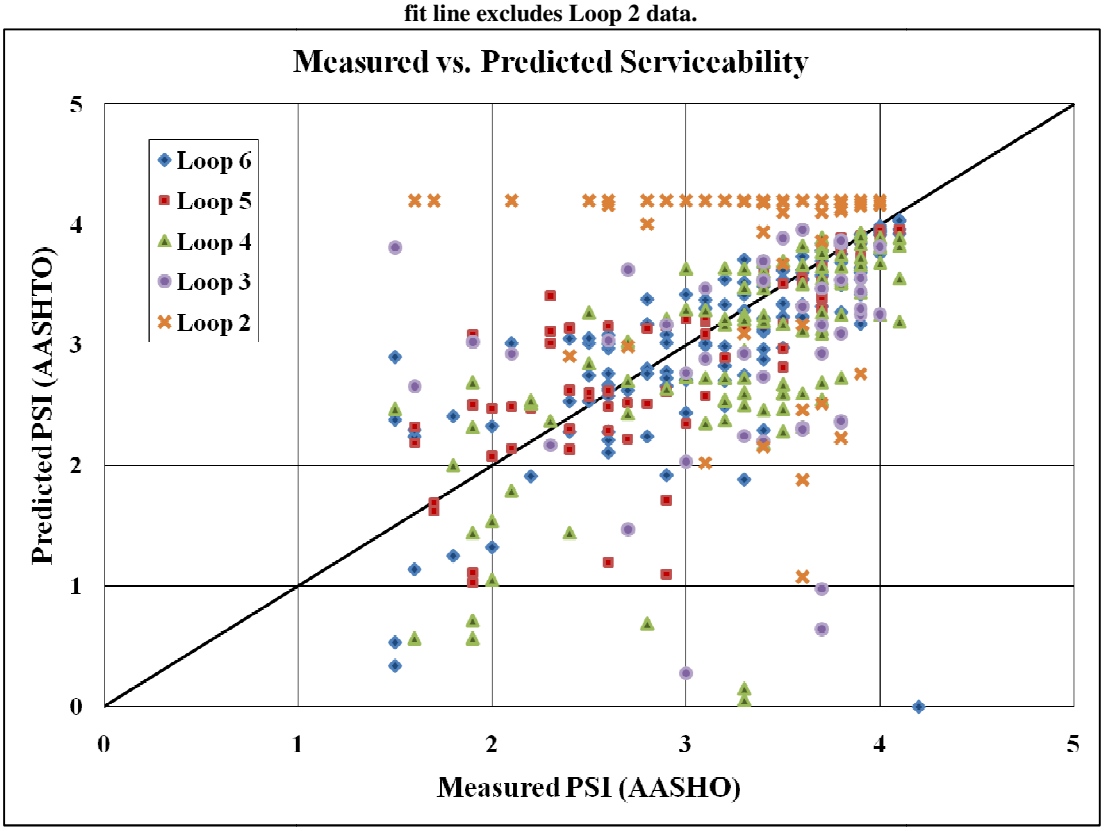

Figure 5.3: Evaluating predicted service life, AASHO measured PSI vs. AASHTO predicted PSI. R^2=0.37 when Loop 2 data is excluded.

5.1.2 Seasonally Weighted Predictions

Briefly discussed in Chapter 3 was the significant seasonal influence on predicted serviceability at the AASHO Road Test. To deal with this the scientists and engineers developed a 'Seasonal Weighting Factor' based upon static load deflection testing from Loop 1. The Seasonal Weighting Factor was applied such that in the spring months, the axle applications were multiplied by a number greater than 1 and in the winter, the axle applications were multiplied by a number less than one. The seasonal factors from the published reports are summarized in Table 5.1. (AASHO, 1961)

Table 5.1: Seasonal weighting factors and weighted axle applications.

Index Day	Axle Applications (Hundreds)		Seasonal Weighting Factor	Seasonally Weighted Applications (Hundreds)	
	Mean	Total		Mean	Total
11	35	797	4.84	169	751
22	162	2,331	0.87	141	2,897
33	368	4,446	0.28	106	4,014
44	355	8,068	1.44	511	9,436
55	142	11,138	0.44	63	12,265

Figure 5.4 and Figure 5.5 show the results of both seasonally weighted and unweighted axle applications for predicted design life and predicted serviceability respectively. As expected, using the seasonally weighted axle applications results in improved predictions and a higher measure of fit, but only slightly.

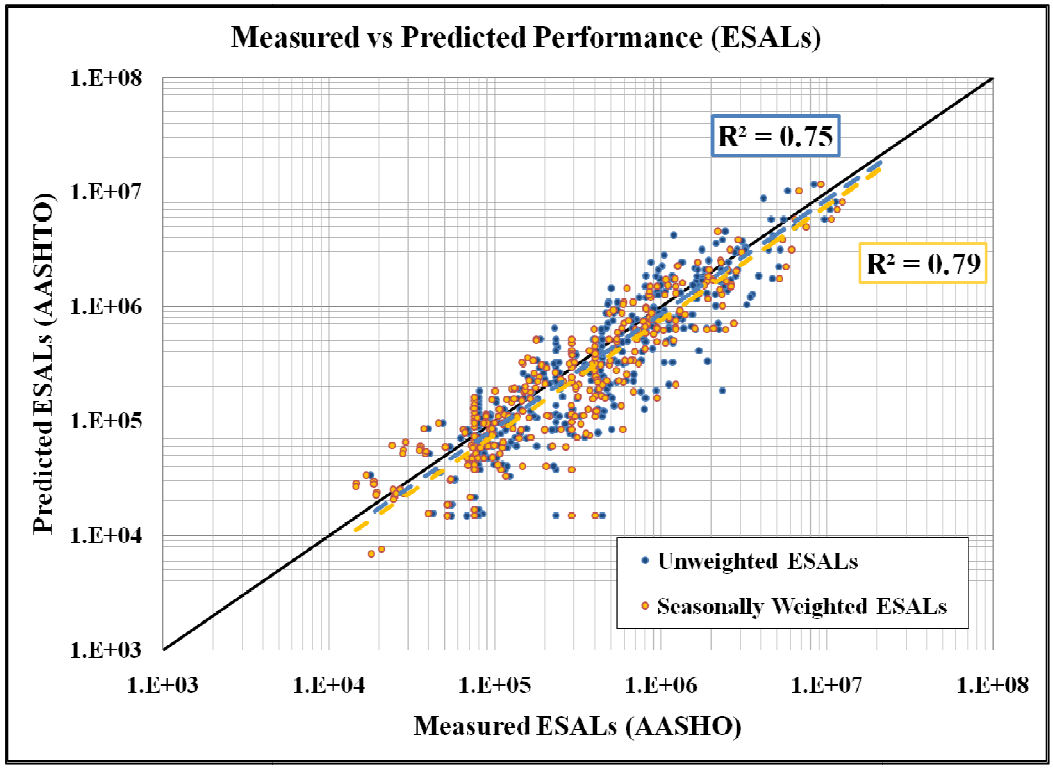

Figure 5.4: Predicted design life vs. measured weighted and unweighted ESALS . In both cases the dependant variable represents predicted service life from AASHO measured PSI. For seasonally weighted data the 'measured' variable is the seasonally adjusted AASHO traffic. For the unweighted data this is just the actual traffic.

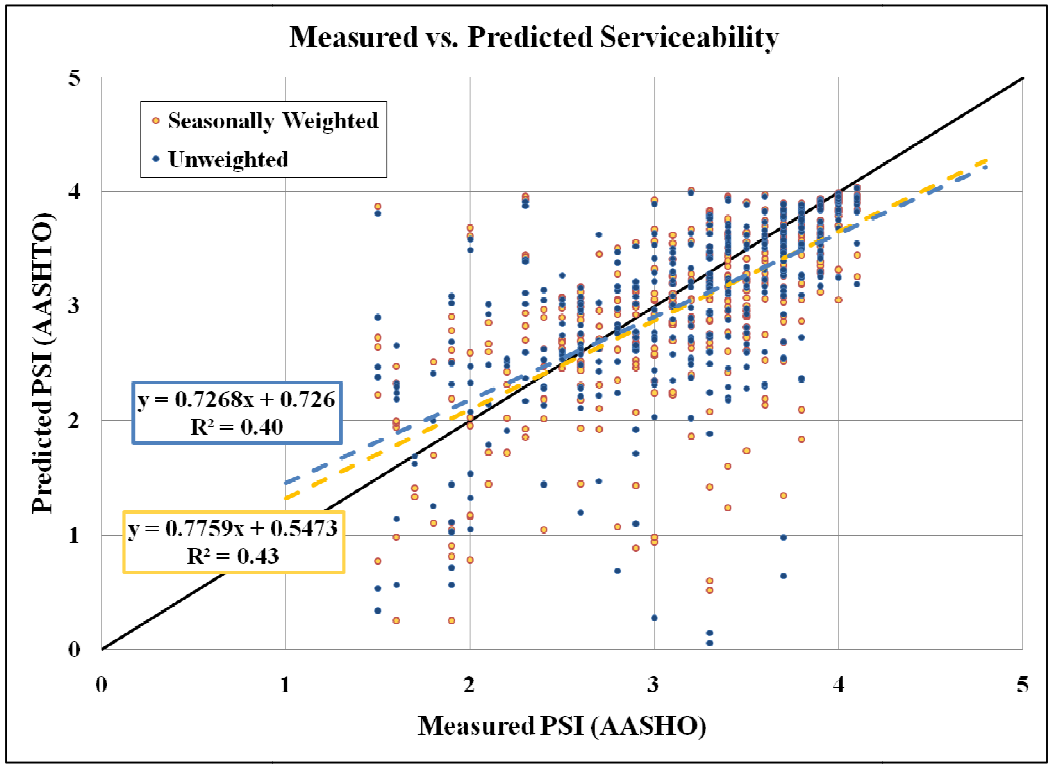

Figure 5.5: Predicted weighted and unweighted PSI vs. measured PSI. In both cases measured PSI is from the historical Road Test Data. For the seasonally weighted case, predicted PSI is based on the seasonally weighted ESALs. For the unweighted case, predicted PSI is based on actual ESALs.

5.2 MEPDG Model

The experimental parameters of the AASHO Road Test are not directly compatible with the design factors of the MEPDG. Therefore, while traffic-to-traffic and PSI-to-PSI comparisons were made for the AASHTO Design Procedure in the proceeding section, the MEPDG distress predictions are presented here individually with respect to the measured AASHO serviceability. The transverse cracking model in the MEPDG v1.1 predicted no thermal cracking for the conditions at the Road Test so only longitudinal cracking, alligator cracking, rut depth, and IRI predictions are discussed.

5.2.1 Fatigue Distress Predictions

When the traffic growth model is applied to all 284 AASHO test sections from Loop 2 – Loop 6, several observations can be made. Rutting is the principal distress recorded at the Road Test and MEPDG predictions support this fact. Nearly no structural sections exhibited predicted longitudinal (Figure 5.6) or alligator cracking (Figure 5.7) that reached significant levels; conversely, almost all the sections have severe predicted rutting (Figure 5.8). The 'Inadequate', 'Fair', and 'Good' thresholds used throughout this section are as suggested in the MEPDG Manual of Practice (AASHTO, 2008).

The data are divided by loop to differentiate any patterns in the distress predictions. Each loop shows decreasing PSI with increasing distress as expected, but the data do not fall into particular ranges depending on loop, nor do the data as a whole exhibit any strong correlations between PSI and predicted distresses.

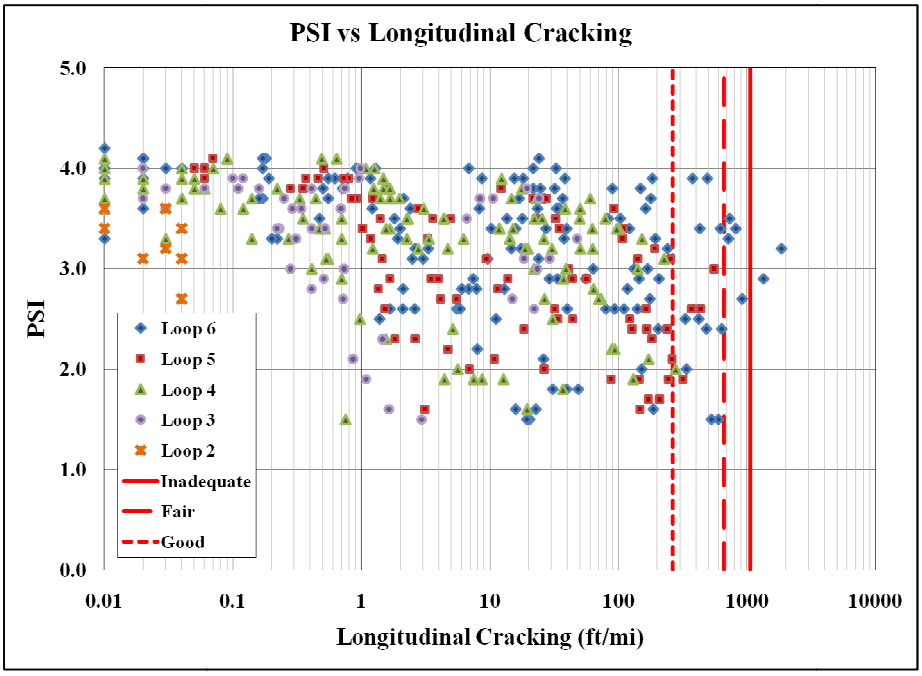

Figure 5.6: MEPDG predicted longitudinal cracking versus AASHO Road Test measured PSI.

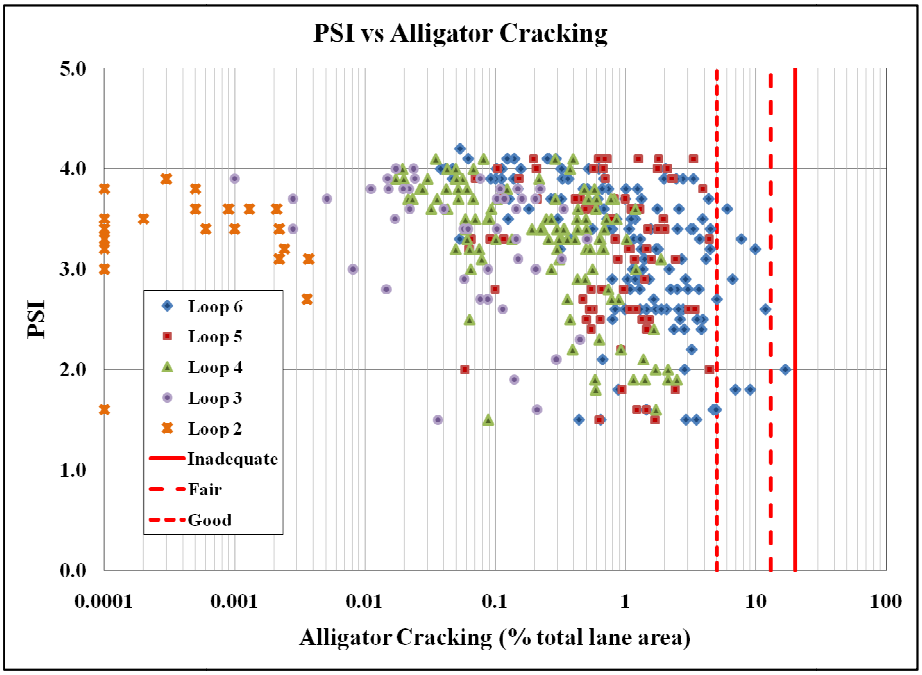

Figure 5.7: MEPDG predicted alligator cracking versus AASHO Road Test measured PSI.

5.2.2 Rutting Distress Predictions

Figure 5.8 shows MEPDG predicted rutting vs. AASHO PSI for all the test sections in Loops 2 through 6 as was discussed in the proceeding section. However, because there is some rutting data published AASHO Road Test Reports, a direct

comparison was also investigated. Transverse profile data was measured over the course of 2 years for 22 unique structural sections (44 pavement-load combinations). Table 5.2 gives a sample data set for a structural section with 3 inches of AC, 9 inches of granular base, and 12 inches of subbase. The raw data in the Road Test reports is recorded as the change in surface elevation at the centerline and at 3, 6, 9, and 12-foot increments from the centerline. The data was converted to absolute change in elevation (the original road profile was graded away from the centerline), then the rut depth was calculated and averaged for the inner and outer wheel paths.

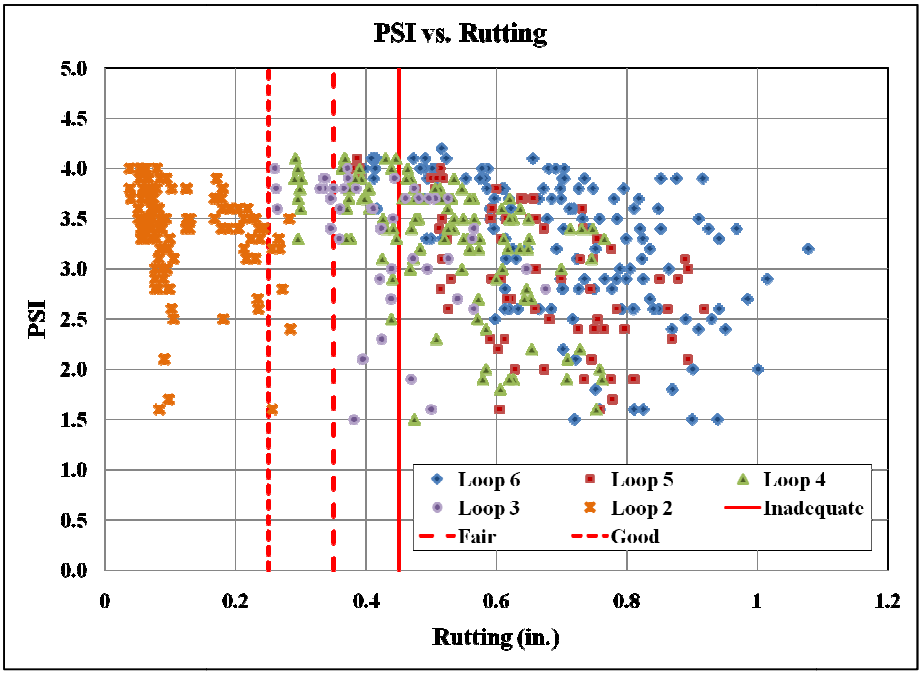

Figure 5.8: MEPDG predicted rut depth versus AASHO Road Test measured PSI.

Table 5.2: Sample of transverse profile data from the AASHO Road Test Reports and rut depth calculations.

AASHO ROAD TEST													MEPDG
LOOP	ID	SN	ESAL	RUTTING DATA									Total Rutting (in)
				TRANSVERSE PROFILE								AVERAGE RD	
				TIME	Origional Profile	12.0	9.0	6.0	3.0	0.0			
5	441	3.90	2,228,276	July 1959	Change in Elevation	-0.1	-0.7	-0.1	-0.7	-0.1		-0.5	0.71
					Transverse Profile	-1.6	-1.6	-0.6	-0.9	-0.1			
					Rut Depth		-0.5		-0.6				
				November 1959	Change in Elevation	-0.2	-0.8	-0.2	-0.8	-0.1		-0.6	0.74
					Transverse Profile	-1.7	-1.7	-0.7	-1.0	-0.1			
					Rut Depth		-0.5		-0.6				
				March 1960	Change in Elevation	0.4	-0.6	0.0	-0.6	0.0		-0.6	0.76
					Transverse Profile	-1.1	-1.5	-0.5	-0.8	0.0			
					Rut Depth		-0.7		-0.6				
5	442	3.90	309,856	July 1959	Change in Elevation	-0.6	-1.3	-0.4	-1.0	-0.1		-0.7	0.84
					Transverse Profile	-2.1	-2.2	-0.9	-1.2	-0.1			
					Rut Depth		-0.7		-0.7				
				November 1959	Change in Elevation	-0.5	-1.3	-0.4	-1.0	-0.1		-0.7	0.88
					Transverse Profile	-2.0	-2.2	-0.9	-1.2	-0.1			
					Rut Depth		-0.8		-0.7				
				March 1960	Change in Profile	0.0	-1.3	-0.1	-1.0	0.0		-1.0	0.91
					Transverse Profile	-1.5	-2.2	-0.6	-1.2	0.0			
					Rut Depth		-1.2		-0.9				
				October 1960	Change in Profile	0.0	-1.3	-0.1	-1.0	0.0		-1.0	1.05
					Transverse Profile	-1.5	-2.2	-0.6	-1.2	0.0			
					Rut Depth		-1.2		-0.9				

Though the data is limited, the results are reassuring. Figure 5.9 shows 2 years of predicted rutting vs. transverse profile measurements for all 175 rutting observations for the 44 pavement-load combinations. The trend for predicted vs. measured rutting for the complete data set is relatively unbiased with an R^2=0.53. Sections trafficked by tandem axles exhibit slightly more scatter (R^2=0.42) as compared to single axle sections (R^2=0.57). These results are promising, but it is important to acknowledge that the data is 10% of the total pavement population and should therefore not be assumed to represent the whole of the AASHO Road Test.

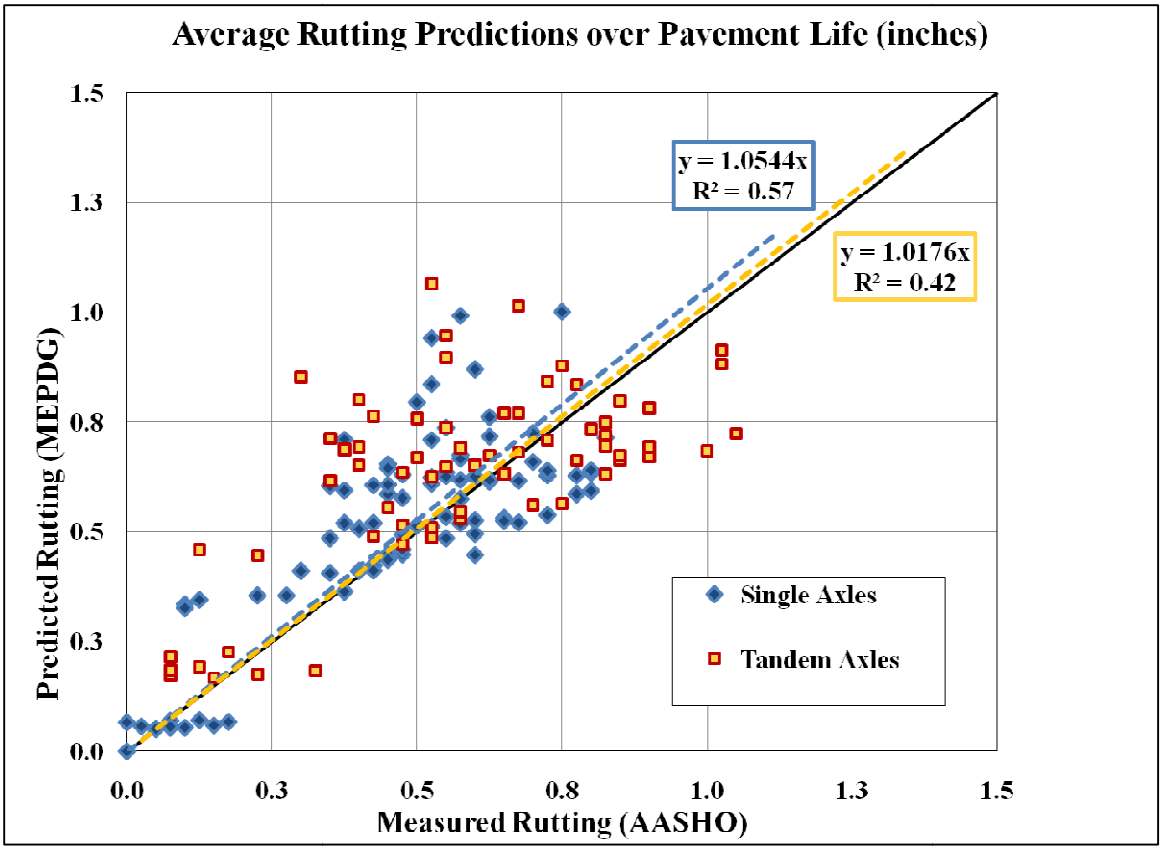

Figure 5.9: AASHO measured rutting vs. MEPDG predicted rutting.

5.2.3 IRI Distress Predictions

The applicability of IRI as a performance measure to compare the MEPDG and AASHTO 1993 design procedures was first explored in the pilot study. It was observed that MEPDG overpredicted design life (underpredicted distresses) in comparison to the AASHTO 1993 design procedure. However, there was ambiguity as to whether the Al-Omari and Darter model (1994) used to convert IRI to PSI introduced too much error.

IRI is considered in Figure 5.10 in the same manner as the previous distresses. As noted before, there is no strong correlation between the measured and predicted data. Moreover, existing models that define a relationship between PSI and IRI are shown to be inadequate for representing the AASHO Road Test data. The Paterson (1987) and Gulen *et al.* (1994) models were developed using data from several countries and the

state of Indiana respectively, while the Al-Omari & Darter model was developed using data from six states, arguably making it more suited to this study. However, the Al-Omari and Darter model is based on data from in-service pavements in generally fair or better condition with few PSI values less than 3.0. A concern raised by the pilot study was that the majority of the PSI values for the AASHO Road Test pavements ranged from 2.5 to 1.5. Consequently, although the Al-Omari and Darter model (IRI_o=45 in/mi) is the best suited of the three to the conditions at the AASHO Road Test, it only fits the data well where PSI>3.0.

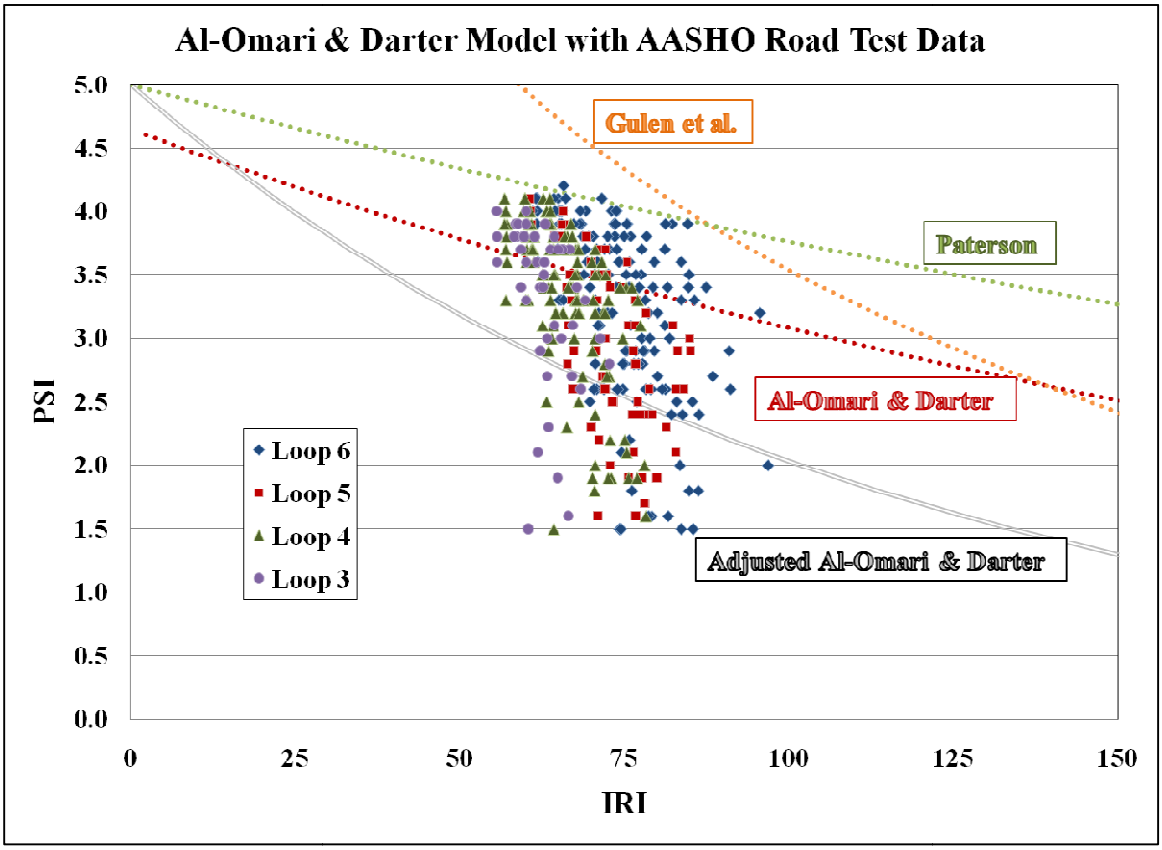

Figure 5.10: AASHO measure PSI vs. MEPDG predicted PSI. The Al-Omari & Darter, Gulen, and Paterson PSI-IRI relationship are also plotted against the data.

A regression was performed on the Road Test data using the same model form as Al-Omari and Darter and is plotted in Figure 5.10 as the double lined 'Adjusted Model'. However, even this adjusted model is still unable to capture the sudden seasonal decrease

in PSI observed in the AASHO Road Test. In Figure 5.11, a log scale is applied to the x-axis to help explain the main functional flaw of this model form.

Based on practical service levels (PSI 0-5), the IRI models are applicable to a range of approximately 40 to 120 in/mi. In that range the AASHO data decreases at a rate far greater than any of the models can capture. The sharp decrease in measured PSI was first observed in the pilot study as a function of traffic and has been discussed in detail. Moreover, the decreases in PSI were highly seasonal at the Road Test, but the MEPDG IRI distress model progresses in an essentially linear fashion with time. Consequently, an entirely new model form to relate PSI to distresses must be developed.

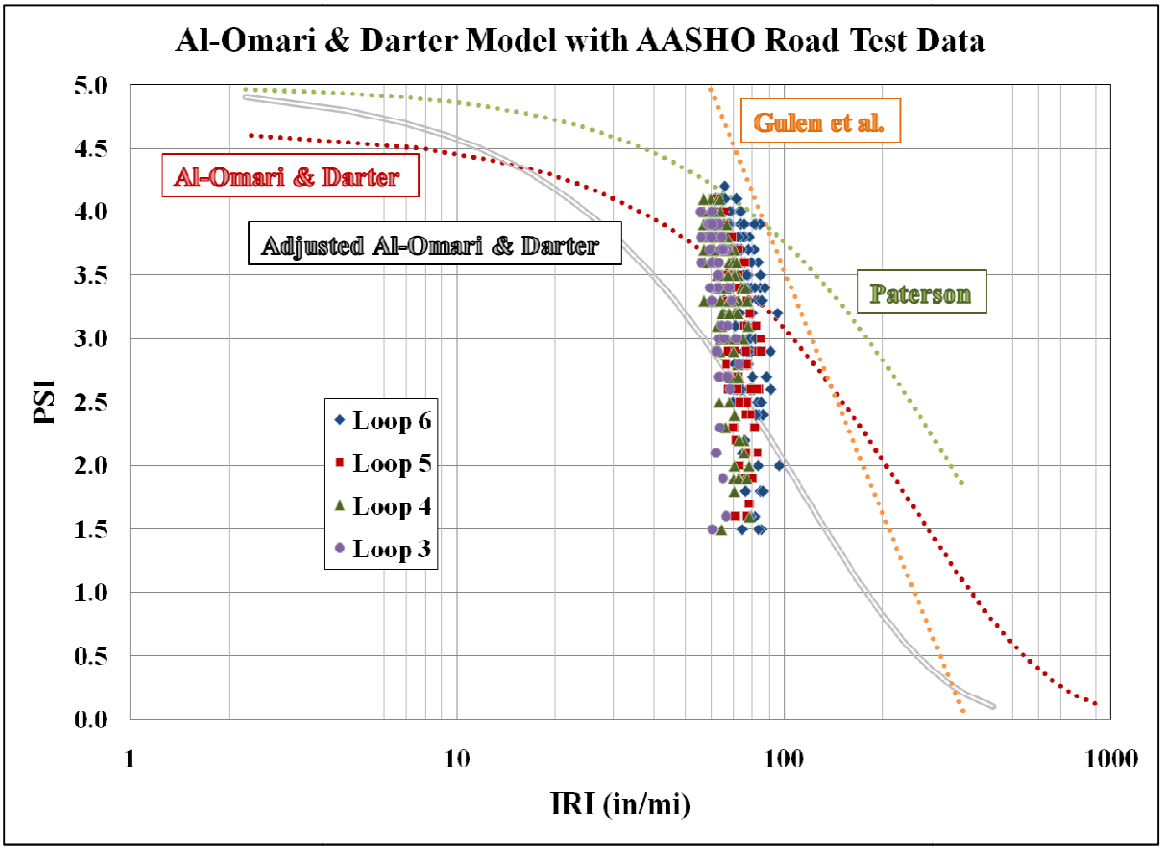

Figure 5.11: Measured AASHO PSI vs. Predicted MEPDG log(IRI).

Chapter 6: Performance and Distress Model Development

Chapter 5 presented the results of modeling the AASHO Road Test using the AASHTO 1993 and MEPDG design procedures. No direct correlations between the predicted MEPDG distresses and AASHO measured serviceability could be drawn and existing relations between IRI and PSI were shown to be inadequate for this application. The following chapter presents several attempts to derive a relationship that can be used as a comparative performance measure between the Road Test, AASHTO 1993 Design Procedure, and the MEPDG.

The Flexible Pavement Database contains the identification and structural data for each section along with the corresponding MEPDG and AASHTO 1993 inputs and distress predictions. Some sections were excluded from the analyses:

- Loop 1 sections, a total of 48 pavement structures, were designed for an environmental affects study and are omitted because they were not subjected to a load.
- Loop 2 sections were used in the initial modeling attempts, but it became increasingly apparent that this loop was substantially under-trafficked with regard to the structural capacity of the pavement as compared to loops 3 through 6; consequently, these 44 structural designs are omitted from final regressions.
- All duplicate sections, totaling 24 structural designs across Loops 3-6, are not used individually but are averaged and cataloged as one result.
- All sections that reached a present serviceability index of 1.5 prior to the first distress record (i.e. the 11^{th} index day record in week 22 of the experiment-

March 1959) were omitted, totaling 39 structural designs across Loops 3-6, because there is no measured data to use in the comparison.

After this screening, 177 of the original 332 structural sections trafficked during the AASHO Road Test main factorial design experiment remained for subsequent analysis. The soundness of each regression model was assessed using at least one statistical test. The coefficient of determination (R^2) was used to assess the 'goodness of fit' in all cases. The T-test was used occasionally as a measure of statistical significance of the individual coefficients in the regression models. For this study a two-tailed test is used and an α=0.05. Thus, if the t-value is greater than 1.960 the coefficient is statistically significant; the practical implication of this is that the given term has an influence in the regression. The residuals of each model were also examined to determine if there was any bias in the regression.

6.1 Multivariate Regression

Several multivariate regressions of the form in Equation 6.1 were conducted using combinations of longitudinal cracking (LC), alligator cracking (AC), and rut depth (RD).

$$PSI = a_0 - a_1 LC - a_2 AC - a_3 RD \quad (6.1)$$

This basic equation was varied to analyze the effect of fatigue distress verses deformation. Based upon the MEPDG predictions and the actual results of the Road Test the rutting term should hold considerable weight in the regression. Therefore, this term was analyzed using multiple forms: $a_i \log(RD)$; $a_i \ln(RD)$; $a_i (RD)^{a_n}$ ($a_n = 2, 3, and\ 4$). The longitudinal and alligator cracking terms were analyzed both separately and as one composite fatigue term (a_iFC). The composite fatigue term was the total area

of fatigue cracking where the top-down crack length was multiplied by 1 ft to convert it to an area basis. The most promising regression was ($R^2 = 0.25$):

$$PSI = 4.390 + 0.00058(LC) - 0.06008(AC) - 1.89974(RD) \quad (6.2)$$

Table 6.1: Statistical Significance of Terms in Regression Equation.

Term	*T-test*
Coefficient	30.4
Longitudinal Cracking (ft/mi)	2.5
Alligator Cracking (%)	-2.5
Rut Depth (in.)	-7.2

Several important observations are made from this initial attempt at developing a relationship between AASHO measured PSI and MEPDG predicted distresses. The final form of the multivariate regression includes a constant term of 4.390, very near the normally assumed initial PSI value of 4.2. Furthermore, not only are all the terms statistically significant by the T-test, but the rutting term is assigned the most weight, as is expected. Finally, the regression fits a normal probability curve reasonably well (Figure 6.1).

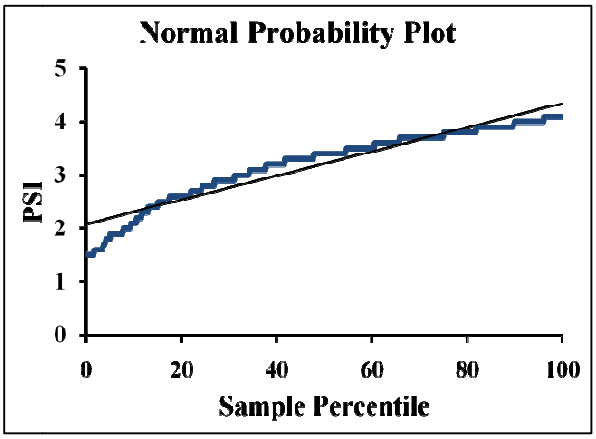

Figure 6.1: Normal probability plot for the most successful multivariate linear regression.

In all the regression attempts, the longitudinal cracking term was assigned a positive coefficient, indicating that PSI would increase with increasing longitudinal cracking. Therefore, while the T-test finds longitudinal cracking to be a statistically

significant variable, it is unreasonable in physical terms. Additionally, while the rutting term is statistically and practically significant further observations suggest a bias in the residuals (Figure 6.2). This, along with the low coefficient of determination (R^2=0.25) indicates that there should be a better model form to relate PSI and distress.

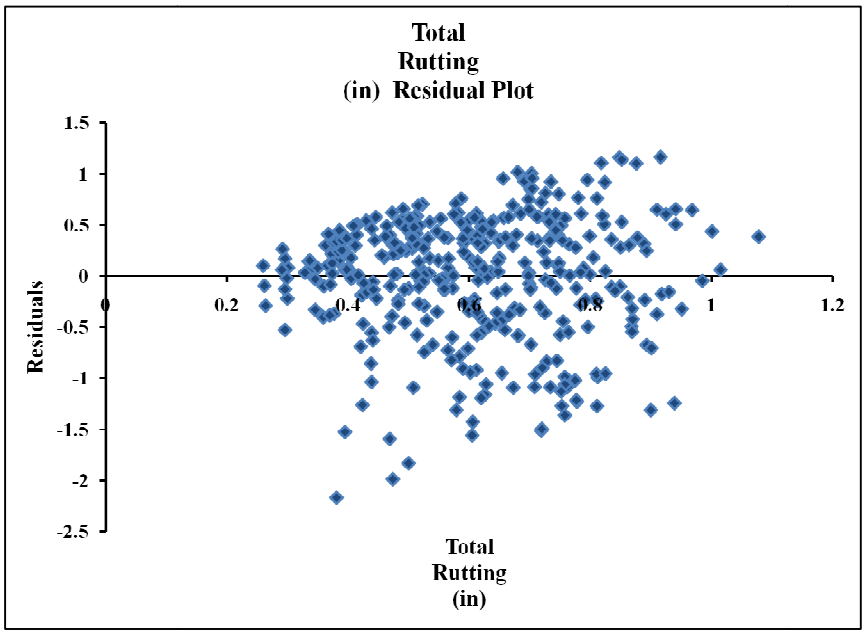

Figure 6.2: Distribution of residuals in the rutting term for the most successful multivariate linear regression. At low rut depth the residuals trend negative while at large rut depths the residuals are positive.

As described previously, the representativeness of the data from Loop 2 is questionable because the ratio of traffic load to structural capacity is much lower than in the other loops. The initial multivariate regressions were therefore conducted twice, both with and without Loop 2 data. In all cases, the exclusion of this data increased the coefficient of determination by approximately one-tenth. Equation 6.2 is representative of Loop 3-6 data.

A linear regression did not provide the required model form to relate PSI to the MEPDG distresses. Because of the high occurrence of rutting at the road test—coupled with promising results from the measured to predicted rutting analysis and indication of statistical significance from the multivariate regression attempts—further analysis was

conducted based solely upon rut depth. Once an adequate model relating PSI to rut depth is developed, it may be further refined by incorporating the fatigue distresses.

6.2 Direct Transformation

To relate PSI and rut depth, a direct transformation was formulated using traffic as a conduit. There are clear and relatively significant relationships between the log of traffic vs. PSI (R^2=0.29) and between the log of traffic vs. rut depth (R^2=0.58) as seen below in Figure 6.3 and Figure 6.4. A linear relationship was derived to fit the log of traffic vs. PSI data (Equation 6.3a), where as both linear and natural log relations were fit to the log of traffic vs. rut depth data (Equation 6.3b and Equation 6.3c). Both cases were resolved so that traffic was the dependant variable and then set equal to each other such that PSI was related directly to rut depth (Equation 6.4a and Equation 6.4b). The final model forms were simplified and manipulated to solve for PSI in terms rut depth (Figure 6.5). The resulting transformations from RD to PSI are shown in Equation 6.5a and Equation 6.5b.

$$\log(W_{18}) = -0.4453PSI + 7.0251 \quad (6.3a)$$

$$\log(W_{18}) = 2.5664RD + 4.0429 \quad (6.3b)$$

$$\log(W_{18}) = 1.4685\ln(RD) + 6.3922 \quad (6.3c)$$

$$-0.4453PSI + 7.0251 = 2.5664RD + 4.0429 \quad (6.4a)$$

$$-0.4453PSI + 7.0251 = 1.4685\ln(RD) + 6.3922 \quad (6.4b)$$

$$PSI = 6.6971 - 5.7633(RD) \quad (6.5a)$$

$$PSI = 1.4213 - 3.2978\ln(RD) \quad (6.5b)$$

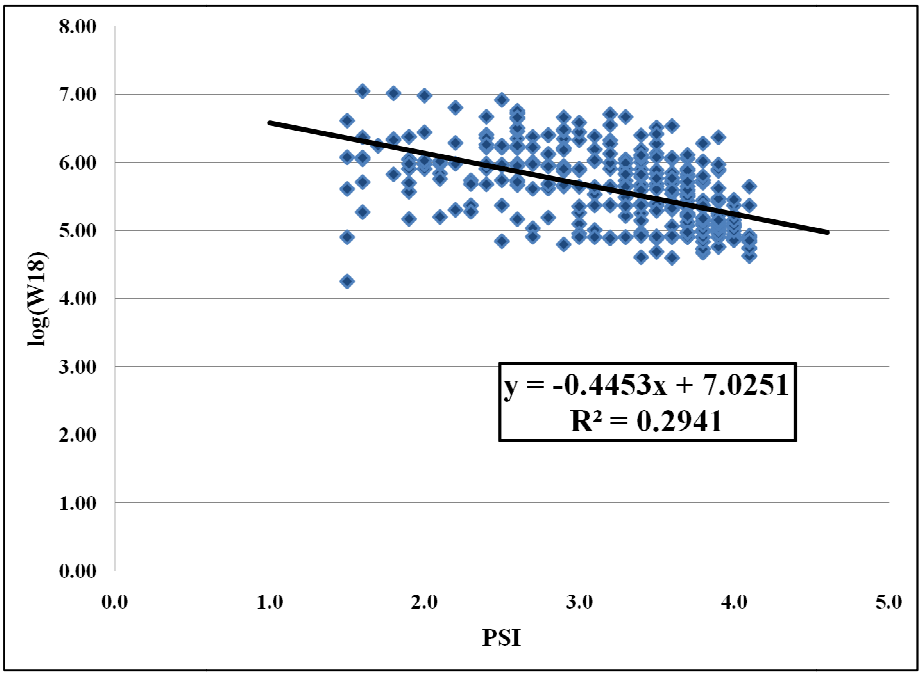

Figure 6.3: Linear regression to establish a relationship between the log of traffic and PSI.

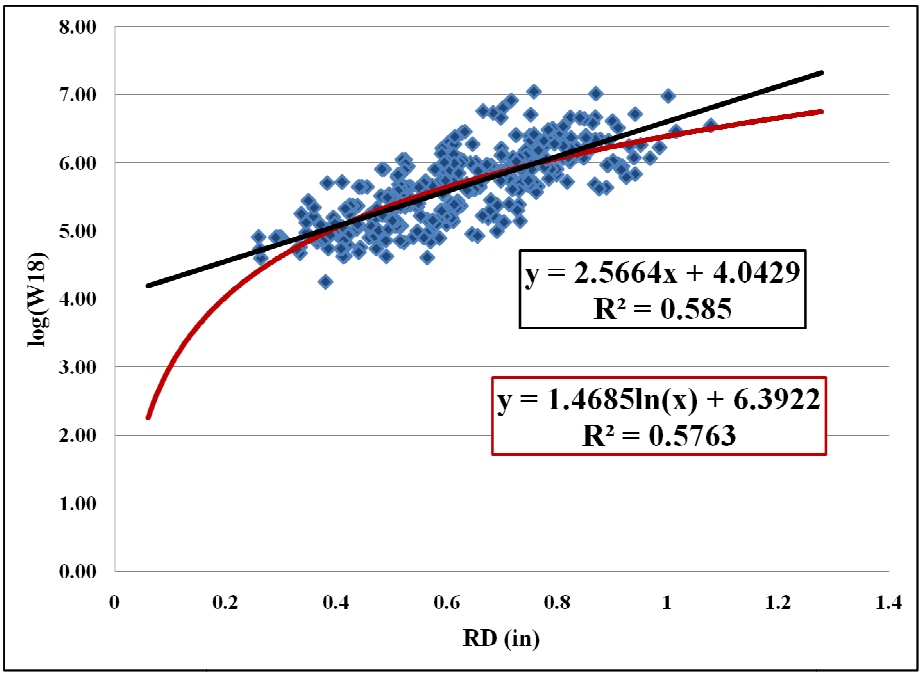

Figure 6.4: Linear and natural log relationships between the log of traffic and rut depth.

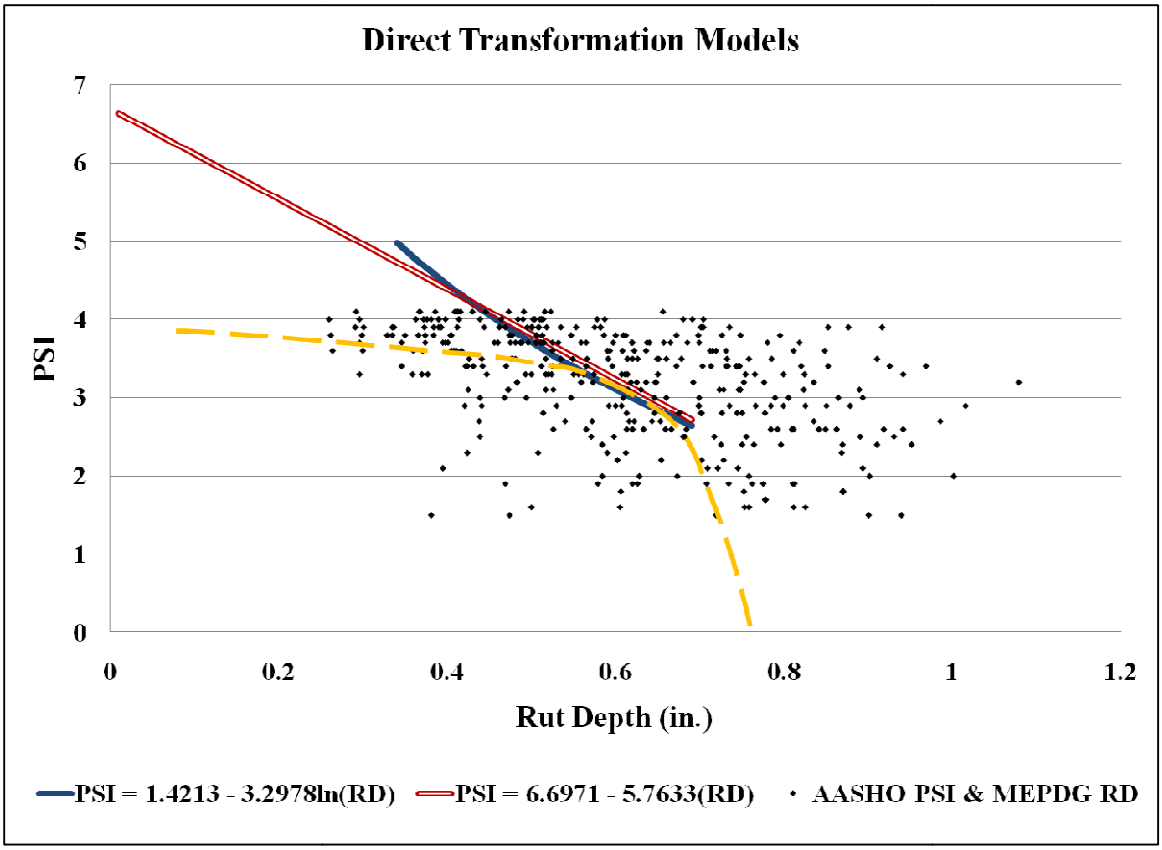

Figure 6.5: Direct transformation relationship between PSI and rut depth. The double red line is Equation 6.5a, the solid blue line is Equation 6.5b, and the dashed yellow line represents the ideal model form.

Figure 6.5 depicts both models superimposed over the AASHO PSI vs. MEPDG RD data. It is clear that neither model provides a very good relationship. If rut depth is zero, the corresponding serviceability of the linear and natural log models are 6.7 and 16.6 respectively. Even accounting for the additional distress that may be expected from including terms for fatigue cracking, these values are too large to represent an end-of-construction serviceability.

There does appear to be a potential trend to the data when considering only PSI and rut depth, as is sketched in Figure 6.5 above as a dashed line. Assuming an initial PSI of 4.2, it is observed that rutting progresses with relatively minimal impact on PSI until approximately 0.4 to 0.8 in. after which PSI rapidly deteriorates. Considering the data in terms of ΔPSI vs. rut depth aids in devising a model that fits these requirements.

6.3 Select Model Forms

As previously discussed, the models must meet the following requirements at a minimum: physical sensibility and significance—i.e., ΔPSI=0 when RD=0; and statistical significance—i.e., acceptable R^2, no bias in residuals. Five separate model forms were attempted (Figure 6.6 and Table 6.2). Model 2 fails both physical and statistical significance tests while the remaining three models meet all physical requirements but have a coefficient of determination R^2 only equal to about 0.2.

The critical flaw in all the model forms is that they fail to capture the point at which the rate of change in PSI to rut depth steepens. Even the bilinear model (Model 5), which was formulated specifically to capture this turn in the relationship, did not produce good results. The slope for the second half of the model should be considerably steeper, indicating that rut depth progresses at a faster rate as PSI increases. However, the spread of data in the upper range (0.5-1 in.) skews this observation and results in nearly identical slopes for both parts of the bilinear model. Moreover, and indicative of the results pertaining to the slopes, the model is not sensitive to changes in the turning point and returns an $R^2 \approx 0.2$ for a turning point range of 0.25 to 0.75 inches of rutting.

To improve the fit (R^2) for these models, each was analyzed multiple times with select data. Data were stratified based on structural number, loop, lane, factorial block, etc. to decrease scatter and then analyzed with each model form. However, no regression yielded an R^2 higher than that achieved using all the data.

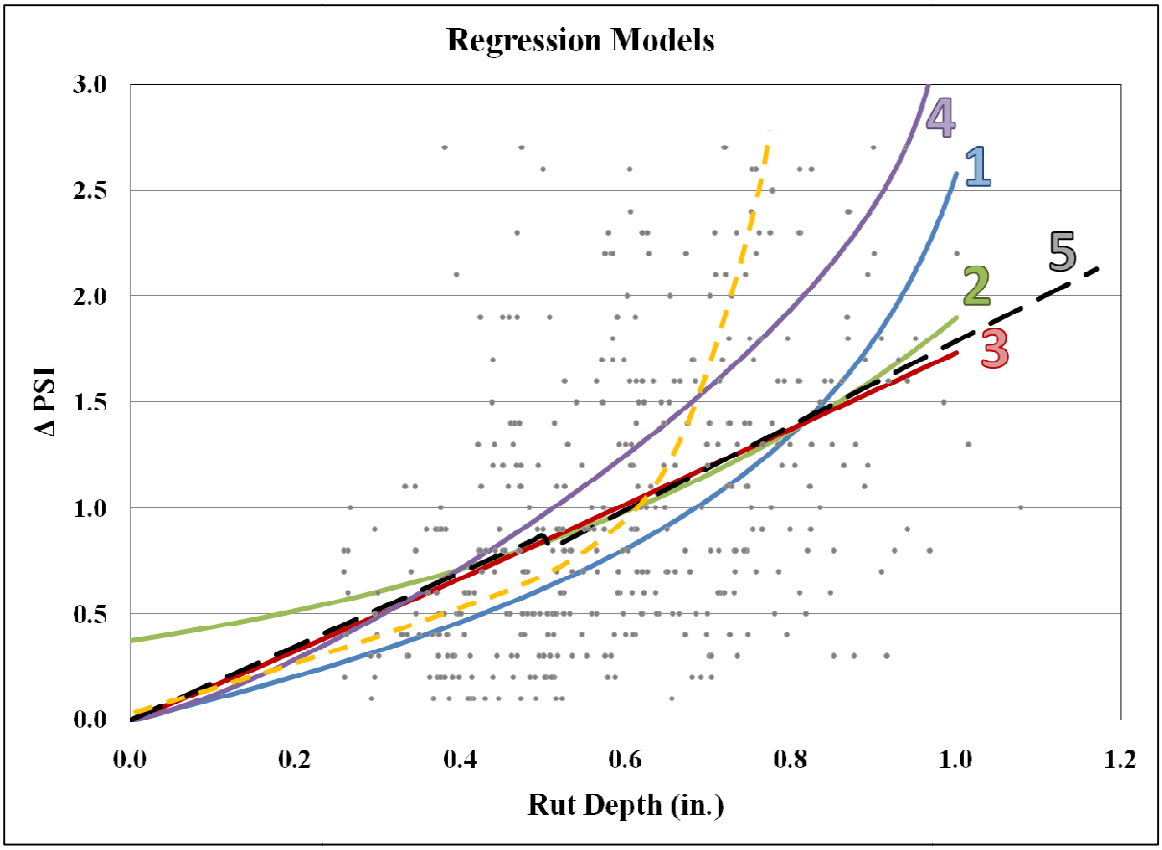

Figure 6.6: PSI vs. RD relationships. Model Forms for curves 1 through 5 are give in Table 6.2 and the yellow line represents the ideal case.

Table 6.2: PSI vs. RD Models and statistical significance.

Model ID	R^2	Model Form
1	0.14	$\Delta PSI = \frac{RD}{(1.1438 - RD)^{0.4878}}$
2	0.09	$\Delta PSI = \frac{1}{\left(1.2452 - 10^{\frac{RD - 57.9407}{93.9247}}\right)^{271.6183}} - \frac{1}{1.2452^{271.6183}}$
3	0.20	$\Delta PSI = \frac{1.5400\ RD}{1.8883 - RD^{0.0368}}$
4	0.20	$\Delta PSI = \frac{2.1864\ RD^{1.2771}}{(0.9950 - RD)^{-0.1011}}$
5	0.20	$\Delta PSI = \begin{cases} 1.7050 * RD & if\ RD \leq 0.5\ in. \\ -0.0449 + 1.7755 * RD & if\ RD > 0.5\ in. \end{cases}$

The most statistically successful model is the multivariate linear regression (R^2=0.25). However, Figure 6.7 shows that while the linear model involves all types of distress, it fails to capture the relationship between ΔPSI and rut depth adequately. To incorporate fatigue cracking while focusing on modeling rut depth, a hybrid model form was used which combined the best components of the linear, power, and piecewise models:

- Linear multivariate model incorporates all distress types.
- Power model best simulates the observed principal distress type (rutting).
- Piecewise model provides the flexibility to split the model into linear and power components

The ideal relationship, plotted as a dashed line in Figure 6.7, is observed to be relatively linear for rut depths less than half an inch and exponential for rutting greater than that. For the first half of the model, longitudinal cracking, alligator cracking, and rut depth terms are derived directly from the multivariate linear model. For the second half, the rutting term is altered to incorporate the most successful of the rut depth model forms.

Ultimately, the most successful model, presented below as Equation 6.6, was achieved using a simple power law for the rutting term. Statically, an R^2 of 0.21 for the piecewise-multivariate-power model is a negligible improvement over previous regressions. However, when the model is superimposed over the AASHO ΔPSI vs. MEPDG rut depth data, the model shows signs of physical significance and very nearly matches the ideal model form (Figure 6.7). Note that Figure 6.7 imposes the multivariate-linear model and piecewise-multivariate-power models on the AASHO

measured ΔPSI vs. MEPDG predicted RD. Since the models are functions of both rut depth and fatigue cracking, they cannot be plotted as a singular line in Figure 6.7.

$$\Delta PSI = \begin{cases} 0.0111(LC) + 0.0138\,(AC) + 1.6593(RD) & if\ RD \leq 0.5\ in. \\ -5.8259 + 7.5577(RD)^{0.2009} & if\ RD > 0.5\ in. \end{cases} \quad (6.6)$$

It is very clear that the piecewise-power model is the most successful model; incorporating both fatigue and rutting terms as well as capturing the PSI vs. RD relationship.

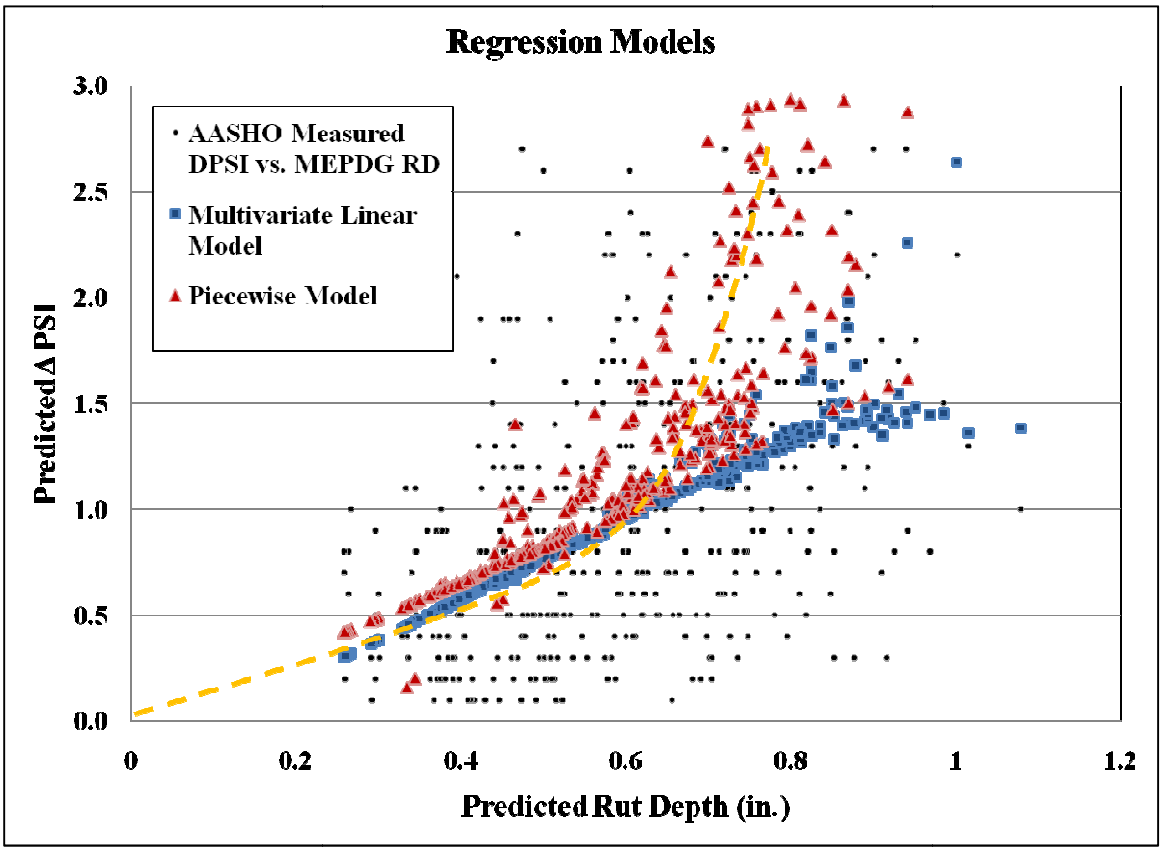

Figure 6.7: Piecewise-power and multivariate-linear distress models plotted over AASHO measured data; dashed yellow line is ideal model form.

Chapter 7: Key Insights and Lessons Learned

The purpose of this thesis is to compare the AASHTO empirical and MEPDG pavement design procedures and evaluate the major practical differences. There were three objectives to this study:

1. Verify the accuracy of the 1993 AASHTO Pavement Design Procedure and the Mechanistic-Empirical Pavement Design Guide predictions in the context of the AASHO Road Test;
2. Evaluate existing pavement performance measures and identify thresholds of serviceability that permit the user to convert between the framework of either procedure;
3. Identify the key practical differences with regard to structural capacity between the MEPDG and AASHTO 1993 design procedures.

This chapter reviews the findings of this research and discusses the overall success towards meeting each of these objectives. Additionally, lessons to learn from these results and future research recommendations are presented.

7.1 Accuracy of Design Predictions for the AASHO Road Test

The AASHO Road Test is used as a historical reference for this study to capitalize upon the weaknesses of the AASHTO empirical design procedure and turn them into strengths instead. Pavement performance based on one location, one environment, one set of materials, and well-defined traffic loads allowed for a high degree of control over the design details, thus minimizing the influence of input variable uncertainty on the final results.

Literature reviewed in preparation for this study suggests that several trends are expected in the data and results. First, because the AASHTO empirical procedure is derived from the Road Test, it is reasonable to anticipate predictions and measured data to agree well. This is found to be the case first in the pilot study and then again for the full data set. When evaluating performance based on design life (Figure 5.2) this result is seen directly with a respectable R^2=0.75. However, when evaluating pavement performance based on predicted distress (serviceability), it is necessary to first understand the shape of the AASHTO model and the context of the Road Test measured records. There is a steep drop off in both the measured results and the model form so that a small change in traffic results in a large change in PSI (Figure 4.2). Additionally, when using the inverted form of the AASHTO equation (solving for serviceability) there is a limiting value of PSI for any given SN and load combination (Figure 3.21). These two factors result in highly variable predictions and a correspondingly low coefficient of determination (R^2=0.37) (Figure 5.3). Once this is understood, it is reasonable to conclude that the AASHTO empirical predictions and measured AASHO records do in fact agree indirectly when using distress to access the accuracy of the AASHTO 1993 design procedure.

The second trend expected to manifest in the data is a prediction of thinner pavement sections by the MEPDG. Findings from the pilot study suggest that when evaluating predicted distress the MEPDG overpredicts measured performance (underpredicts distress accumulation) by approximately 1.0 PSI (Figure 4.1). Additionally, for the case of predicted service life MEPDG once again is found to overpredict the number of ESALs to reach failure (Figure 4.3). Practically, these results

translate to a prediction of thinner pavement sections as anticipated. Moreover, based on the observed distresses at the AASHO Road Test (Figure 3.10) it is expected that MEPDG will predict minimal fatigue distress and excessive rutting. The results presented in Chapter 5 confirm this expectation. In addition, the available measured rutting data agrees well with the MEPDG rut depth predictions (R^2=0.53) (Figure 5.9). While the specific rutting results only represent 10% of the population, they are a key component in both verifying the MEPDG rutting model and the development of the new performance measure relation discussed in Chapter 6.

7.2 Evaluation of Pavement Performance Measures

Defining an appropriate performance measure to compare the MEPDG and AASHTO 1993 design procedures has proven a difficult task. Because the AASHTO 1993 procedure is evaluated in terms of the semi-qualitative present serviceability index and MEPDG predicts individual distresses there is no direct correlation. As discussed in Chapter 2, there are several existing empirical relationships between PSI and IRI, with the Al-Omari and Darter (1994) model most applicable to this research. However, because this relationship was developed using in-service pavements it was ultimately found to not fit the AASHO Road Test data (Figure 5.10). Moreover, even the basic model form suggested by Al-Omari and Darter is unsuitable for the Road Test data. The discrepancy is due to the inherent conditions at the Road Test. Observation of the distress histories reveals a significant seasonal influence on distress accumulation. In the most extreme cases, PSI rapidly decreases between February and March each year and nearly halts during the remainder of the year (Figure 3.19). The root of the disagreement between measured PSI and predicted IRI lies in the MEPDG IRI model itself. The nearly

linear MEPDG predictions of IRI vs. time fail to capture the dramatic seasonal drops in PSI that actually occurred at the Road Test.

A database of the AASHO Road Test structural pavement sections, AASHTO 1993, and MEPDG predictions was therefore created for developing credible alternative models relating AASHO PSI directly to MEPDG distress predictions. Several approaches were used to develop these models, as detailed in Chapter 6. The largest coefficient of determination achieved for a physically sensible model is R^2=0.21 for a piecewise-multivariate-power model. Predicted serviceability vs. rut depth plays a critical role in the development of this model. Measured PSI decreases gradually with predicted rut depth until approximately 0.4 inches of rutting, after which PSI then rapidly deteriorates. Although the R^2 value for this model is still quite low, it is successful in mirroring the measured ΔPSI vs. predicted RD trends observed in Figure 6.7.

7.3 Discussion

The purpose of this research is not just to evaluate how AASHTO and MEPDG predictions relate to each other, but also how close they match actual performance. The AASHO Road Test was chosen as a real-world comparison to put the design predictions in perspective. Furthermore, it was expected that the AASHTO predictions would correspond well with the AASHO measured data while MEPDG would overpredict design life. As discussed above, AASHTO and MEPDG expectations based upon past studies were met, verifying the accuracy of the design procedures.

However, difficulty arose in quantifying the differences between the two procedures. Lacking a suitable comparative performance measure to fit the conditions of the Road Test, one was derived based on measured serviceability and predicted distress

with limited success (R^2=0.21). There are several likely causes to explain the weak correlation between predicted distresses and measured serviceability including:

- Limited availability of AASHO Road Test data. Access to more detailed distress histories will unlikely change the results, but would improve confidence in the final model.
- The seasonal influence on the pavement performance at the Road Test. This is particularly important because there are only two years worth of data to analyze making it critical to fit the traffic and climate models accurately.
- Use of the nationally calibrated MEPDG models to predict distresses for localized conditions. Both Kim *et al.* (2010) and Li *et al.* (2009) found that calibrating the MEPDG models was vital to successful implementation on the state level. No flexible pavements from Illinois were used in the national calibration of the MEPDG implying that agreement may be particularly poor for this state. (NCHRP, 2004)

Efforts were made to develop a correlation between the AASHTO predicted PSI and MEPDG predicted distresses as well, with no improvement over the initial attempts. Furthermore, neither stratification of the data nor use of weighted PSIs improved the model fit. Therefore, it is concluded that the model presented in Equation 6.6 with an R^2=0.21 is the best possible result for these conditions.

7.4 Lessons Learned and Future Research Recommendations

The main criticism of the AASHO Road Test relative to this study is the limited range of traffic loading. Beyond 2 million ESALs the AASHO Road Test is no longer useful for comparison; there is no longer a 'real' result to compare against the AASHTO

1993 and MEPDG predictions. As such, all findings discussed above should be viewed within that context and may not necessarily hold true for traffic levels above 2 million ESALs. Even within the scope of the AASHO Road Test, the range of data is extremely limited. Except for about two dozen test sections having measured rutting data, the subjective PSI values are the only performance measure available. This makes it impossible to evaluate directly any of the performance measures predicted by the MEPDG. Future research efforts will benefit from using a more realistic historic source that better accommodates comparison under 'real' circumstances. For example, a more substantial design life as well as materials and traffic similar to those in practice today. The FHWA Long Term Pavement Performance (LTPP) database is the obvious source for these data. However, given the wide range of pavement structures, material properties, traffic, and environmental conditions spanned in the LTPP database, performing a comparative study between the MEPDG and 1993 AASHTO procedures for a large set of LTPP sections is a major undertaking.

Ultimately, the link between empirical design and the MEPDG will be found in historical pavement data. The AASHO Road Test is a great source for detailed material, traffic, and climate inputs. However, it is only useful for considering the broad strokes in performance trends. To quantify the key practical differences with regard to structural capacity between the MEPDG and AASHTO 1993 design procedures a more modern source like the LTPP database should be employed. This is presently the biggest hurdle to implementing the MEPDG. State agencies will need to refine what data is collected for their pavement management information systems before the MEPDG will be useful as an independent design tool.

Appendix A: Flexible Pavement Database

The Flexible Pavement Database contains all pertinent information about the AASHO Road Test, AASHTO 1993 predictions, and MEPDG predictions for this thesis. There are several software options that serve as a suitable platform for this application; the options were narrowed down to Microsoft Access and Microsoft Excel due to universal acceptance and availability. Access provides more flexibility to cluster, link, quarry, and protect information; however Excel was chosen for more powerful regression and plotting options.

The Flexible Pavement Database is a complete compilation of the AASHO Road Test Main Factorial Design and houses the data for roughly 284 individual structural sections. An example of the database layout is given below in Figure A.1. It includes all pertinent Road Test identification information (loop, lane, factorial block, SID, layer thicknesses, SN) and result data available in the AASHO reports (axle applications and PSI). Alongside the measured data for each structural section is the corresponding MEPDG and AASHTO 1993 distress predictions.

The AASHTO analysis is carried out with the two methodologies discussed in Chapter 3. Predicted distress is determined using the AASHO measured ESALs while predicted design life is determined using the AASHO measured PSI. AASHTO predictions are computed directly in Excel and, though not show in Figure A.1, a full breakdown of calculations is available in the attached electronic database. Rutting measurements are available for 24 structural sections. To preserve continuity in the main

database this data is stored separately but follows the same logic and design concepts as previously described.

The MEPDG generates an Excel file summarizing predictions as part of the analysis procedure. The predictions are stored as links in the database and refer directly to the original summary outputs generated by the MEPDG software itself. This provides the flexibility to alter various components of the MEPDG analysis and re-run a project, the database will automatically update the new content when next opened. However, users without access to the MEPDG source files should disable links to avoid corrupting the data.

SECTION ID									AASHO					MEPDG						AASHTO	
LANE	LOOP	Block	ID	D1 SURFACE (in.)	D2 BASE (in.)	D3 SUBBASE (in.)	TOTAL (in.)	SN	Time	Axle Applications	Truck Applications	ESAL	PSI	Month	Longitudinal Cracking (ft/mi)	Alligator Cracking (%)	Total Rutting (in)	IRI	Heavy Trucks	PSI	ESALs
									Nov-58	7,047	3,523	31,922	3.5	Nov-58	0.14	0.134	0.436	62.6	15,493	2.9	97,806
														Dec-58	0.39	0.326	0.492	65.1	30,985		
														Jan-59	0.59	0.479	0.521	66.4	46,478		
									Feb-59	69,502	34,751	439,285	3.0	Feb-59	1.28	0.783	0.57	68.6	61,971	1.2	155,660
									Mar-59	71,450	35,725	745,406	1.5	Mar-59	3.31	1.26	0.631	71.5	77,463	0.7	313,187
														Apr-59	7.49	2.03	0.676	73.9	92,956		
														May-59	20.5	3.74	0.763	78.5	108,449		
														Jun-59	34.2	5.34	0.813	81.5	123,942		
														Jul-59	50	7.2	0.859	84.5	139,434		
														Aug-59	65.5	8.84	0.888	86.7	154,927		
														Sep-59	78.3	10.1	0.906	88.2	170,420		
1	6	3	269	4	3	8	15	3.06						Oct-59	83	10.7	0.911	88.9	185,912		
														Nov-59	86.7	11.3	0.917	89.5	216,882		
														Dec-59	89.7	11.8	0.921	90	247,852		
														Jan-60	90.5	12	0.923	90.3	278,822		
														Feb-60	96	12.8	0.929	91	309,792		
														Mar-60	104	13.7	0.935	91.9	340,762		
														Apr-60	120	15.1	0.945	93.2	371,732		
														May-60	164	18	0.973	96.2	402,701		
														Jun-60	222	21.5	1.011	100.1	433,671		
														Jul-60	289	25.2	1.058	104.6	464,641		
														Aug-60	336	27.6	1.076	107.1	495,611		
														Sep-60	366	29.1	1.086	108.7	526,581		
														Oct-60	379	29.8	1.09	109.5	557,551		
														Nov-58	0.09	0.107	0.433	62.5	15,493		
														Dec-58	0.27	0.261	0.486	64.8	30,985		
														Jan-59	0.39	0.378	0.512	66	46,478		
														Feb-59	0.88	0.624	0.559	68.1	61,971		
									Mar-59	79,616	39,808	218,051	3.7	Mar-59	2.12	0.997	0.619	70.8	77,463	3.3	111,645
									Apr-59	85,901	42,951	307,218	3.5	Apr-59	4.66	1.59	0.664	73.1	92,956	1.9	166,215
									May-59	107,152	53,576	587,610	3.0	May-59	12.2	2.96	0.755	77.7	108,449	1.7	314,434
									Jun-59	132,739	66,370	959,521	2.5	Jun-59	19.4	4.18	0.797	80.2	123,942	1.4	474,722
									Jul-59	188,799	94,400	1,674,391	2.0	Jul-59	29.6	5.66	0.841	82.9	139,434	1.1	643,984
									Aug-59	233,346	116,673	2,217,305	1.8	Aug-59	39.4	6.99	0.869	84.9	154,927		713,788
														Sep-59	47.2	8.04	0.886	86.2	170,420		
														Oct-59	49.6	8.52	0.891	86.7	185,912		
1	6	2	299	4	3	12	19	3.5						Nov-59	51.4	9.02	0.897	87.3	216,882		
									Dec-59	372,392	186,196	3,885,016	1.5	Dec-59	52.8	9.46	0.901	87.8	247,852	0.6	820,482
														Jan-60	53.4	9.66	0.903	88.1	278,822		
														Feb-60	56.2	10.4	0.911	88.9	309,792		
														Mar-60	60.4	11.2	0.917	89.7	340,762		
														Apr-60	69.3	12.4	0.927	90.9	371,732		
														May-60	93.7	14.8	0.952	93.4	402,701		
														Jun-60	128	17.6	0.986	96.6	433,671		
														Jul-60	174	20.8	1.032	100.6	464,641		
														Aug-60	204	23	1.05	102.8	495,611		
														Sep-60	222	24.3	1.059	104.1	526,581		
														Oct-60	229	25	1.062	104.8	557,551		

Figure A.1: Example of Flexible Pavement Database containing AASHO Road Test SID and distress history data, AASHTO predictions, and MEPDG predictions.

Appendix B: AASHO Road Test Transverse Profile Data

AASHO ROAD TEST												MEPDG
LOOP	ID	SN	ESAL	RUTTING DATA								Total Rutting (in)
				TRANSVERSE PROFILE							AVERAGE RD	
				TIME	Original Profile	12.0	9.0	6.0	3.0	0.0		
2	749	2.16	4,041	July 1959	Change in Elevation	0.4	0.0	0.0	-0.2	-0.1	-0.1	0.1
					Transverse Profile	-1.1	-0.9	-0.5	-0.4	-0.1		
					Rut Depth		-0.1		-0.1			
				October 1959	Change in Elevation	0.1	-0.1	-0.1	-0.2	-0.1	0.0	0.1
					Transverse Profile	-1.4	-1.0	-0.6	-0.4	-0.1		
					Rut Depth		0.0		-0.1			
				March 1960	Change in Elevation	1.2	0.6	0.5	X	0.4	-0.2	0.1
					Transverse Profile	-0.3	-0.3	0.0	X	0.4		
					Rut Depth		-0.2		X			
				August 1960	Change in Elevation	0.0	-0.2	-0.2	-0.5	-0.4	-0.1	0.1
					Transverse Profile	-1.5	-1.1	-0.7	-0.7	-0.4		
					Rut Depth		0.0		-0.2			
				October 1960	Change in Elevation	0.0	-0.2	-0.1	-0.5	-0.4	-0.1	0.1
					Transverse Profile	-1.5	-1.1	-0.6	-0.7	-0.4		
					Rut Depth		-0.1		-0.2			
2	763	2.6	11,122	July 1959	Change in Elevation	0.2	0.0	0.2	0.1	0.1	-0.1	0.1
					Transverse Profile	-1.3	-0.9	-0.3	-0.1	0.1		
					Rut Depth		-0.1		0.0			

				October 1959	Change in Elevation	-0.1	-0.4	-0.1	-0.1	-0.1	-0.1	0.1
					Transverse Profile	-1.6	-1.3	-0.6	-0.3	-0.1		
					Rut Depth		-0.2		0.0			
				March 1960	Change in Elevation	0.6	0.1	0.2	0.2	0.2	-0.1	0.1
					Transverse Profile	-0.9	-0.8	-0.3	0.0	0.2		
					Rut Depth		-0.2		0.1			
				August 1960	Change in Elevation	-0.1	-0.2	-0.1	-0.2	-0.2	0.0	0.1
					Transverse Profile	-1.6	-1.1	-0.6	-0.4	-0.2		
					Rut Depth		0.0		0.0			
				October 1960	Change in Elevation	-0.2	-0.4	-0.1	-0.4	-0.2	-0.2	0.1
					Transverse Profile	-1.7	-1.3	-0.6	-0.6	-0.2		
					Rut Depth		-0.2		-0.2			
3	123	3.04	163,926	July 1959	Change in Elevation	-0.1	-0.2	0.1	0.0	0.2	-0.1	0.3
					Transverse Profile	-1.6	-1.1	-0.4	-0.2	0.2		
					Rut Depth		-0.1		-0.1			
				October 1959	Change in Elevation	0.0	-0.5	-0.1	-0.2	0.0	-0.2	0.4
					Transverse Profile	-1.5	-1.4	-0.6	-0.4	0.0		
					Rut Depth		-0.4		-0.1			
				March 1960	Change in Elevation	-0.1	-0.5	0.4	0.2	0.5	-0.4	0.4
					Transverse Profile	-1.6	-1.4	-0.1	0.0	0.5		
					Rut Depth		-0.6		-0.2			
3	139	3.48	522,242	July 1959	Change in Elevation	0.1	-0.1	0.0	-0.2	0.0	-0.1	0.3
					Transverse Profile	-1.4	-1.0	-0.5	-0.4	0.0		
					Rut Depth		-0.1		-0.2			
				October 1959	Change in Elevation	0.0	-0.2	0.0	-0.2	0.0	-0.1	0.3

					Transverse Profile	-1.5	-1.1	-0.5	-0.4	0.0		
					Rut Depth		-0.1		-0.2			
					Change in Elevation	0.5	-0.1	0.2	-0.1	0.1		
				March 1960	Transverse Profile	-1.0	-1.0	-0.3	-0.3	0.1	-0.3	0.4
					Rut Depth		-0.4		-0.2			
					Change in Elevation	-0.2	-0.5	0.0	-0.5	-0.1		
				August 1960	Transverse Profile	-1.7	-1.4	-0.5	-0.7	-0.1	-0.4	0.4
					Rut Depth		-0.3		-0.4			
					Change in Elevation	-0.2	-0.5	-0.1	-0.5	-0.1		
				October 1960	Transverse Profile	-1.7	-1.4	-0.6	-0.7	-0.1	-0.3	0.4
					Rut Depth		-0.3		-0.4			
					Change in Elevation	-0.2	-0.6	-0.1	-0.5	-0.2		
				July 1959	Transverse Profile	-1.7	-1.5	-0.6	-0.7	-0.2	-0.4	0.4
					Rut Depth		-0.5		-0.3			
					Change in Elevation	-0.1	-0.6	-0.1	-0.6	-0.2		
				November 1959	Transverse Profile	-1.6	-1.5	-0.6	-0.8	-0.2	-0.5	0.4
					Rut Depth		-0.5		-0.4			
					Change in Elevation	0.4	-0.4	0.0	-0.5	0.0		
4	581	4.36	1,114,000	March 1960	Transverse Profile	-1.1	-1.3	-0.5	-0.7	0.0	-0.5	0.4
					Rut Depth		-0.5		-0.5			
					Change in Elevation	-0.8	-1.2	-0.5	-1.1	-0.6		
				August 1960	Transverse Profile	-2.3	-2.1	-1.0	-1.3	-0.6	-0.5	0.5
					Rut Depth		-0.5		-0.5			
					Change in Elevation	-0.5	-1.0	-0.2	-1.0	-0.4		
				October 1960	Transverse Profile	-2.0	-1.9	-0.7	-1.2	-0.4	-0.6	0.5
					Rut Depth		-0.5		-0.7			

4	601	3.48	621,000	July 1959	Change in Elevation	-0.2	-0.7	-0.1	-0.4	-0.1	-0.4	0.6
					Transverse Profile	-1.7	-1.6	-0.6	-0.6	-0.1		
					Rut Depth		-0.5		-0.3			
				November 1959	Change in Elevation	-0.2	-0.7	-0.1	-0.6	-0.1	-0.5	0.6
					Transverse Profile	-1.7	-1.6	-0.6	-0.8	-0.1		
					Rut Depth		-0.5		-0.5			
				March 1960	Change in Elevation	0.0	-0.7	-0.2	-0.6	-0.1	-0.5	0.7
					Transverse Profile	-1.5	-1.6	-0.7	-0.8	-0.1		
					Rut Depth		-0.5		-0.4			
4	629	3.48	593,500	July 1959	Change in Elevation	-0.5	-0.8	-0.1	-0.5	-0.1	-0.4	0.4
					Transverse Profile	-2.0	-1.7	-0.6	-0.7	-0.1		
					Rut Depth		-0.5		-0.4			
				October 1959	Change in Elevation	-0.2	-0.6	0.0	-0.4	0.1	-0.5	0.5
					Transverse Profile	-1.7	-1.5	-0.5	-0.6	0.1		
					Rut Depth		-0.5		-0.4			
				March 1960	Change in Elevation	0.4	-0.4	0.2	-0.1	0.4	-0.5	0.5
					Transverse Profile	-1.1	-1.3	-0.3	-0.3	0.4		
					Rut Depth		-0.6		-0.4			
4	621	3.52	589,000	July 1959	Change in Elevation	-0.4	-1.0	-0.1	-0.5	-0.1	-0.4	0.4
					Transverse Profile	-1.9	-1.9	-0.6	-0.7	-0.1		
					Rut Depth		-0.5		-0.4			
				October 1959	Change in Elevation	-0.4	-1.0	-0.2	-0.6	-0.1	-0.5	0.4
					Transverse Profile	-1.9	-1.9	-0.7	-0.8	-0.1		
					Rut Depth		-0.5		-0.4			
				March 1960	Change in Elevation	0.1	-0.8	0.0	-0.5	0.0	-0.6	0.4

					Transverse Profile	-1.4	-1.7	-0.5	-0.7	0.0		
					Rut Depth		-0.8		-0.5			
5	425	3.92	1,131,815	July 1959	Change in Elevation	-0.4	-0.1	-0.2	-0.1	-0.2	-0.5	0.6
					Transverse Profile	-1.9	-1.0	-0.7	-0.3	-0.2		
					Rut Depth		-0.5		-0.4			
				March 1960	Change in Elevation	0.2	-0.8	0.0	-0.8	0.1	-0.8	0.6
					Transverse Profile	-1.3	-1.7	-0.5	-1.0	0.1		
					Rut Depth		-0.8		-0.8			
5	427	4.78	1,882,743	July 1959	Change in Elevation	-0.1	-0.5	0.0	-0.4	0.0	-0.4	0.5
					Transverse Profile	-1.6	-1.4	-0.5	-0.6	0.0		
					Rut Depth		-0.4		-0.4			
				November 1959	Change in Elevation	-0.2	-0.6	-0.1	-0.6	-0.1	-0.4	0.5
					Transverse Profile	-1.7	-1.5	-0.6	-0.8	-0.1		
					Rut Depth		-0.4		-0.5			
				March 1960	Change in Elevation	0.7	-0.2	0.1	-0.2	0.1	-0.4	0.5
					Transverse Profile	-0.8	-1.1	-0.4	-0.4	0.1		
					Rut Depth		-0.5		-0.3			
				August 1960	Change in Elevation	-0.7	-0.8	-0.2	-0.7	-0.2	-0.4	0.6
					Transverse Profile	-2.2	-1.7	-0.7	-0.9	-0.2		
					Rut Depth		-0.3		-0.5			
				October 1960	Change in Elevation	-0.8	-1.0	0.2	-0.7	-0.2	-0.6	0.6
					Transverse Profile	-2.3	-1.9	-0.3	-0.9	-0.2		
					Rut Depth		-0.6		-0.7			
5	441	3.9	2,228,276	July 1959	Change in Elevation	-0.1	-0.7	-0.1	-0.7	-0.1	-0.5	0.7

					Transverse Profile	-1.6	-1.6	-0.6	-0.9	-0.1		
					Rut Depth		-0.5		-0.6			
					Change in Elevation	-0.2	-0.8	-0.2	-0.8	-0.1		
				November 1959	Transverse Profile	-1.7	-1.7	-0.7	-1.0	-0.1	-0.6	0.7
					Rut Depth		-0.5		-0.6			
					Change in Elevation	0.4	-0.6	0.0	-0.6	0.0		
				March 1960	Transverse Profile	-1.1	-1.5	-0.5	-0.8	0.0	-0.6	0.8
					Rut Depth		-0.7		-0.6			
					Change in Elevation	-0.1	-0.8	-0.1	-0.7	-0.1		
				November 1959	Transverse Profile	-1.6	-1.7	-0.6	-0.9	-0.1	-0.6	0.5
					Rut Depth		-0.6		-0.6			
					Change in Elevation	0.5	-0.5	0.1	-0.5	0.2		
				March 1960	Transverse Profile	-1.0	-1.4	-0.4	-0.7	0.2	-0.7	0.5
					Rut Depth		-0.7		-0.6			
5	445	4.36	1,583,314		Change in Elevation	-1.0	-1.3	-0.4	-1.1	-0.2		
				August 1960	Transverse Profile	-2.5	-2.2	-0.9	-1.3	-0.2	-0.6	0.6
					Rut Depth		-0.5		-0.8			
					Change in Elevation	-0.8	-1.4	-0.4	-1.2	-0.2		
				October 1960	Transverse Profile	-2.3	-2.3	-0.9	-1.4	-0.2	-0.8	0.6
					Rut Depth		-0.7		-0.9			
					Change in Elevation	0.0	-0.5	0.0	-0.5	-0.1		
				November 1959	Transverse Profile	-1.5	-1.4	-0.5	-0.7	-0.1	-0.4	0.5
					Rut Depth		-0.4		-0.4			
5	447	4.34	2,392,259		Change in Elevation	0.8	0.0	0.4	-0.1	0.2		
				March 1960	Transverse Profile	-0.7	-0.9	-0.1	-0.3	0.2	-0.4	0.5
					Rut Depth		-0.5		-0.4			

				August 1960	Change in Elevation	-0.6	-0.7	-0.1	-0.8	-0.2	-0.4	0.6
					Transverse Profile	-2.1	-1.6	-0.6	-1.0	-0.2		
					Rut Depth		-0.3		-0.6			
				October 1960	Change in Elevation	-0.6	-1.0	-0.1	-1.0	-0.2	-0.7	0.6
					Transverse Profile	-2.1	-1.9	-0.6	-1.2	-0.2		
					Rut Depth		-0.6		-0.8			
5	469	3.92	1,254,839	July 1959	Change in Elevation	-0.1	-0.7	0.0	-0.5	-0.1	-0.5	0.5
					Transverse Profile	-1.6	-1.6	-0.5	-0.7	-0.1		
					Rut Depth		-0.6		-0.4			
				November 1959	Change in Elevation	-0.2	-1.0	-0.1	-0.8	-0.2	-0.7	0.5
					Transverse Profile	-1.7	-1.9	-0.6	-1.0	-0.2		
					Rut Depth		-0.8		-0.6			
				March 1960	Change in Elevation	0.5	-0.4	0.2	-0.4	0.0	-0.6	0.5
					Transverse Profile	-1.0	-1.3	-0.3	-0.6	0.0		
					Rut Depth		-0.7		-0.5			
				October 1960	Change in Elevation						-0.6	0.6
					Transverse Profile	-1.0	-1.3	-0.3	-0.6	0.0		
					Rut Depth		-0.7		-0.5			
5	475	3.9	1,222,384	July 1959	Change in Elevation	-0.2	-0.8	-0.1	-0.7	-0.1	-0.6	0.5
					Transverse Profile	-1.7	-1.7	-0.6	-0.9	-0.1		
					Rut Depth		-0.6		-0.6			
				November 1959	Change in Elevation	0.0	-0.6	0.2	-0.4	0.0	-0.5	0.5
					Transverse Profile	-1.5	-1.5	-0.3	-0.6	0.0		
					Rut Depth		-0.6		-0.5			
				March 1960	Change in Elevation	0.4	-0.5	0.1	-0.5	0.1	-0.6	0.5
					Transverse Profile	-1.1	-1.4	-0.4	-0.7	0.1		

					Rut Depth		-0.7		-0.6			
				October 1960	Change in Elevation Transverse Profile Rut Depth	-1.1	-1.4 -0.7	-0.4	-0.7 -0.6	0.1	-0.6	0.6
5	477	4.34	2,480,338	July 1959	Change in Elevation Transverse Profile Rut Depth	0.0 -1.5	-0.7 -1.6 -0.6	0.0 -0.5	-0.6 -0.8 -0.6	0.0 0.0	-0.6	0.6
				March 1960	Change in Elevation Transverse Profile Rut Depth	0.4 -1.1	-0.6 -1.5 -0.8	0.1 -0.4	-0.4 -0.6 -0.4	0.0 0.0	-0.6	0.6
				June 1960	Change in Elevation Transverse Profile Rut Depth	-0.7 -2.2	-1.3 -2.2 -0.7	-0.3 -0.8	-0.8 -1.0 -0.5	-0.3 -0.3	-0.6	0.7
				August 1960	Change in Elevation Transverse Profile Rut Depth	-1.1 -2.6	-1.6 -2.5 -0.6	-0.7 -1.2	-1.7 -1.9 -1.1	-0.5 -0.5	-0.8	0.7
				October 1960	Change in Elevation Transverse Profile Rut Depth	-0.6 -2.1	-1.2 -2.1 -0.8	-0.1 -0.6	-0.8 -1.0 -0.7	-0.1 -0.1	-0.7	0.7
5	479	3.94	1,366,759	July 1959	Change in Elevation Transverse Profile Rut Depth	-0.1 -1.6	-1.0 -1.9 -0.8	-0.2 -0.7	-0.8 -1.0 -0.5	-0.4 -0.4	-0.6	0.5
				November 1959	Change in Elevation Transverse Profile Rut Depth	0.1 -1.4	-0.7 -1.6 -0.7	0.1 -0.4	-0.6 -0.8 -0.6	0.0 0.0	-0.7	0.5

				March 1960	Change in Elevation	0.7	-0.2	0.4	-0.4	0.5	-0.7	0.5
					Transverse Profile	-0.8	-1.1	-0.1	-0.6	0.5		
					Rut Depth		-0.7		-0.8			
				June 1960	Change in Elevation	-0.7	-1.5	-0.2	-0.8	-0.1	-0.8	0.6
					Transverse Profile	-2.2	-2.4	-0.7	-1.0	-0.1		
					Rut Depth		-1.0		-0.6			
				August 1960	Change in Elevation	-1.1	-1.7	-0.6	-1.3	-0.5	-0.7	0.6
					Transverse Profile	-2.6	-2.6	-1.1	-1.5	-0.5		
					Rut Depth		-0.8		-0.7			
				October 1960	Change in Elevation	-0.8	-1.6	-0.2	-1.1	0.0	-0.7	0.6
					Transverse Profile	-0.8	-1.1	-0.1	-0.6	0.5		
					Rut Depth		-0.7		-0.8			
6	255	4.82	3,793,657	July 1959	Change in Elevation	-0.8	-1.1	-0.2	-0.6	-0.1	-0.5	0.6
					Transverse Profile	-2.3	-2.0	-0.7	-0.8	-0.1		
					Rut Depth		-0.5		-0.4			
				October 1959	Change in Elevation	-0.7	-1.0	-0.2	-0.6	0.0	-0.5	0.6
					Transverse Profile	-2.2	-1.9	-0.7	-0.8	0.0		
					Rut Depth		-0.5		-0.5			
				March 1960	Change in Elevation	-0.6	-1.3	-0.3	-0.8	0.1	-0.7	0.7
					Transverse Profile	-2.1	-2.2	-0.8	-1.0	0.1		
					Rut Depth		-0.8		-0.7			
6	263	4.78	4,170,789	July 1959	Change in Elevation	-0.5	-1.2	-0.1	-1.0	-0.2	-0.8	0.6
					Transverse Profile	-2.0	-2.1	-0.6	-1.2	-0.2		
					Rut Depth		-0.8		-0.8			
				October 1959	Change in Elevation	-0.7	-1.0	-0.4	-1.2	-0.4	-0.6	0.6

					Transverse Profile	-2.2	-1.9	-0.9	-1.4	-0.4		
					Rut Depth		-0.4		-0.8			
				March 1960	Change in Elevation	0.0	-1.0	0.0	-0.7	0.1	-0.8	0.6
					Transverse Profile	-1.5	-1.9	-0.5	-0.9	0.1		
					Rut Depth		-0.9		-0.7			
6	309	4.78	7,005,006	July 1959	Change in Elevation	-0.5	-1.1	-0.2	-0.6	-0.2	-0.5	0.8
					Transverse Profile	-2.0	-2.0	-0.7	-0.8	-0.2		
					Rut Depth		-0.7		-0.4			
				October 1959	Change in Elevation	-0.6	-1.1	-0.2	-0.7	-0.2	-0.5	0.8
					Transverse Profile	-2.1	-2.0	-0.7	-0.9	-0.2		
					Rut Depth		-0.6		-0.5			
				March 1960	Change in Elevation	-0.1	-1.0	-0.1	-0.5	0.0	-0.6	0.9
					Transverse Profile	-1.6	-1.9	-0.6	-0.7	0.0		
					Rut Depth		-0.8		-0.4			
				June 1960	Change in Elevation	-1.0	-1.3	-0.3	-0.8	-0.2	-0.5	0.9
					Transverse Profile	-2.5	-2.2	-0.8	-1.0	-0.2		
					Rut Depth		-0.6		-0.5			
				August 1960	Change in Elevation	-1.2	-1.3	-0.4	-1.1	-0.2	-0.6	1.0
					Transverse Profile	-2.7	-2.2	-0.9	-1.3	-0.2		
					Rut Depth		-0.4		-0.8			
				October 1960	Change in Elevation	-1.3	-1.7	-0.4	-1.2	-0.4	-0.8	1.0
					Transverse Profile	-2.8	-2.6	-0.9	-1.4	-0.4		
					Rut Depth		-0.8		-0.8			
6	333	5.66	7,619,718	July 1959	Change in Elevation	-0.4	-1.0	-0.2	-0.7	-0.4	-0.5	0.6
					Transverse Profile	-1.9	-1.9	-0.7	-0.9	-0.4		

					Rut Depth		-0.6		-0.4			
				October 1959	Change in Elevation	-0.6	-1.1	-0.4	-1.0	-0.4	-0.5	0.6
					Transverse Profile	-2.1	-2.0	-0.9	-1.2	-0.4		
					Rut Depth		-0.5		-0.6			
				March 1960	Change in Elevation	0.0	-1.0	-0.4	-0.8	-0.4	-0.5	0.6
					Transverse Profile	-1.5	-1.9	-0.9	-1.0	-0.4		
					Rut Depth		-0.7		-0.4			
				June 1960	Change in Elevation	-1.2	-1.6	-0.5	-1.1	-0.6	-0.6	0.7
					Transverse Profile	-2.7	-2.5	-1.0	-1.3	-0.6		
					Rut Depth		-0.7		-0.5			
				August 1960	Change in Elevation	-1.2	-1.3	-0.5	-1.0	-0.6	-0.4	0.7
					Transverse Profile	-2.7	-2.2	-1.0	-1.2	-0.6		
					Rut Depth		-0.4		-0.4			
				October 1960	Change in Elevation	-1.3	-1.8	-0.6	-1.2	-0.7	-0.6	0.7
					Transverse Profile	-2.8	-2.7	-1.1	-1.4	-0.7		
					Rut Depth		-0.8		-0.5			
2	750	2.16	40,809	July 1959	Change in Elevation	0.1	-0.2	-0.4	-0.4	-0.1	0.0	0.0
					Transverse Profile	-1.4	-1.1	-0.9	-0.6	-0.1		
					Rut Depth		0.0		-0.1			
				October 1959	Change in Elevation	-0.1	-0.4	-0.4	-0.4	-0.1	-0.1	0.2
					Transverse Profile	-1.6	-1.3	-0.9	-0.6	-0.1		
					Rut Depth		-0.1		-0.1			
				March 1960	Change in Elevation	0.8	0.0	0.2	0.0	0.4	-0.3	0.2
					Transverse Profile	-0.7	-0.9	-0.3	-0.2	0.4		
					Rut Depth		-0.4		-0.3			
				August 1960	Change in Elevation	-0.4	-0.7	-0.4	-0.5	-0.4	-0.1	0.2

					Transverse Profile	-1.9	-1.6	-0.9	-0.7	-0.4		
					Rut Depth		-0.2		0.0			
					Change in Elevation	-0.2	-0.5	-0.2	-0.5	-0.4		
				October 1960	Transverse Profile	-1.7	-1.4	-0.7	-0.7	-0.4	-0.2	0.2
					Rut Depth		-0.2		-0.2			
					Change in Elevation	0.1	-0.1	0.1	0.0	0.1		
				July 1959	Transverse Profile	-1.4	-1.0	-0.4	-0.2	0.1	-0.1	0.2
					Rut Depth		-0.1		-0.1			
					Change in Elevation	-0.2	-0.4	-0.2	-0.4	-0.1		
				October 1959	Transverse Profile	-1.7	-1.3	-0.7	-0.6	-0.1	-0.2	0.2
					Rut Depth		-0.1		-0.2			
					Change in Elevation	0.6	-0.1	0.1	0.0	0.2		
2	764	2.6	110,083	March 1960	Transverse Profile	-0.9	-1.0	-0.4	-0.2	0.2	-0.2	0.2
					Rut Depth		-0.4		-0.1			
					Change in Elevation	-0.4	-0.4	-0.2	-0.4	-0.2		
				August 1960	Transverse Profile	-1.9	-1.3	-0.7	-0.6	-0.2	-0.1	0.2
					Rut Depth		0.0		-0.2			
					Change in Elevation	-0.4	-0.5	-0.4	-0.5	-0.2		
				October 1960	Transverse Profile	-1.9	-1.4	-0.9	-0.7	-0.2	-0.1	0.2
					Rut Depth		0.0		-0.2			
					Change in Elevation	0.5	0.0	0.2	-0.1	0.2		
				July 1959	Transverse Profile	-1.0	-0.9	-0.3	-0.3	0.2	-0.3	0.5
3	124	3.04	193,365		Rut Depth		-0.3		-0.3			
					Change in Elevation	0.2	0.2	0.1	-0.4	0.0		
				October 1959	Transverse Profile	-1.3	-0.7	-0.4	-0.6	0.0	-0.1	0.5

					Rut Depth		0.2		-0.4			
				March 1960	Change in Elevation	1.1	0.1	0.5	0.0	0.5	-0.5	0.5
					Transverse Profile	-0.4	-0.8	0.0	-0.2	0.5		
					Rut Depth		-0.6		-0.5			
3	140	3.48	539,790	July 1959	Change in Elevation	0.1	-0.2	0.0	-0.2	0.0	-0.2	0.4
					Transverse Profile	-1.4	-1.1	-0.5	-0.4	0.0		
					Rut Depth		-0.2		-0.2			
				October 1959	Change in Elevation	0.0	-0.2	-0.1	-0.5	0.0	-0.2	0.5
					Transverse Profile	-1.5	-1.1	-0.6	-0.7	0.0		
					Rut Depth		-0.1		-0.4			
				March 1960	Change in Elevation	0.7	-0.2	0.1	-0.4	0.1	-0.5	0.5
					Transverse Profile	-0.8	-1.1	-0.4	-0.6	0.1		
					Rut Depth		-0.5		-0.5			
				August 1960	Change in Elevation	-0.1	-0.6	-0.1	-0.5	0.1	-0.4	0.6
					Transverse Profile	-1.6	-1.5	-0.6	-0.7	0.1		
					Rut Depth		-0.4		-0.5			
				October 1960	Change in Elevation	0.0	-0.6	-0.1	-0.5	0.1	-0.5	0.6
					Transverse Profile	-1.5	-1.5	-0.6	-0.7	0.1		
					Rut Depth		-0.5		-0.5			
4	582	4.36	998,681	July 1959	Change in Elevation	-0.1	-0.6	-0.2	-0.8	-0.2	-0.5	0.5
					Transverse Profile	-1.6	-1.5	-0.7	-1.0	-0.2		
					Rut Depth		-0.5		-0.6			
				November 1959	Change in Elevation	-0.1	-0.6	-0.2	-0.8	-0.2	-0.5	0.5
					Transverse Profile	-1.6	-1.5	-0.7	-1.0	-0.2		
					Rut Depth		-0.5		-0.6			

				March 1960	Change in Elevation	0.4	-0.5	0.0	-0.7	0.0	-0.6	0.6
					Transverse Profile	-1.1	-1.4	-0.5	-0.9	0.0		
					Rut Depth		-0.5		-0.7			
				August 1960	Change in Elevation	-0.6	-1.1	-0.5	-1.1	0.2	-0.7	0.6
					Transverse Profile	-2.1	-2.0	-1.0	-1.3	0.2		
					Rut Depth		-0.5		-0.9			
				October 1960	Change in Elevation	-0.2	-0.7	-0.2	-0.8	-0.6	-0.5	0.6
					Transverse Profile	-1.7	-1.6	-0.7	-1.0	-0.4		
					Rut Depth		-0.5		-0.5			
4	602	3.48	513,114	July 1959	Change in Elevation	-0.6	-0.8	-0.2	-0.6	-0.1	-0.5	0.7
					Transverse Profile	-2.1	-1.7	-0.7	-0.8	-0.1		
					Rut Depth		-0.5		-0.4			
				November 1959	Change in Elevation	-0.4	-0.8	-0.4	-0.6	-0.1	-0.4	0.7
					Transverse Profile	-1.9	-1.7	-0.9	-0.8	-0.1		
					Rut Depth		-0.5		-0.3			
				March 1960	Change in Elevation	0.0	-0.8	-0.2	-0.7	-0.1	-0.6	0.8
					Transverse Profile	-1.5	-1.7	-0.7	-0.9	-0.1		
					Rut Depth		-0.6		-0.5			
4	630	3.48	566,396	July 1959	Change in Elevation	-0.1	-0.8	-0.1	-1.0	-0.1	-0.7	0.5
					Transverse Profile	-1.6	-1.7	-0.6	-1.2	-0.1		
					Rut Depth		-0.5		-0.9			
				October 1959	Change in Elevation	0.1	-0.5	0.1	-0.6	0.1	-0.6	0.6
					Transverse Profile	-1.4	-1.4	-0.4	-0.8	0.1		
					Rut Depth		-0.5		-0.7			
				March 1960	Change in Elevation	0.7	-0.2	0.4	-0.5	0.4	-0.8	0.6

					Transverse Profile	-0.8	-1.1	-0.1	-0.7	0.4		
					Rut Depth		-0.7		-0.9			
4	622	3.52	564,956	July 1959	Change in Elevation	0.1	-0.5	0.0	X	-0.1	-0.5	0.5
					Transverse Profile	-1.4	-1.4	-0.5	X	-0.1		
					Rut Depth		-0.5		X			
				October 1959	Change in Elevation	0.0	-0.5	-0.1	-0.6	-0.1	-0.5	0.5
					Transverse Profile	-1.5	-1.4	-0.6	-0.8	-0.1		
					Rut Depth		-0.5		-0.5			
				March 1960	Change in Elevation	0.6	-0.4	0.1	-0.5	0.0	-0.6	0.6
					Transverse Profile	-0.9	-1.3	-0.4	-0.7	0.0		
					Rut Depth		-0.7		-0.5			
5	426	3.92	368,653	July 1959	Change in Elevation	-0.4	-1.1	-0.2	-1.1	-0.2	-0.8	0.7
					Transverse Profile	-1.9	-2.0	-0.7	-1.3	-0.2		
					Rut Depth		-0.7		-0.9			
				March 1960	Change in Elevation	0.4	-1.0	0.0	-1.0	0.1	-1.1	0.8
					Transverse Profile	-1.1	-1.9	-0.5	-1.2	0.1		
					Rut Depth		-1.1		-1.0			
5	428	4.78	2,118,495	July 1959	Change in Elevation	-0.5	-0.7	-0.1	-0.4	0.0	-0.3	0.6
					Transverse Profile	-2.0	-1.6	-0.6	-0.6	0.0		
					Rut Depth		-0.3		-0.3			
				November 1959	Change in Elevation	-0.6	-1.0	-0.5	-0.7	-0.1	-0.4	0.6
					Transverse Profile	-2.1	-1.9	-1.0	-0.9	-0.1		
					Rut Depth		-0.4		-0.4			
				March 1960	Change in Elevation	0.2	-0.7	-0.1	-0.5	0.1	-0.6	0.7
					Transverse Profile	-1.3	-1.6	-0.6	-0.7	0.1		

					Rut Depth		-0.7		-0.5			
				August 1960	Change in Elevation	-0.7	-1.2	-0.6	-1.0	-0.2	-0.5	0.8
					Transverse Profile	-2.2	-2.1	-1.1	-1.2	-0.2		
					Rut Depth		-0.5		-0.6			
				October 1960	Change in Elevation	-0.8	-1.2	-0.5	-0.8	-0.2	-0.4	0.8
					Transverse Profile	-2.3	-2.1	-1.0	-1.0	-0.2		
					Rut Depth		-0.5		-0.4			
5	442	3.9	309,856	July 1959	Change in Elevation	-0.6	-1.3	-0.4	-1.0	-0.1	-0.7	0.8
					Transverse Profile	-2.1	-2.2	-0.9	-1.2	-0.1		
					Rut Depth		-0.7		-0.7			
				November 1959	Change in Elevation	-0.5	-1.3	-0.4	-1.0	-0.1	-0.7	0.9
					Transverse Profile	-2.0	-2.2	-0.9	-1.2	-0.1		
					Rut Depth		-0.8		-0.7			
				March 1960	Change in Elevation	0.0	-1.3	-0.1	-1.0	0.0	-1.0	0.9
					Transverse Profile	-1.5	-2.2	-0.6	-1.2	0.0		
					Rut Depth		-1.2		-0.9			
				October 1960	Change in Elevation							
					Transverse Profile	-1.5	-2.2	-0.6	-1.2	0.0	-1.0	1.1
					Rut Depth		-1.2		-0.9			
5	446	4.36	1,559,929	November 1959	Change in Elevation	-0.4	-1.1	-0.2	-1.0	-0.1	-0.8	0.7
					Transverse Profile	-1.9	-2.0	-0.7	-1.2	-0.1		
					Rut Depth		-0.7		-0.8			
				March 1960	Change in Elevation	0.2	-0.8	0.0	-0.7	0.2	-0.8	0.7
					Transverse Profile	-1.3	-1.7	-0.5	-0.9	0.2		
					Rut Depth		-0.8		-0.8			
				August 1960	Change in Elevation	-0.5	-1.3	0.2	-1.0	-0.2	-1.0	0.8

					Transverse Profile	-2.0	-2.2	-0.3	-1.2	-0.2		
					Rut Depth		-1.1		-1.0			
					Change in Elevation	-0.5	-1.2	-0.4	-1.0	-0.2		
				October 1960	Transverse Profile	-2.0	-2.1	-0.4	-1.2	-0.2	-0.9	0.8
					Rut Depth		-0.9		-0.9			
					Change in Elevation	-0.7	-0.8	-0.1	-0.5	-0.1		
				November 1959	Transverse Profile	-2.2	-1.7	-0.6	-0.7	-0.1	-0.3	0.7
					Rut Depth		-0.3		-0.4			
					Change in Elevation	0.5	-0.5	0.1	-0.4	0.2		
				March 1960	Transverse Profile	-1.0	-1.4	-0.4	-0.6	0.2	-0.6	0.7
					Rut Depth		-0.7		-0.5			
5	448	4.34	1,632,621		Change in Elevation	-0.6	-1.2	-0.2	-0.8	-0.2		
				August 1960	Transverse Profile	-2.1	-2.1	-0.7	-1.0	-0.2	-0.6	0.8
					Rut Depth		-0.7		-0.6			
					Change in Elevation	-0.6	-1.3	-0.4	-1.0	-0.2		
				October 1960	Transverse Profile	-2.1	-2.2	-0.9	-1.2	-0.2	-0.7	0.8
					Rut Depth		-0.7		-0.7			
					Change in Elevation	-0.1	-1.0	-0.2	-0.7	-0.1		
				July 1959	Transverse Profile	-1.6	-1.9	-0.7	-0.9	-0.1	-0.6	0.6
					Rut Depth		-0.8		-0.5			
					Change in Elevation	-0.2	-1.2	-0.2	-1.0	-0.2		
5	470	3.92	755,535	November 1959	Transverse Profile	-1.7	-2.1	-0.7	-1.2	-0.2	-0.8	0.7
					Rut Depth		-0.9		-0.8			
					Change in Elevation	0.5	-1.0	0.0	-0.7	0.0		
				March 1960	Transverse Profile	-1.0	-1.9	-0.5	-0.9	0.0	-0.9	0.7
					Rut Depth		-1.2		-0.7			

				October 1960	Change in Elevation Transverse Profile Rut Depth	-1.0	-1.9 -1.2	-0.5	-0.9 -0.7	0.0	-0.9	0.8
5	476	3.9	712,872	July 1959	Change in Elevation Transverse Profile Rut Depth	-0.4 -1.9	-1.0 -1.9 -0.6	-0.2 -0.7	-1.0 -1.2 -0.8	-0.1 -0.1	-0.7	0.6
				November 1959	Change in Elevation Transverse Profile Rut Depth	-0.4 -1.9	-0.8 -1.7 -0.5	0.0 -0.5	-0.6 -0.8 -0.6	0.0 0.0	-0.5	0.7
				March 1960	Change in Elevation Transverse Profile Rut Depth	0.4 -1.1	-0.8 -1.7 -1.0	0.1 -0.4	-0.7 -0.9 -0.8	0.1 0.1	-0.9	0.7
5	478	4.34	2,132,626	July 1959	Change in Elevation Transverse Profile Rut Depth	-0.1 -1.6	-0.7 -1.6 -0.6	0.0 -0.5	-0.6 -0.8 -0.6	0.0 0.0	-0.6	0.7
				March 1960	Change in Elevation Transverse Profile Rut Depth	0.6 -0.9	-0.6 -1.5 -0.9	0.1 -0.4	-0.6 -0.8 -0.6	0.0 0.0	-0.7	0.8
				June 1960	Change in Elevation Transverse Profile Rut Depth	-0.4 -1.9	-1.2 -2.1 -0.8	-0.3 -0.8	-0.9 -1.1 -0.6	-0.3 -0.3	-0.7	0.8
				August 1960	Change in Elevation Transverse Profile Rut Depth	-0.5 -2.0	-1.4 -2.3 -0.8	-0.6 -1.1	-1.4 -1.6 -0.8	-0.5 -0.5	-0.8	0.9
				October 1960	Change in Elevation	-0.2	-1.2	-0.1	-0.7	-0.1	-0.8	0.9

					Transverse Profile	-1.7	-2.1	-0.6	-0.9	-0.1		
					Rut Depth		-1.0		-0.6			
5	480	3.94	1,237,863	July 1959	Change in Elevation	-0.4	-1.1	-0.4	-0.7	-0.4	-0.4	0.6
					Transverse Profile	-1.9	-2.0	-0.9	-0.9	-0.4		
					Rut Depth		-0.6		-0.3			
				November 1959	Change in Elevation	-0.1	-0.8	0.0	-0.7	0.0	-0.7	0.7
					Transverse Profile	-1.6	-1.7	-0.5	-0.9	0.0		
					Rut Depth		-0.7		-0.7			
				March 1960	Change in Elevation	0.8	-0.5	0.2	-0.5	0.5	-0.9	0.7
					Transverse Profile	-0.7	-1.4	-0.3	-0.7	0.5		
					Rut Depth		-0.9		-0.8			
				June 1960	Change in Elevation	-0.1	-1.1	-0.2	-1.0	-0.1	-0.8	0.7
					Transverse Profile	-1.6	-2.0	-0.7	-1.2	-0.1		
					Rut Depth		-0.9		-0.8			
				August 1960	Change in Elevation	-0.5	-1.6	-0.5	-1.2	-0.5	-0.8	0.8
					Transverse Profile	-2.0	-2.5	-1.0	-1.4	-0.5		
					Rut Depth		-1.0		-0.7			
				October 1960	Change in Elevation	-0.1	-1.2	-0.1	-0.8	0.0	-0.9	0.8
					Transverse Profile	-0.7	-1.4	-0.3	-0.7	0.5		
					Rut Depth		-0.9		-0.8			
6	256	4.82	4,523,570	July 1959	Change in Elevation	0.1	-0.7	0.0	-0.7	-0.1	-0.6	0.7
					Transverse Profile	-1.4	-1.6	-0.5	-0.9	-0.1		
					Rut Depth		-0.7		-0.6			
				October 1959	Change in Elevation	-0.2	-0.7	0.0	-0.7	0.0	-0.6	0.7
					Transverse Profile	-1.7	-1.6	-0.5	-0.9	0.0		

					Rut Depth		-0.5		-0.7			
				March 1960	Change in Elevation	0.6	-0.6	0.1	-0.7	0.1	-0.8	0.8
					Transverse Profile	-0.9	-1.5	-0.4	-0.9	0.1		
					Rut Depth		-0.9		-0.8			
6	264	4.78	4,442,005	July 1959	Change in Elevation	0.1	-1.0	-0.1	-0.8	-0.2	-0.8	0.7
					Transverse Profile	-1.4	-1.9	-0.6	-1.0	-0.2		
					Rut Depth		-0.9		-0.6			
				October 1959	Change in Elevation	-0.4	-1.2	-0.4	-1.1	-0.4	-0.7	0.7
					Transverse Profile	-1.9	-2.1	-0.9	-1.3	-0.4		
					Rut Depth		-0.7		-0.7			
				March 1960	Change in Elevation	0.5	-0.7	0.1	-0.7	0.1	-0.8	0.7
					Transverse Profile	-1.0	-1.6	-0.4	-0.9	0.1		
					Rut Depth		-0.9		-0.8			
6	310	4.78	3,547,770	July 1959	Change in Elevation	-0.1	-0.7	-0.2	-0.7	-0.2	-0.5	0.9
					Transverse Profile	-1.6	-1.6	-0.7	-0.9	-0.2		
					Rut Depth		-0.5		-0.5			
				October 1959	Change in Elevation	-0.5	-0.8	-0.4	-0.7	-0.2	-0.3	0.9
					Transverse Profile	-2.0	-1.7	-0.9	-0.9	-0.2		
					Rut Depth		-0.3		-0.4			
				March 1960	Change in Elevation	0.5	-0.5	0.0	-0.5	0.0	-0.6	0.9
					Transverse Profile	-1.0	-1.4	-0.5	-0.7	0.0		
					Rut Depth		-0.7		-0.5			
				June 1960	Change in Elevation	-0.3	-1.0	-0.2	-0.7	-0.2	-0.6	1.0
					Transverse Profile	-1.8	-1.9	-0.7	-0.9	-0.2		
					Rut Depth		-0.7		-0.5			

				August 1960	Change in Elevation	-0.4	-1.2	-0.2	-0.8	-0.2	-0.7	1.1
					Transverse Profile	-1.9	-2.1	-0.7	-1.0	-0.2		
					Rut Depth		-0.8		-0.6			
				October 1960	Change in Elevation	-0.4	-1.2	-0.4	-0.8	-0.4	-0.5	1.1
					Transverse Profile	-1.9	-2.1	-0.9	-1.0	-0.4		
					Rut Depth		-0.7		-0.4			
6	334	5.66	3,447,869	July 1959	Change in Elevation	-0.1	-0.7	-0.4	-0.8	-0.4	-0.4	0.7
					Transverse Profile	-1.6	-1.6	-0.9	-1.0	-0.4		
					Rut Depth		-0.4		-0.4			
				October 1959	Change in Elevation	-0.3	-1.0	-0.5	-0.8	-0.4	-0.4	0.7
					Transverse Profile	-1.8	-1.9	-1.0	-1.0	-0.4		
					Rut Depth		-0.5		-0.3			
				March 1960	Change in Elevation	0.0	-0.8	-0.5	-0.8	-0.4	-0.4	0.7
					Transverse Profile	-1.5	-1.7	-1.0	-1.0	-0.4		
					Rut Depth		-0.5		-0.3			
				June 1960	Change in Elevation	-0.5	-1.0	-0.7	-1.1	-0.6	-0.4	0.8
					Transverse Profile	-2.0	-1.9	-1.2	-1.3	-0.6		
					Rut Depth		-0.3		-0.4			
				August 1960	Change in Elevation	-0.5	-1.2	-0.5	-1.0	-0.6	-0.5	0.8
					Transverse Profile	-2.0	-2.1	-1.0	-1.2	-0.6		
					Rut Depth		-0.6		-0.4			
				October 1960	Change in Elevation	-0.6	-1.2	-0.6	-1.0	-0.7	-0.4	0.8
					Transverse Profile	-2.1	-2.1	-1.1	-1.2	-0.7		
					Rut Depth		-0.5		-0.3			

Appendix C: References

AASHO (1961). "The AASHO Road Test: Report." *Publication 816, No. 61A-61G*, Highway Research Board, National Research Council, National Academy of Sciences, Washington, D.C.

AASHTO (1993). *AASHTO Guide for Design of Pavements Structures*, American Association of State Highway and Transportation Officials, Washington, DC.

AASHTO (2008). *Mechanistic-Empirical Pavement Design Guide: A Manual of Practice*. American Association of State Highway and Transportation Officials, Washington, D.C.

Al-Omari, B., and M.I. Darter. (1994). *Relationships between International Roughness Index and Present Serviceability Rating.* Transportation Research Record 1435, Washington, D.C., pp.130-136.

Crawford, G. (2009, January 11). *National Update of MEPDG Activities*. (Power Point). Washington, D.C.: 88th Annual Transportation Research Board Meeting.

Gulen, S., R. Woods, J. Weaver, and V.L. Anderson. (1994). *Correlation of Present Serviceability Ratings and International Roughness Index.* Transportation Research Record 1435, Washington, D.C., pp. 27-37.

Hung, Y.H. (2004). *Pavement Analysis and Design*. Prentice-Hall, Upper Saddle River, N.J.

Kim, S., Ceylan, H., Copalakrishnan, K., Smadi, O., Brakke, C., and Behnami, F. (2010). *Verification of Mechanistic-Empirical Pavement Design Guide (MEPDG) Performance Predictions Using Pavement Management Information System (PMIS).* Transportation Research Board 2010 Annual Meeting, TRB Paper 10-2395, p. 20. Washington, D.C.

Li, J., Uhlmeyer, J. S., Mahoney, J. P., & Muench, S. T. (2009). *Use of the AASHTO 1993 Guide, MEPDG, and Historical Performance to Update the WSDOT Pavement Design Catalog*. Transportation Research Board 2010 Annual Meeting, (p. 15). Washington, D.C.

NCHRP (2004). *Guide for Mechanistic-Empirical Design of New and Rehabilitated Pavement Structures.* Draft Final Report NCHRP Project 1-37A, Transportation Research Board, National Research Council, Washington, D.C.

Paterson, W.D.O. (1987). *Road Deterioration and Maintenance Effects: Models for Planning and Management.* The World Bank, Washington, D.C.

Schwartz, C.W. (2009). "Influence of Unbound Materials on Flexible Pavement Performance: A Comparison of the AASHTO and MEPDG Methods," *Eighth International Conference on the Bearing Capacity of Roads, Railways, and Airfields*, Urbana-Champaign IL, July, p. 951-959.

The Department of the Treasury with the Council of Economic Advisors. (2010, October 11). *An Economic Analysis of Infrastructure Investment*. Washington, D.C.

This page has been intentionally left blank.